ISHAM, LINCOLN & BEALE
COUNSELORS AT LAW

1120 CONNECTICUT AVENUE, N.W. • SUITE 840
WASHINGTON, D.C. 20036
202 833-9730

EDWARD S. ISHAM 1872-1902
ROBERT T. LINCOLN 1872-1889
WILLIAM G. BEALE 1885-1923

CHICAGO OFFICE
THREE FIRST NATIONAL PLAZA
CHICAGO, ILLINOIS 60602
TELEPHONE 312 558-7500
TELEX: 2-5288

June 20, 1983

Peter B. Bloch, Esquire
Administrative Judge
Atomic Safety and Licensing
Board Panel
U.S. Nuclear Regulatory
Commission
Washington, D.C. 20555

Dr. Oscar H. Paris
Administrative Judge
Atomic Safety and Licensing
Board Panel
U.S. Nuclear Regulatory
Commission
Washington, D.C. 20555

Mr. Frederick J. Shon
Administrative Judge
Atomic Safety and Licensing
Board Panel
U.S. Nuclear Regulatory Commission
Washington, D.C. 20555

Gentlemen:

I am enclosing two documents that provide information concerning the structural integrity of the concrete in the Big Rock spent fuel pool at elevated temperatures (Subcontention (5) of intervenors' contentions 8 and IIIE-2). These documents are:

1. June 8, 1983 letter from Consumers Power Company to Mr. Crutchfield of the NRC; and
2. June 10, 1983 letter from Consumers Power Company to Mr. Crutchfield.

The foregoing documents provide additional information in response to questions posed by the NRC Staff during their review of Amendment 2 of Consumers Power Company's Consolidated Application in this case. I am also enclosing a copy of pertinent work papers that can be identified by the title on the front page, namely, "Crack Spacing of Two Way Slab".

Sincerely,

Joseph Gallo

Joseph Gallo

cc: Service list
JG/gym

D503

Consumers Power Company

General Offices: 1945 West Parnall Road, Jackson, MI 49201 • (517) 788-0550

COPY

June 8, 1983

Dennis M Crutchfield, Chief
Operating Reactors Branch No 5
Nuclear Reactor Regulation
US Nuclear Regulatory Commission
Washington, DC 20555

DOCKET 50-155 - LICENSE DPR-6 - BIG ROCK POINT PLANT -
RESPONSE TO NRC STAFF CONCERNS - AMENDMENT 2 TO SPENT
FUEL RACK ADDITION - "CONSOLIDATED APPLICATION"

Consumers Power Company letter dated January 10, 1983 enclosed our analysis of the structural integrity of the spent fuel pool at elevated temperatures, and identified it as Amendment 2 to the "Consolidated Application." NRC review and response to our submittal yielded a Safety Evaluation Report (SER) transmitted by letter dated May 16, 1983 . The SER concluded that ". . . the licensee must provide the requested additional information to the staff and receive staff approval before plant start-up." This submittal is intended to provide that information.

The May 16, 1983 SER identified in general terms the five unresolved items that remain open. NRC letter dated May 24, 1983 provided a summary of a May 9, 1983 meeting and further clarified the five remaining unresolved items as follows: 1. Shear key capacity and factor of safety; 2. Effects of cracking on development length; 3. Orthotropic plate assumptions; 4. Shear capacity of the pool slab in the vicinity of the east support wall; and 5. Deflections of the west and south walls in the vicinity of the expansion joints. An additional item was transmitted via telephone conference call and was subsequently discussed during a meeting in Bethesda on June 2, 1983. This item concerned orthotropic plate assumptions and we were requested to consider the effects of time on the stress loadings.

In order to expedite Staff review, we have attached responses to the above five items. These responses (excepting renumbering of items to correlate with the NRC May 9, 1983 summary of issues letter) have been reproduced as originally forwarded. In addition, the following discussion of the issues as presented during the June 2, 1983 meeting is provided:

1. Shear Key Capacity and Factor of Safety -

   The capacity of the shear key and bearing support wall were evaluated with respect to the imposed deadweight and deadweight-plus-thermal loading conditions. It was concluded that the shear key has sufficient capacity to support deadweight pool loads when the capacity of the key is determined from very conservative shear allowables. The key can also support the deadweight-plus-thermal pool loads (except perhaps at the very northern edge of the key). It was noted that the bearing wall in the vicinity of the northern edge of the shear key is actually in a parallel load path with respect to the shear key and the very stiff bearing wall will preclude any local failure of the shear key. It was also noted that the bearing wall is of sufficient capacity to support the entire weight of the fuel pool. It was determined that the shear key/bearing wall support system was of sufficent capacity to support the imposed loads due to either loading condition.

2. Effects of Cracking on Development Length -

   Considering the most unfavorable concrete cracking pattern and a conservative post cracking bond strength, the margin of safety associated with the development length of embedment steel was evaluated at various critical locations. It was determined that there was sufficient margin of safety at all but one of those locations. Consideration of the loading environment in the neighborhood of the location of concern, the conservative nature of the evaluation assumptions and the small size of the deviation from allowables resulted in the conclusion that the condition was structurally insignificant.

3. Orthotropic Plate Assumptions -

   An apparent inconsistency exists in the ANSYS computer code with respect to the material property development for orthotropic plates. The empirical relationship of material properties employed in ANSYS was compared with a theoretical relationship in order to determine the effect the ANSYS relationship might have on the fuel pool concrete cracking patterns. It was concluded that where the ANSYS material input approximations differ from theoretical values, the bending moments calculated by the ANSYS approximation for cracked elements were overestimated. While such an overestimation can alter the theoretical crack pattern throughout the pool structure, it was determined that overestimation of bending moments introduced overall conservatism into the analysis.

4. Shear Capacity of the Pool Slab in the Vicinity of the East Support Wall

   This concern was over the potential for the development of diagonal cracking at the pool floor/east support wall juncture. An evaluation of the stress pattern in the areas of potential concern resulted in the judgment that the stress field was dominated by compression induced by deadweight pool loads. Application of Mohr's circle resulted in the

conclusion that the tensile stresses required to induce diagonal cracking could not be developed and thus no support/pool floor juncture failure would occur.

5. Deflections of the West and South Walls in the Vicinity of the Expansion of Joints -

   Pool deflections induced by thermal expansion were extracted from computer code output and reported. The deflections were very small. The small deflections ensure that pool expansion will not take up the expansion gap and introduce additional undesirable stiffness (hence more cracking) into the fuel pool structure and support system.

6. Transient Time

   A significant amount of discussion focused on the issue of employing stepwise increments of temperature gradient as a function of the peak gradient rather than as a function of the time of the transient in the sequential analysis of concrete cracking. It was noted that the temperature gradient steps were employed for convenience as a reasonable approximation of the cracking phenomenon and it was judged that this approach had little if any effect on the final conclusions of the analysis.

Consumers Power Company committed during the June 2, 1983 meeting to provide documentation of the basis for resolution of concerns identified by items 3 and 6 above. This information will be supplied directly.

Thomas C Bordine/wgf (Signed)

Thomas C Bordine
Staff Licensing Engineer

CC Administrator, Region III, USNRC
NRC Resident Inspector-Big Rock Point

Attachment

Consumers Power Company
Big Rock Point Plant
Docket 50-155

1. SHEAR KEY DESCRIPTION
June 8, 1983

16 pages

Consumers Power Company

OPERATING SERVICES DEPARTMENT

Subject: NRC DISCUSSION ITEM # 5: SHEAR KEY CAPACITY

Sketch No _____ Cal No _____
Project No _____
Originator E T Wong
Reviewed by R B Goldin
Approved by _____
Date 7/16/83 Page 1 of 2

1. SHEAR KEY DESCRIPTION

PLAN VIEW DWG. C-113
ELEVATION VIEW C-117

DIMENSION: 6" x 4'-0" @ RUNS CONTINUOUS ON THE W. SIDE OF POOL WITH A 45° DOGLEG ON THE N.W. CORNER.
UNABLE TO CONFIRM THE EXISTENCE OF THE SHEAR KEY ON THE 45° PORTION, BUT MAY BE GROUTED COSMETICALLY.

REINF. : # 7 @ 18" , 40,000 psi STEEL.

DESIGN CONCEPT: THE CONSTRUCTION DWG. WAS ISSUED IN EARLY 1961, PRIOR TO THE EXISTENCE OF THE ACI 318-63. ASSUME ACI 318-56 WAS USED. IN THAT CODE $N < 90$ psi (REVISED TO 60 psi) FOR BEAMS W/O WEB REINFORCEMENT. FOR THE SHEAR KEY, IT IS BELIEVED THAT THE REINFORCEMENT IS FOR SHRINKAGE CONTROL ONLY.
FROM DWG. C-116, WHERE SEVERAL (OTHER) SHEAR KEYS COUPLING THE REACTOR CAVITY STRUCTURE TO THE SURROUNDING STRUCTURES HAVE ASPHALT COATED BEARING SURFACES, IT IS ASSUMED THAT THE SHEAR KEY ONLY TRANSMITS VERTICAL LOAD.

2. LOADING CONDITION

PRESENTLY, WE ARE CONCERNED WITH 2 LOADING CONDITIONS, DEAD LOAD (D.L.) AND THERMAL LOAD (T.L.) THE INPUT ARE FROM THE ANUS ANALYSIS, WHICH IS EXCERPTED & ATTACHED.

3. SHEAR KEY CAPACITY (SEE ATTACHMENT 1)

PRESENT CODE ALLOWS A SHEAR STRESS

$$v_c = 2\sqrt{f_c'} \qquad \text{(ACI 318-77 EQ. 11-3)}$$

$$\phi\, v_u \leq \phi\, v_c \qquad \text{when } \phi = 0.85$$

OR, ALTERNATELY

$$v_c = \left(1.9\sqrt{f_c'} + 2500\,\rho_w \frac{V_u d}{M_u}\right) \leq 3.5\sqrt{f_c'} \qquad \text{(Eq. 11-6)}$$

FOR THE SHEAR KEY, Eq 11-6 BECOMES

$$v_c = 2.35\sqrt{f_c'}$$

i.e. 18% HIGHER THAN EQ. 11-3. BOTH EQS. 11-3 & 11-6 ARE RELEVANT FOR A DIAGONAL TENSION FAILURE MODE IN BEAMS. IT SHOULD BE NOTED THAT THE COMPUTED SHEAR STRESS IS ONLY A MEASURE OF THE DIAGONAL TENSION AS THE TRUE STRESS DISTRIBUTION IS SELDOM KNOWN. THE CURRENT CODE USES A NOMINAL SHEAR STRESS OBTAINED BY DIVIDING THE SHEAR FORCE BY THE EFFECTIVE AREA bd.

THE USE OF DIAGONAL TENSION FAILURE MODE IS JUSTFIED IN LIGHT OF THE EXPERIMENTAL WORK CITED IN REFERENCES 1 & 2. IN THOSE EXPERIMENTS, THE BEHAVIOR OF CONCRETE FAILED BY PURE SHEAR (SHEAR-FRICTION FAILURE) WAS STUDIED. IT IS OBSERVED THAT, FOR A MONOLITHIC & INITIALLY UNCRACKED CONCRETE BLOCK SUBJECTED TO SHEARING FORCE WHICH TENDS TO 'SHEAR' IT IN HALF, THERE IS NO MOVEMENT UNTIL DIAGONAL TENSION CRACKS ARE FORMED. A MOHR CIRCLE TYPE EVALUATION PREDICTS THAT FOR A SPECIMEN WITHOUT ANY SHEAR REINFORCEMENT, DIAGONAL CRACKING OCCURS AT

A NOMINAL ULTIMATE SHEAR STRESS OF APPROXIMATELY $8\sqrt{f_c'}$. TEST RESULT OF ONE SUCH SPECIMEN GIVE RESULTS THAT ARE VERY CLOSE TO THIS VALUE ($7.6\sqrt{f_c'}$, SEE REF. 1)

THEREFORE IT IS CONSIDERED CONSERVATIVE TO USE THE FOLLOWING ACCEPTANCE CRITERIA

$$V_u < 2\phi\sqrt{f_c'} \qquad \text{(EQ 11-3)}$$

or

$$< 2.35\phi\sqrt{f_c'} \qquad \text{(DERIVED FROM EQ 11-6)}$$

4. SUPPORT WALL CAPACITY (SEE ATTACHMENT II)

FURTHERMORE, THERE ARE WALLS SUPPORTING THE WEST POOL WALL ON ITS SOUTH & NORTH ENDS. (SEE C-113 AND C-107 attached, shade area) THE CONFIGURATION OF THESE WALLS DOES NOT LEND ITSELF TO 'EXACT' ANALYSIS. FOR THE PURPOSE OF THIS EVALUATION, THE FOLLOWING CONSERVATIVE METHOD WILL BE USED.

- ONLY AREAS DIRECTLY BELOW THE POOL WALL ARE CONSIDERED EFFECTIVE IN LOAD DISSIPATION.
- WHERE THERE ARE DOOR OPENING, THE AREA IS IGNORED, i.e. LOAD DISTRIBUTION EFFECTS ARE IGNORED (SEE SUPPORT WALL ON NORTH SIDE). HOWEVER, THEIR RIGIDITY AS A UNIT IS RECOGNIZED & THE WEAK AXIS OF THE WALL ARE DETERMINED ACCORDINGLY.
- THE LATERAL BRACING OF THE FLOOR SLAB ON THE N. WALL IS RECOGNIZED. BUT THE STIFFENING EFFECTS OF PERPENDICULARLY INTERCEPTING WALLS (BOTH N & S) HAS BEEN IGNORED.
- THE ANALYSIS METHOD PER ACI 349-80 SECTION 14.2 "EMPIRACAL DESIGN METHOD" WAS USED. THE CONSERVATISM WITH REGARD TO CHOICE OF ℓ_p/r RATIO AND EFFECTIVE AREA SHOULD PROVIDE A LOWER BOUND VALUE.

Consumers Power Company	OPERATING SERVICES DEPARTMENT Subject:	Sketch No ____ Cal No ____ Project No ____ Originator GAWong Reviewed by RBQ[illegible] Approved by ____ Date 5/16/83 Page 4 of 6

- SINCE THE WALLS MAY ALREADY HAVE BEEN CARRYING DEAD & LIVE LOAD, THE APPLIED THERMAL LOAD WILL NOT BE EVALUATED BY THE MARGIN OF SAFETY, INSTEAD, IT WILL BE COMPARED TO THE CAPACITY AS AN INCREMENTAL FRACTION. IT SHOULD BE NOTED HERE THAT CONTAINMENT INTERNAL STRUCTURES ARE OFTEN SIZED FOR REASONS OTHER THAN EXPECTED LOADING, AS e.g. LATERAL STIFFNESS AND SHIELDING.

5. SUMMARY AND CONCLUSIONS

THE MARGINS OF SAFETY ARE COMPUTED IN THE FOLLOWING PAGE. WITH EXCEPTION OF THE LAST TWO NODES (NODES 232 & 233) ON THE NORTH SIDE, THE SHEAR KEY HAS ADEQUATE CAPACITY FOR BOTH THE DEAD LOAD CASE & DEAD + THERMAL LOAD CASE. FURTHERMORE, THE BEARING WALLS SUPPORTING THE POOL STRUCTURE CAN SUPPORT THE WORST LOADING CONDITION, EVEN ASSUMING A VERY CONSERVATIVE ESTIMATION OF ITS CAPACITY. THE MAXIMUM INCREMENTAL LOAD DUE TO THERMAL CONDITION IS 7.3%.

IT IS WORTHY TO NOTE THAT, IGNORING THE SHEAR KEY CAPACITY ENTIRELY, AND ASSUMING EACH WALL WILL TAKE HALF THE LOAD, THE DEAD LOAD IS ONLY 12.4% OF THE NORTH WALL (WEAKER WALL) CAPACITY. UNDER THE DEAD AND THERMAL LOAD CASE, THERE ARE LESS NET DOWNWARD LOAD.

GIVEN THE LARGE DEGREE OF CONSERVATISM IN CAPACITY COMPUTATION, & GIVEN THE ABOVE JUSTIFICATION, IT CAN BE CONCLUDED THAT THE SHEAR KEY / BEARING WALL SUPPORT IS ADEQUATE.

Consumers Power Company

OPERATING SERVICES DEPARTMENT

Subject:

Sketch No. ____ Cal No. ____
Project No. ____
Originator SW Jones
Reviewed by [illegible]
Approved by ____
Date 5/16/85 Page 5 of 6

SUMMARY OF LOADS & MARGINS

NODE NO.	225	226	227	228	229	230	231	232	233	Σ
DEAD LOAD	118,000#	55,100	69,200	68,000	70,200	65,600	57,300	54,300	161,000#	709,700#
$(F.S.)_1$	2.07	2.34	2.14	1.89	1.83	1.96	2.25	2.85	1.60	
THERMAL LOAD	77,100#	-65,000	-98,600	-100,300	-91,700	-65,100	-42,900	37,500	170,000	
THERMAL + DEAD LOAD	195,100#	-9,900	-38,400	-32,300	-21,500	500	14,400	91,800	331,000	
$(F.S.)_1$	1.25	13.0	3.35	3.99	5.99	258	8.94	1.68 (0.79)*	(0.78) —*	
$(F.S.)_2$	1.47	—	—	—	—	—	—	1.98 (0.99)*	(0.91) —*	
INCREMENTAL FRACTION OF BEARING WALL CAPACITY (%) THERMAL LOAD	1.8%	← N.A. →						7.3%**		
INCREMENTAL FRACTION OF BEARING WALL CAPACITY (%) THERMAL + DEAD LOAD	4.6%	← N.A. →						14.8%**		

FOOTNOTE: 1. $(F.S.)_1$ - FACTOR OF SAFETY W/ SHEAR CAPACITY (EQ 11-3 $V_c = 2\sqrt{f'_c}$) DIVIDED BY SHEAR LOAD

2. $(F.S.)_2$ - F.S. W/ SHEAR CAPACITY COMPUTED BY EQ 11-6 $V_c = 2.35\sqrt{f'_c}$

3. * - ASSUMING SHEAR KEY DOES NOT EXTEND INTO 45° DOG LEG

4. INSUFFICIENT MARGINS ($F.S. \leq 1.0$) ARE ENCIRCLED.

5. INCREMENTAL FRACTIONS OF BEARING WALL CAPACITY ARE COMPUTED IGNORING SHEAR KEY LOAD CARRYING CAPACITY AT THAT NODE.

6. ** - ASSUMING THE LOADS FROM BOTH NODES 232 & 233 BEING DUMPED ONTO NORTH BEARING WALL.

6 REFERENCES:

1. HOFBECK J. A, IBRAHIM I. O., AND MATTOCK A. H., "SHEAR TRANSFER IN REINFORCED CONCRETE", ACI JOURNAL, Vol. 66, No. 2, Feb. 1969 pp 119-128.

2. MATTOCK A.H. AND HAWKINS N.M., "SHEAR TRANSFER IN REINFORCED CONCRETE - RECENT RESEARCH", JOURNAL OF PRESTRESSED CONCRETE INSTITUTE, Vol 17, No. 2, MAR.-APR. 1972, pp. 55-75.

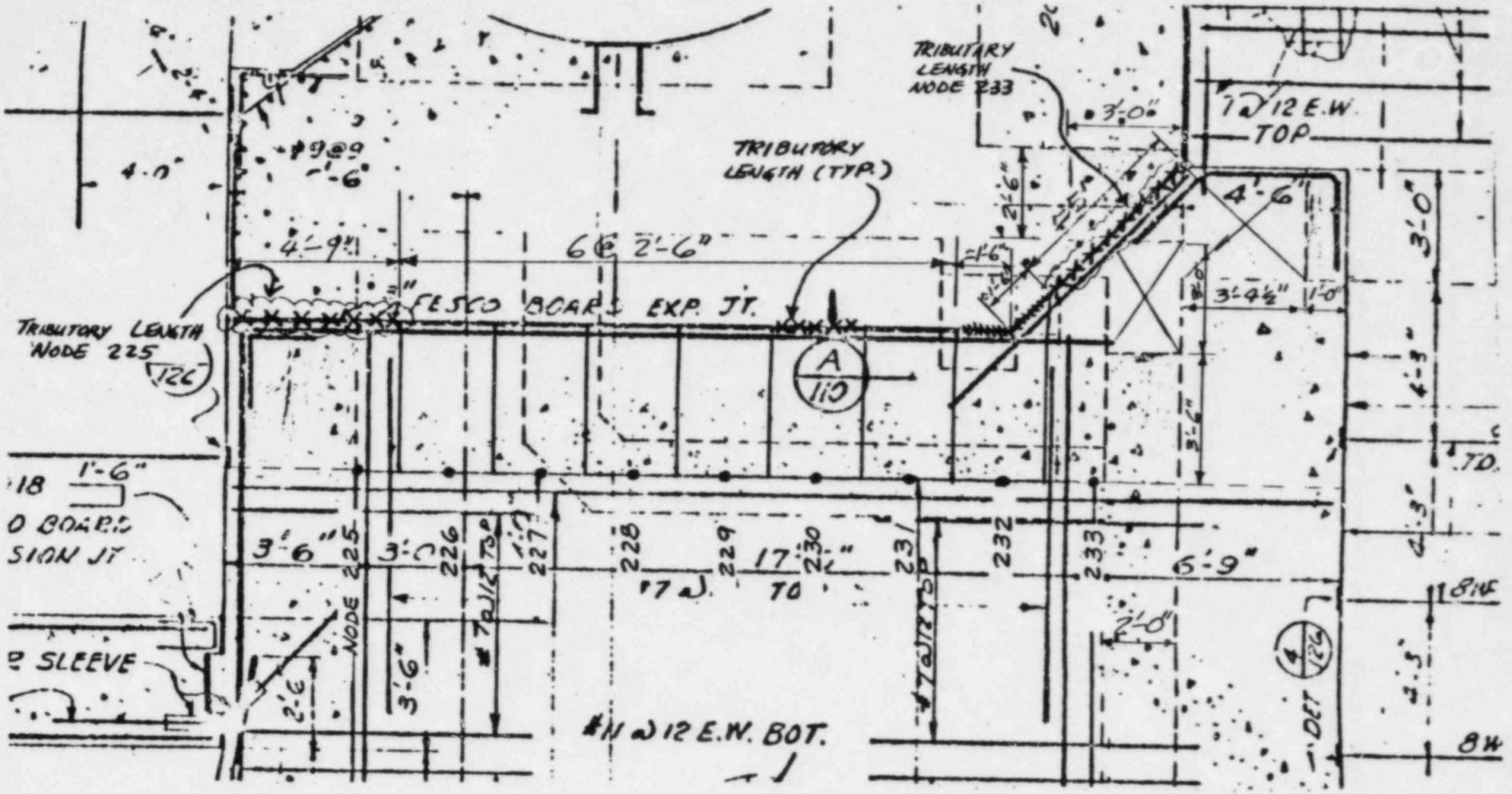

FIGURE 1 Node Points, Tributary Length
& Effective Bearing Wall Area

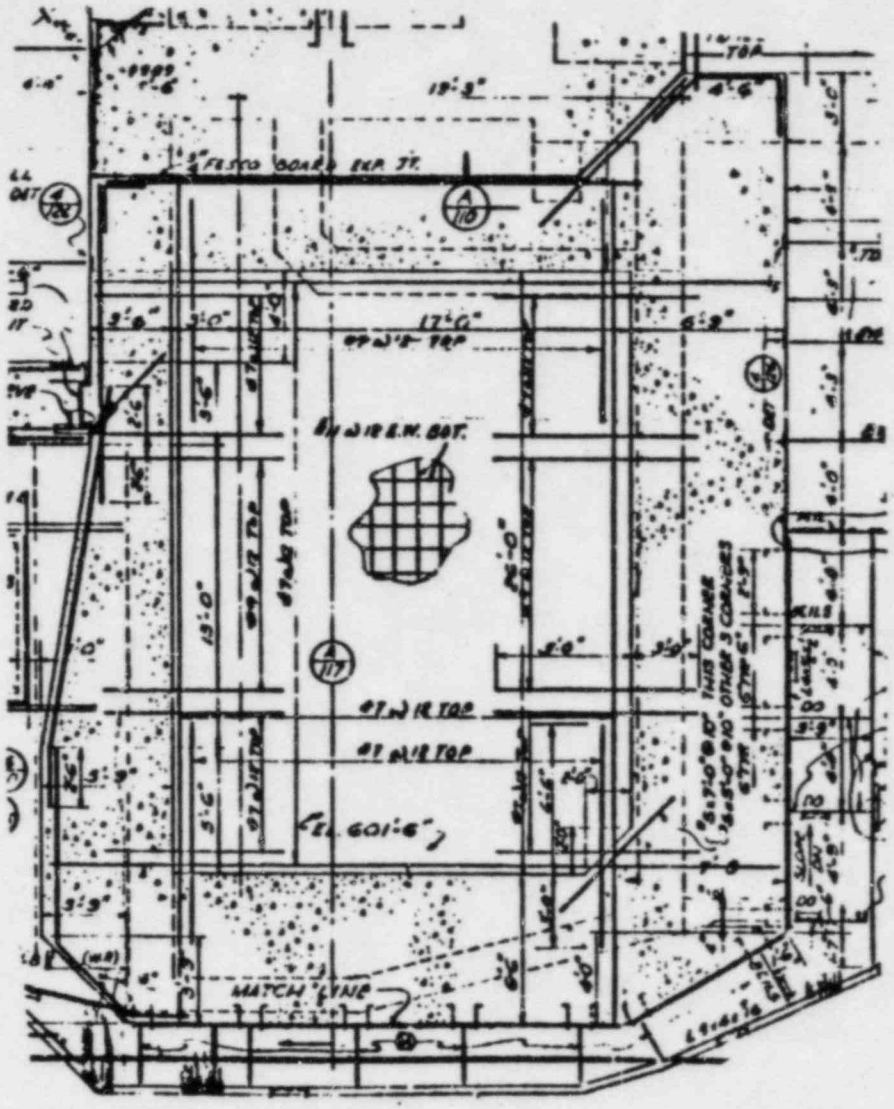

BIG ROCK POINT PLANT CHARLEVOIX, MICHIGAN CONSUMERS POWER COMPANY			
REACTOR BUILDING PLAN • ELEV 599'-5"			
BECHTEL	3759	FORMER DWG. NO. C-113	7

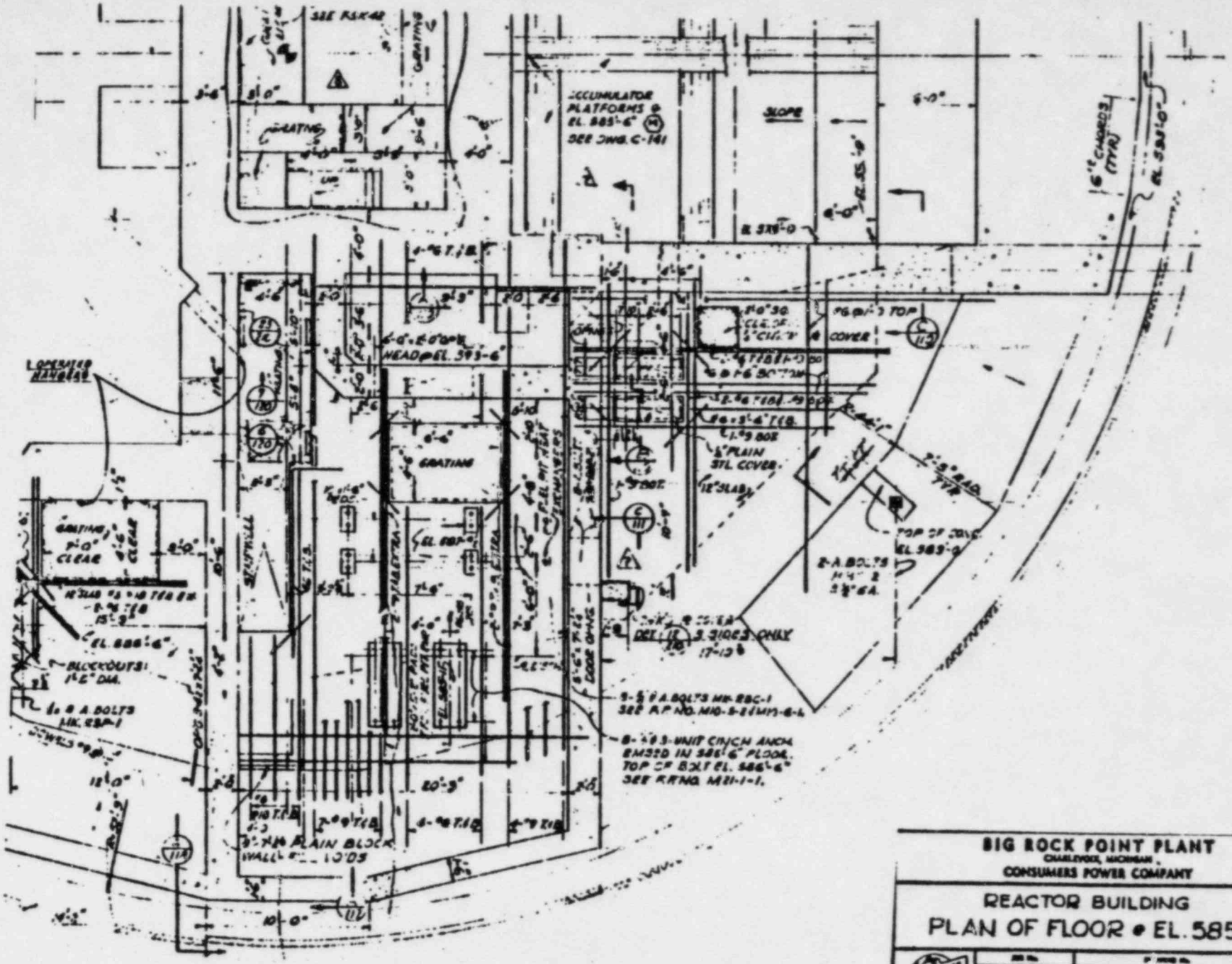

BIG ROCK POINT PLANT CHARLEVOIX, MICHIGAN CONSUMERS POWER COMPANY			
REACTOR BUILDING PLAN OF FLOOR @ EL. 585'-6"			
BECHTEL	3159	FORMER DWG. NO. C-111	8

NEW DWG. NO. 07406-0111 REV. A

1-3-63

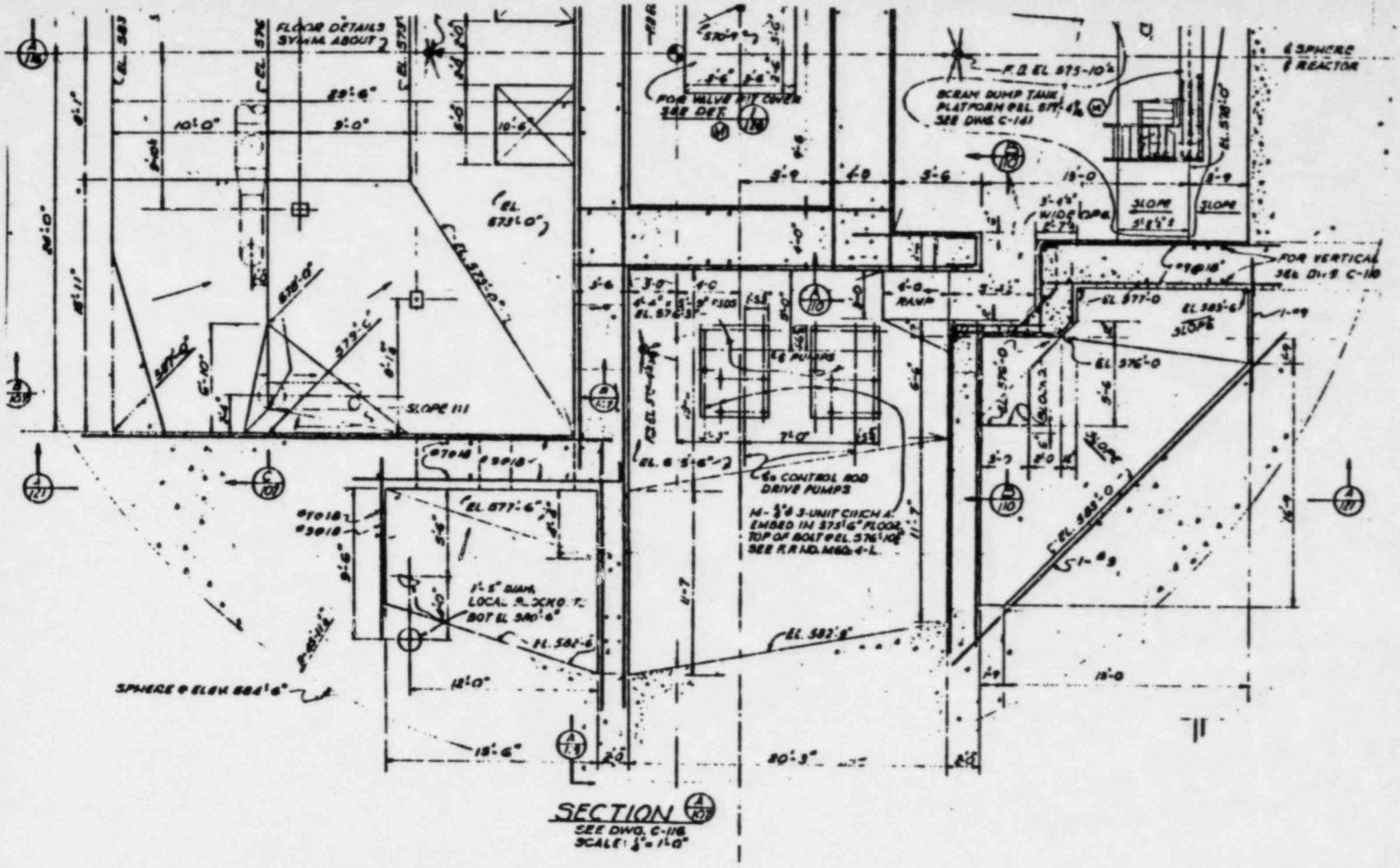

BIG ROCK POINT PLANT CHARLEVOIX, MICHIGAN CONSUMERS POWER COMPANY			
REACTOR BUILDING PLAN OF FLOOR @ EL. 573'-0"			
BECHTEL	3159	FORMER DWG. NO. C-107	6

NEW DWG. NO. 07406201 07 REV. A 11-14-62

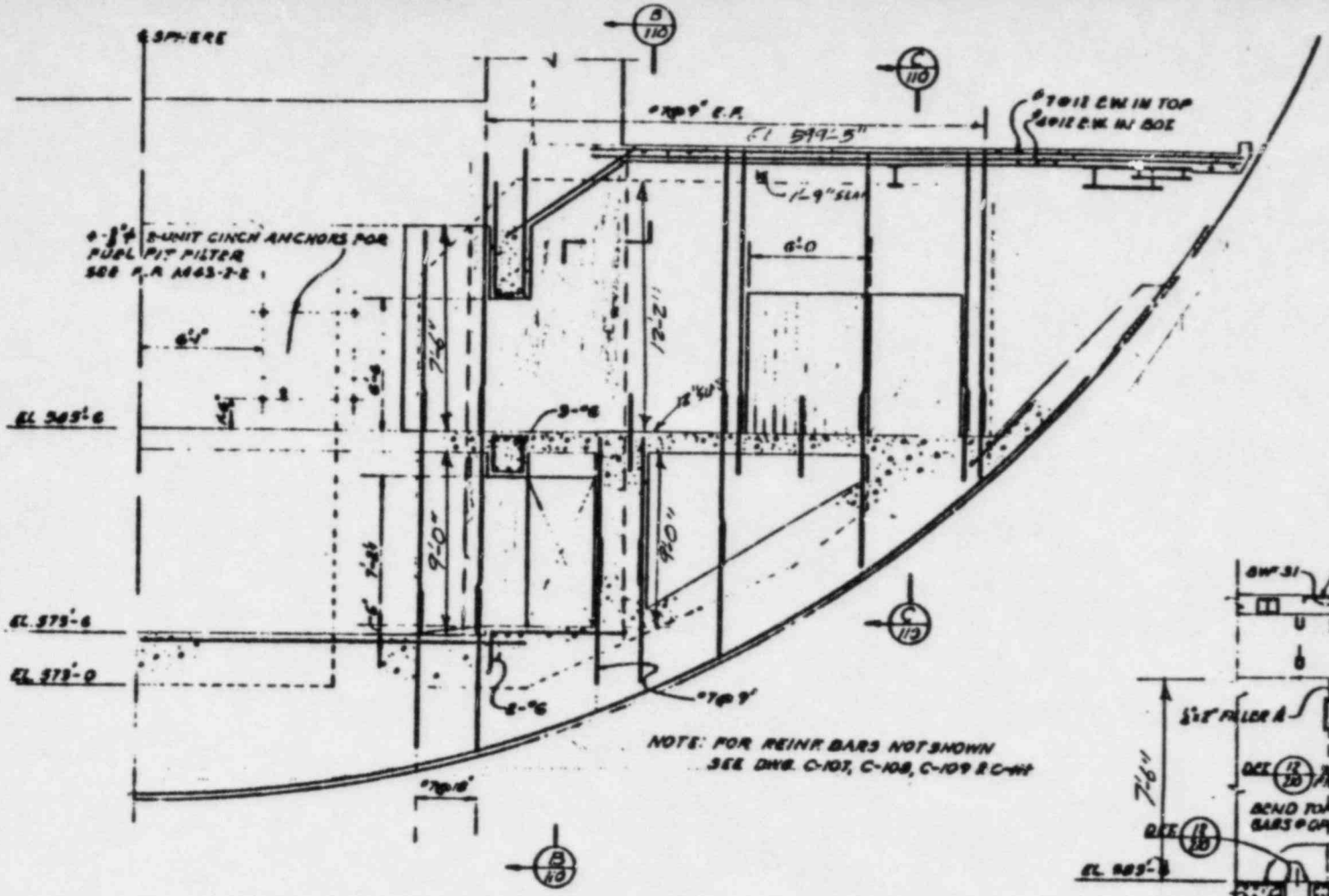

SECTION (A/110)

– SEE DWG. C-113

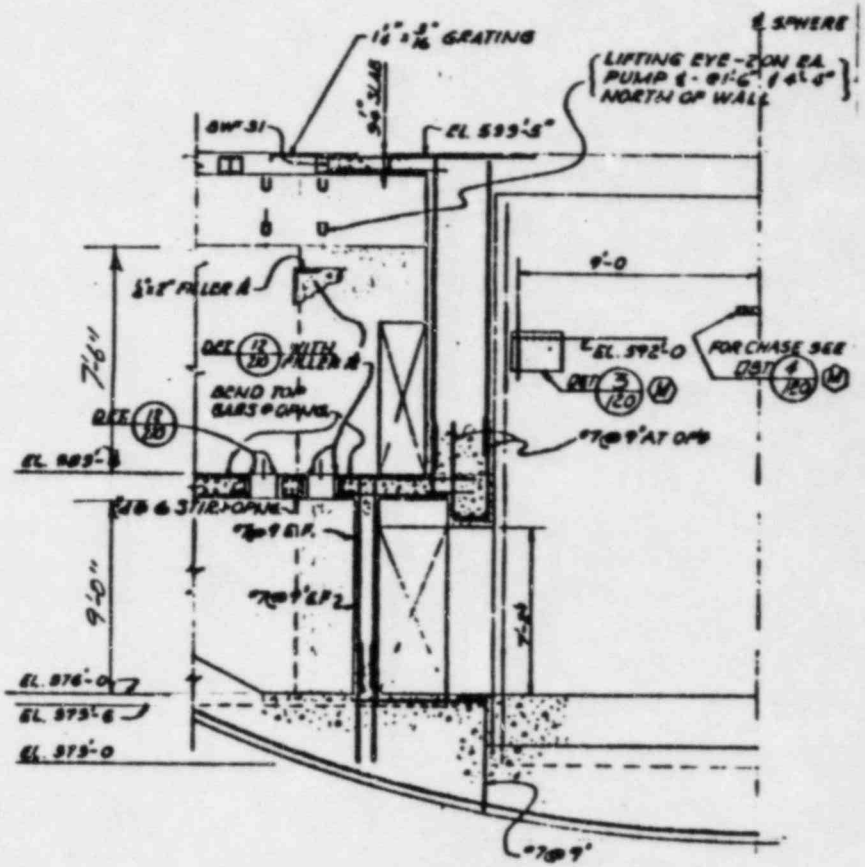

SECTION (B/110)

SEE THIS DWG. & DWG. C-107

BIG ROCK POINT PLANT CHARLEVOIX, MICHIGAN CONSUMERS POWER COMPANY		
REACTOR BUILDING SECTIONS & DETAILS SHT. 1.		
	3159	C-110 FORMER DWG. NO. 5

0740G20110 Rev. A 9/3/68

Consumers Power Company

OPERATING SERVICES DEPARTMENT

Subject: ATTACHMT. I
SHEAR CAPACITY CALCULATION

Sketch No _____ Cal No _____
Project No _____
Originator ETulon
Reviewed by RBQ
Approved by _____
Date 5/16/83 Page 1 of 2

ATTACHMENT I

SHEAR CAPACITY OF KEY

PER ACI 349-80

$V_c = 2\sqrt{f'_c}\, b w d$ (EQ 11-3)

OR

$= (1.9\sqrt{f'_c} + 2{,}500 \rho_w \frac{V_u d}{M_u}) b w d$ (EQ 11-6)

$\leq 3.5\sqrt{f'_c}\, b w d$

where $M_u = V_u \times 3.38''$ } SEE DWG. AT RIGHT

$d = 46.1''$

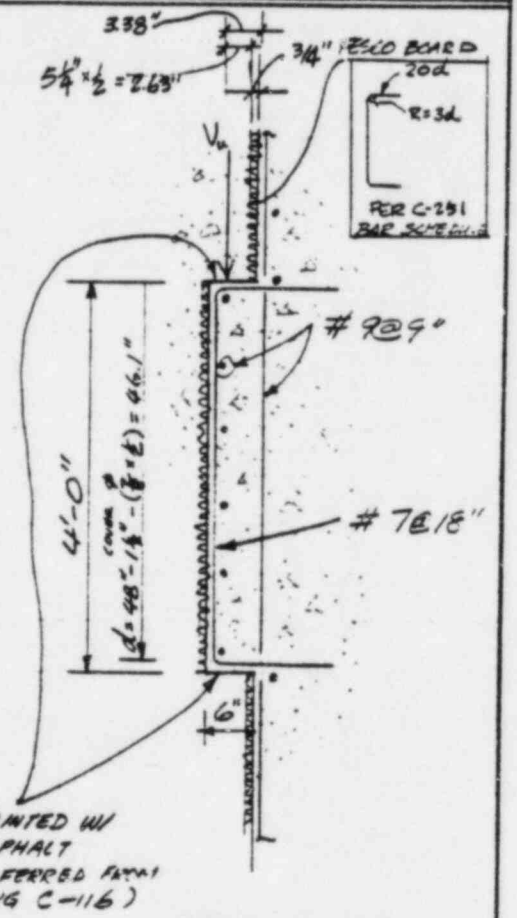

$$\rho_w = \frac{A_s}{b w d} = \frac{0.60\ in^2 / 18\ in}{46.1'' \times 1''/in} = .000723$$

∴ EQ. 11-6 BECOMES

$$V_c = \left(1.9\sqrt{f'_c} + 2{,}500 \times 0.000723 \frac{V_u \times 46.1}{V_u \times 3.38}\right) b w d$$

$= (104.07 + 24.65)\, b w d$

$= 128.72\, b w d$

$= 2.35\sqrt{f'_c}\, b w d \leq 3.5\sqrt{f'_c}\, b w d$ O.K.

$V_n = V_c$

$\phi V_n = \phi V_c = 0.85 V_c$

FOR $V_c = 2\sqrt{f'_c}\, b w d$

$\phi V_n = 0.85 \times 2\sqrt{3000} \times 46.1/in$

$= \underline{4292.5\ \#/in}$ (FROM EQ 11-3)

FOR $V_c = 2.35\sqrt{f'_c}\, b w d$

$\phi V_n = 0.85 \times 128.72 \times 46.1/in$

$= \underline{5043.9\ \#/in}$ (FROM EQ 11-6)

Consumers Power Company

OPERATING SERVICES DEPARTMENT

Subject: ATTACHMT I

Sketch No_____ Cal No_____
Project No_____
Originator E T Wood
Reviewed by RBG
Approved by_____
Date 5/11/83 Page 2 of 2

THE TRIBUTARY LENGTH OF EACH NODE IS AS SHOWN IN FIG. 1. THE CAPACITY OF EACH NODE IS TABULATED BELOW:

NODE	ϕV_n	
	(EQ. 11-3)	(EQ 11-6)
225	244,700 #	287,500 #
226 – 231	128,800 #	151,300 #
232	154,500 # 72,300 # (*)	181,600 # 90,800 # (*)
233	257,600 # 0 (*)	302,600 # 0 (*)

* IF SHEAR KEY DOES NOT EXTEND INTO 45° DOG LEG PORTION OF POOL STRUCTURE.

Consumers Power Company

OPERATING SERVICES DEPARTMENT

Subject: ATTACHMT. II
BEARING WALL CAPACITY

Sketch No _____ Cal No _____
Project No _____
Originator _____
Reviewed by _____
Approved by _____
Date 5/6/93 Page 1 of 1

ATTACHMENT II

BEARING WALL CAPACITY PER ACI 349-80 § 14.2

$$\phi P_{nw} = 0.55(0.70) f_c' A_g \left[1 - \left(\frac{k l_c}{32 h}\right)^2\right]$$

SOUTH BEARING WALL

$l_c = 18'$ (DWG C-121 & FIG 1)
$h = 3'-6"$
$A_g = 4'-0" \times 3'-6" = 3{,}744\ in^2$
$k = 1.0$ (CONSERVATIVELY ASSUMED PIN - P.T.)

$$\phi P_{nw} = 0.55 \times 0.70 \times 3{,}000 \times 3{,}744 \times \left[1 - \left(\frac{18 \times 12}{32 \times 3.5 \times 12}\right)^2\right]$$

$$= \underline{4{,}212{,}600\ \#}$$

NOTE: SLENDERNESS EFFECT IS SMALL

NORTH BEARING WALL
(SEE DWG C-110 & C-107)

$$\phi P_{nw} = 0.55(0.70)\, 3000 \times 144 \times \left\{ \begin{array}{l} 26 \times 3.0 \left[1 - \left(\frac{9.0}{32 \times 2.5}\right)^2\right] \quad .0127 \\ + 1.0 \times 3.0 \left[1 - \left(\frac{12.17}{32 \times 3.0}\right)^2\right] \quad .0161 \\ + 7.0 \times 3.5 \left[1 - \left(\frac{9.0}{32 \times 2.0}\right)^2\right] \quad .0198 \end{array} \right.$$

$$= 0.55(0.70)\, 3{,}000 \times 144 \left(\underbrace{7.41 + 2.95 + 6.86}_{17.22}\right)$$

$$= \underline{2{,}864{,}000\ \#}$$

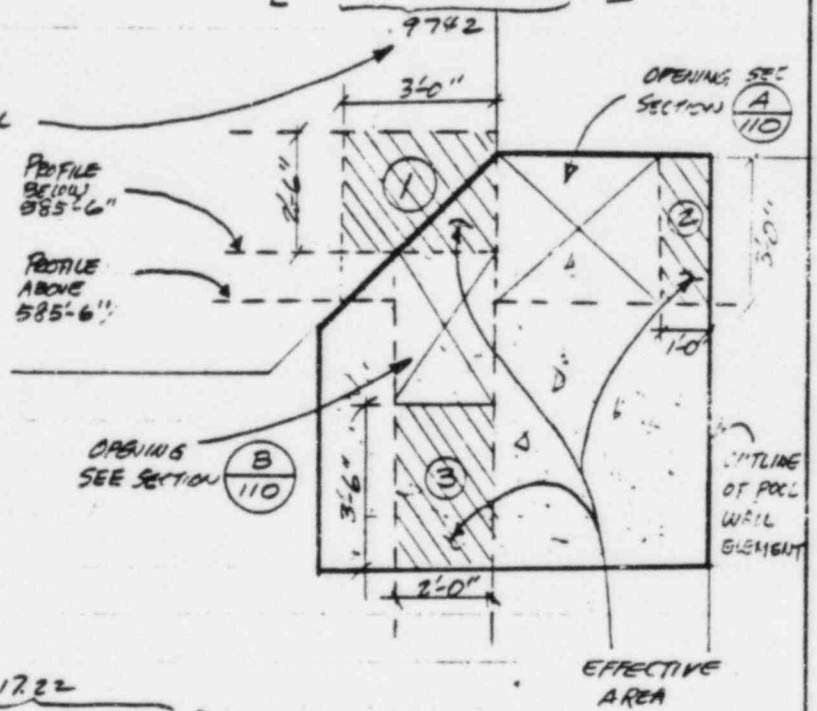

NORTH BEARING WALL PLAN

NUS
of MICHIGAN, INC

May 2, 1983
5803-NUS-393
5803-002

Mr. Rolfe B. Jenkins
Consumers Power Company
1945 West Parnall Road
Jackson, Michigan 49201

Dear Rolfe:

Enclosed please find the reaction forces at the key on the west wall of Big Rock Point spent fuel pool.

Sincerely,

G.J. Antonucci
Project Manager

GJA/lav

Enclosure

cc: NUS of Michigan w/enc.
D. Mullholand w/enc.
P. Arrowsmith
B. Reckman
S. Gerges
File w/enc.
DCC w/enc.

Reaction Forces at the Key on the West wall of Big Rock Point Spent Fuel Pool

Node No.	225	226	227	228	229	230	231	232	233
Dead Load	118000 lbs.	55100 lbs	60200 lbs	68000 lbs	70200 lbs	65600 lbs	57300 lbs	54300 lbs	161000 lbs
Thermal Load (150°F)	77100 lbs	-65000* lbs	-98600* lbs	-100300* lbs	-91700* lbs	-65100* lbs	-42900* lbs	87500 lbs	170000 lbs

(-) sign indivates the force is acting upwards.

Node 225 corresponds to the junction of West and south walls.

Node 233 corresponds to the junction of West and north walls.

There are nine nodes (223 to 233) along the key. The distance between the adjacent nodes is 30 inches.

ENUS CORPORATION

Page ___ of ___

CLIENT CPC-FLP FILE NO 5168-FA- BY MKP DATE 5-3-93

SUBJECT ___ Checked By M.L

Consumers Power Company
Big Rock Point Plant
Docket 50-155

2. EFFECTS OF CRACKING ON DEVELOPMENT LENGTH
June 8, 1983

34 pages

ic0683-0205b142

2. EFFECTS OF CRACKING ON DEVELOPMENT LENGTH

In order to assess the effects of hairline cracks on the development length of rebars running parallel to the cracks, it is necessary to investigate stages of crack pattern, and the sources of bond strength.

It was pointed out in Ref. 1 that, " The cracking pattern was similar for most specimens regardless of the variables in consideration. After the initial flexural and main diagonal cracks had developed, longitudinal splitting began to develop after at least half of the ultimate load had been reached. The longitudinal crack progressed down the center of beam crossing the transverse flexural cracks that had previously formed. After approximately 80% of the ultimate load, short diagonal or stitch cracks began to form on the side of the beam adjacent to the main

diagonal crack at the level of longitudinal steel. At ultimate load, the stitch cracks joined together and the concrete split on a horizontal plane through the reinforcement."

Corresponding to the stages of cracking pattern in the previous paragraph, different sources of bond strength begin to show up. From Ref. 2, the basic features of bond resistance are

(1) for a plain bar, the bond resistance is often thought of as chemical adhesion between concrete and bar surface, and

(2) Once the adhesion is broken up, further bond can be developed by means of friction and by the wedge action of small dislodged sand particles between the bar and the surrounding concrete. It is noted that

when plain round bars are subjected to standard load tests, failure occurs when the adhesion and frictional resistance are overcome, and the bars usually pull out from the encasing concrete. But for deformed bars, other sources of bond resistance begin to show up.

(3) Bearing of steel bar ribs against the concrete. The action-reaction between the steel bar ribs and concrete can be best pictured by a figure from Ref. 4, which is shown on next page. It is noted that in the internally cracked zone, there are numerous internal cracks, some of which will propagate to the external surface of the concrete to form the major primary cracks which run perpendicular to the rebars.

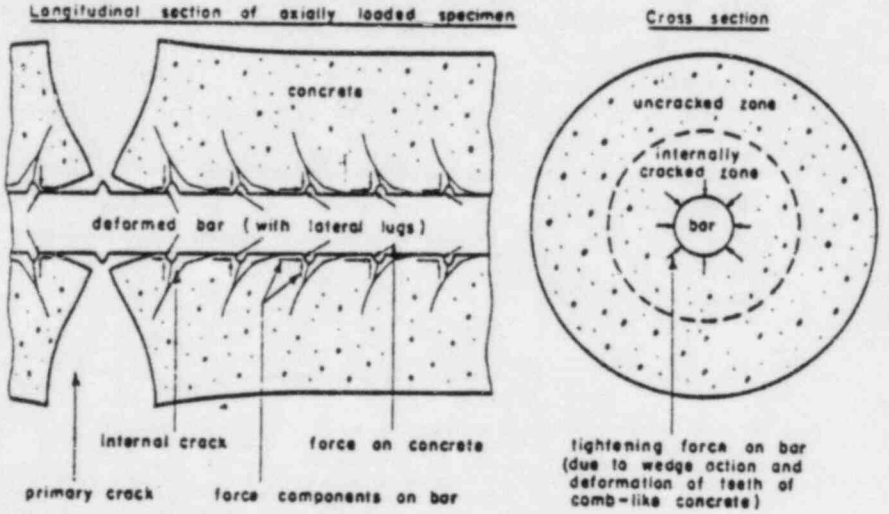

Fig. 3--Deformation of concrete around reinforcing bars (after formation of internal cracks)

(4) when the concrete separates itself from around a bar at a primary crack, the circumference of the concrete surface, previously in contact with the bar, increases; hence circumferential tensile stresses are induced. The stresses can lead to longitudinal splitting cracks.

In Ref. 3, it is written, " Although splitting is the usual bond failure mode, it is noted than an initial splitting crack on one face of a beam does not constitute failure. Progressive splitting is the first sign of bond distress and may be considered the usual cause of bond collapse." This is in agreement with the test done in Ref. 1. Test Results in Ref. 1 showed that the longitudinal splitting began to develop after at least half of the ultimate load had been reached. And the longitudinal crack started to progress after approximately 80% of the ultimate load.

In conclusion, the hairline cracks caused

by the flexural bending in one direction do not indicate an impending bond failure of rebars running parallel to the hairline cracks, and it is estimated the bearing of steel rebar ribs against concrete contributes at least half of the bond strength.

However, for the following calculations, we will conservatively assume that the bond strength between steel and concrete will be zero wherever a hairline crack appears. From Ref. 5, the space between cracks was actually measured by Beeby in the tests as 1.33 h_o, where h_o is the crack height.

The crack will penetrate nearly to the neutral axis, and its height may be calculated by standard elastic theory using the steel content and the modular ratio. In the analysis of the spent fuel pool, it is noted that $h_o = 48" - 5.95" = 42.05"$ for the north wall (see page 2-75 of analysis report). h_o is about 87% of total wall thickness. The crack spacing for a wall of thickness h will be

$1.33 h_o = 1.33 \times 0.87 \times h = 1.165 h$

Substitute $h = 48"$, we obtain crack spacing $= 56"$.

The rebar in this region is #7@12". The percentage of steel discredited for development evaluation will be $12/56 \times 100\% = 21.4\%$

Then l_d required should be revised to

$$l_d = 12.5 \times \frac{1}{(1 - 0.214)} = 15.9"$$

l_d provided $= 30"$

∴ SAFETY MARGIN = 1.88, which is cut down from 2.40 (see page 13-75 of analysis report.)

This procedure shall be performed for every critical spot to check for the adequacy of development length.

WEST WALL

a) At West wall and floor intersection

From Page 13-9 of analysis report, wall cracked along the vertical reinforcement, # 7 @ 12".

crack spacing = 1.33 h_o

$\approx 1.33 (0.87 h)$

$= 1.165 h$ ($h = 48"$)

$= 56"$

Percentage of steel discredited for development evaluation will be $12/56 \times 100\% = 21.4\%$

l_d (Revised) $= 5.14 \times \frac{1}{1-0.214} = 6.5"$

But, never less than 12",

l_d revised = 12"

l_d provided = 66"

Safety margin = 5.5

(b) West Wall, the splice above the shear key.

the wall in this region also cracks along the vertical splice. Similar to (a),

$$\text{Splice length (Revised)} = 17.77 \times \frac{1}{1-0.214}$$

$$= 22.6''$$

splice length provided = 26.25"

safety margin = 1.16

(c) West Wall, splice at 10' above floor

As stated in the analysis report, page 13-63, the splice is located in the compression side and is not included when calculating moment capacity. The adequacy of splice is not critical.

d) l_d at south end of west wall.

The wall cracked along the horizontal reinforcement, # 9 @ 10".

crack spacing $= 1.33(h_o)$
$\approx 56"$

percentage of reinforcement discredited will be $10/56 \times 100\% = 17.8\%$

l_d (Revised) $= 10.49 \times \frac{1}{1-0.178} = 12.8"$

l_d provided $= 36"$

∴ safety margin $= 2.82$ o.k

e) l_d at North end of West Wall

Similar to d)

l_d (Revised) $= 23.62 \times \frac{1}{1-0.178} = 28.7"$

l_d provided $= 30'$

safety margin $= 1.04$ o.k.

North Wall

a) At north wall and floor intersection.

the wall cracked along the vertical reinforcement at elements 63 & 64. Wall thickness is 81".

Rebar is #7 @ 12" at outer face.

crack spacing = $1.33 \times h_o$

$\simeq 1.33 \times (0.875\, h)$

$= 1.165\, h$

$= 94"$

percentage of Rebars to be discredited

$= 12/94 \times 100\% = 12.7\%$

l_d (Revised) $= 13.67 \times \frac{1}{1-0.127} = 15.6"$

l_d provided $= 30"$

Safety factor = 1.92 ok.

The splice right above the intersection

splice length (Revised) $= 17.77 \times \frac{1}{1-0.127} = 20.4"$

splice length provided = 30"

Safety margin = 1.47 ok.

North Wall

b) splice at 10' above the floor

There is no need to check the adequacy of this splice since the concrete does not crack in this region and the contribution of steel is ignored entirely as explained in the analysis report.

c) l_d at where the thickness of wall reduces, i.e, 8'-6" from top of wall.

From page 13-9 of analysis report, the wall cracks along the vertical reinforcement in this region. Wall thickness = 48"

crack spacing $\approx 1.165 \times 48 = 56$"

percentage of reinforcement discredited for development evaluation will be $13/56 \times 100\% = 21.4\%$

l_d (Revised) $= 12.5 \times \frac{1}{1-0.214} = 15.9$"

l_d provided = 30"

Safety margin = 1.88 o.k.

NORTH WALL

d) splice at where the thickness of wall reduces.

From page 13-9, the wall does not crack in this region, no revision is needed.

The safety margin remains to be 1.69

NORTH WALL

e) l_d at WEST Wall END.

The wall cracks at element 17.

Wall thickness = 48"

crack spacing $\approx 1.165h = 56$"

Rebar = #9 @ 10"

percentage of reinforcement discredited $= \frac{10}{56} \times 100\% = 17.9\%$

l_d revised $= 6.24 \times \frac{1}{1-0.179} = 7.60$"

But never less than 12"

$\therefore$ l_d revised = 12"

l_d Provided = 42"

Safety margin = 3.5

NORTH WALL

f) ld at East Wall End

For the Top 8'-6", the wall cracks at element 24. The wall thickness is 48",

crack spacing $= 1.165 \times 48 = 56$"

Rebar is #9@10",

percentage of rebar discredited $= \frac{10}{56} \times 100\% = 17.8\%$

ld (Revised) $= 6.19 \times \frac{1}{1-0.178}$

$= 7.53$"

But never less than 12"

$\therefore$ ld (Revised) = 12"

ld (Provided) = 18"

Safety margin = 1.5

For the rest of the wall, the wall thickness is 81".

crack spacing $= 1.165 \times 81 = 94$"

Rebar = #9 @ 10"

percentage of rebar discredited $= 10/94 \times 100\% = 10.6\%$

ld (revised) $= 23.98 \times \frac{1}{1-0.106} = 26.82$

ld provided = 30"

Safety margin = 1.12. OK.

EAST WALL

a) At the wall and floor intersection

Since the wall does not crack in this region, no revision is needed.

b) Splice at 10' above the floor

The wall cracks along the splice in this region. Wall thickness is 78".

crack spacing = $1.165 \times 78 = 90.8$"

Rebar: # 7 @ 6"

percentage of steel discredited is $\frac{6}{90.8} \times 100\% = 6.6\%$.

Splice length (Revised) $= 23.24 \times \frac{1}{1-0.066}$

$= 24.88$"

Splice provided $= 30$"

Safety margin $= 1.21$.

East Wall

c) l_d at 8'-6" From TOP OF WALL

The wall cracks along the vertical reinforcement in this region. Wall thickness is 78"

Crack spacing = 1.165 × 78 = 90.8

Rebar is #7 @ 12"

percentage of steel discredited will be $\frac{12}{90.8} \times 100\% = 13.2\%$

l_d (Revised) = $8.76 \times \frac{1}{1-0.132} = 10.09$"

But not less than 12"

∴ l_d revised = 12"

l_d provided = 30"

Safety margin = 2.5 O.K.

d) Splice at 8'-6" From top of wall

The wall cracks along the vertical splices.

percentage of steel discredited will be 13.2%

Splice length revised = $17.77 \times \frac{1}{1-0.132} = 20.47$"

Splice provided = 30"

Safety margin = 1.46

East Wall

e) ld at south wall end

For the top 8'-6" of the wall, the wall cracks at element 24 along the horizontal reinforcement.

Wall thickness = 24"

crack spacing = 1.165 × 24 = 27.9"

Rebar = #9 @ 10"

percentage of steel discredited = $\frac{10}{27.9} \times 100\% = 35.7\%$

ld Revised = $5.06 \times \frac{1}{1-0.357} = 7.9$"

But never less than 12"

ld provided = 18"

Safety margin = 1.5

For the rest of the wall, it doesn't crack, no revision is needed. The safety margin remains as 2.0.

EAST WALL

f) l_d AT north wall end

For the top 8'-6", the wall cracks along the horizontal reinforcement.

Wall thickness = 24"

crack spacing = $24 \times 1.165 = 27.9$"

Rebar : #9 @ 10"

percentage of steel discredited = $\frac{10}{27.9} \times 100\% = 35.8\%$

l_d (Revised) = $4.12 \times \frac{1}{1-0.358} = 6.4$"

But never less than 12"

l_d provided = 42"

Safety Margin = 3.5 o.k

For the bottom portion of east wall,

Wall thickness = 78"

Crack spacing = $1.165 \times 78 = 90.8$"

Rebar : #9 @ 10"

percentage of steel discredited = $\frac{10}{90.8} \times 100\% = 11.0\%$

East Wall

l_d Revised $= 22.78 \times \frac{1}{1-0.11}$

$= 25.6"$

l_d provided $= 30"$

Safety Margin $= 1.17$

South Wall

a) l_d AT floor and Wall intersection

From page 13-10, the concrete in the region cracks along the vertical reinforcement.

Wall thickness varies from 42" to 69".

Use minimum wall thickness. 42".

Crack spacing = $1.165 \times 42 = 49$"

Rebar used : #7 @ 12"

percentage of rebar discredited : $\frac{12}{49} \times 100\% = 24.5\%$

l_d Revised $= 13.67 \times \frac{1}{1-0.245} = 18.1$"

l_d provided = 30"

Safety Margin = 1.66. ok.

Check splice right above the intersection.

splice length revised $= 17.77 \times \frac{1}{1-0.245} = 23.5$"

Splice length provided = 30"

Safety Margin = 1.27

South Wall

b) Splice at 10' above the floor

The contribution of splice is entirely neglected in the analysis report. No revision is needed

c) ld at 7'-0" from top of wall

The wall cracks along the vertical reinforcement.

Use minimum wall thickness, 42".

Crack spacing = $1.165 \times 42 = 49$"

Rebar used = # 7 @12".

percentage of rebar discredited = $\frac{12}{49} \times 100\% = 24.5\%$

ld Revised = $5.42 \times \frac{1}{1-0.245} = 7.18$"

But never less than 12"

ld provided = 30"

Safety margin = 2.5

South Wall

d) Splice at 7'-0" from top

percentage of steel discredited is the same as c)

Splice length revised $= 17.77 \times \frac{1}{1-0.245} = 23.54"$

Splice length provided = 30"

Safety Margin = 1.27 OK.

e) ld at east wall end:
For the bottom portion of wall, the wall cracks along the horizontal rebars in this region. Wall thickness = 69"

crack spacing $= 1.165 \times 69$
$= 80.4"$

Rebar used: #9 @ 10"

percentage of steel discredited $= \frac{10}{80.4} \times 100\% = 12.4\%$

ld revised $= 31.90 \times \frac{1}{1-0.124} = 36.4"$

ld provided = 66"

safety margin = 1.81

South Wall

For the top 7'-0" of wall, the wall also cracks along the horizontal reinforcement.

The wall thickness = 24"

crack spacing = 1.165 × 24 = 28"

rebar used = #9 @ 10"

percentage of steel discredited = $\frac{10}{28} \times 100\% = 35.7\%$

l_d Revised = $4.76 \times \frac{1}{1-0.357} = 7.4$"

But never less than 12"

l_d provided = 18 INCH

Safety margin = 1.5

f) Splice at 5'-6" from east wall.

For the top 7'-0", the thickness of wall is 2'-0" straight, there is no splice to be checked.

For the remainder of the wall, the wall cracks along the horizontal reinforcement at

SOUTH WALL

element 50 only.

Wall thickness is 69".

Crack spacing $1.165 \times 69 = 80.4$"

Rebar used = #9 @ 10"

Percentage of Rebar discredited for bond evaluation will be $(10/80.4) \times 100\% = 12.4\%$

Splice length required $= 28.25 \times \frac{1}{1-0.124}$

$= 32.25$"

Splice provided = 30"

Safety margin = 0.93*

* Although the safety margin is less than one, it is considered satisfactory because this occurs at only one of the 8 elements. Moreover, the concrete of the 3 elements above element 50 do not crack in the vertical

South Wall

direction, i.e., the stress in the rebar is very small, and the element below it has adequate splice length. Thus, this is a local phenomenon. Furthermore, the 50% of bond strength contributed by the bearing of steel rebar ribs on concrete has been conservatively neglected in this calculation.

SOUTH WALL

g) Splice at 7'-6" From West Wall

The wall cracks along the horizontal reinforcement.

Wall thickness = 42"

crack spacing = $1.165 \times 42 = 49$"

Rebar used = #9 @ 10"

percentage discredited = $\frac{10}{49} \times 100\% = 20.4\%$

Splice length revised = $54.23 \times \frac{1}{1-0.204}$

$= 68.13$"

Splice length provided = 60"

Safety margin = 0.88

Using the equation given by Reference 19 of analysis file, the splice length required can be calculated as follows:

Applicable modified factors

1, Grade 40 Reinforcement 0.6

2, Top Reinforcement 1.3

$C_b = 6"$ MIN.

$C_s = 10" - 1.128" = 8.872"$

$C = C_b = 6"$

$d_b = 1.128.$

$C/d_b = \frac{6}{1.128} = 5.31 > 2.5$

$\therefore C/d_b = 2.5$ (maximum allowed)

$$l_s = \frac{1}{1-0.204} \times 0.6 \times 1.3 \times \frac{10200 \times 1.128}{\sqrt{3000}\,(1 + 2.5 \times 2.5 + 0) \times 0.8}$$

$= 35.0"$

l_s provided $= 60"$

Safety margin $= 1.69$ O.K.

h) l_d at West Wall end

The wall cracks along the horizontal reinforcement. Wall thickness $= 42"$

crack spacing $= 1.165 \times 42 = 49"$

Rebar : #9 @ 10"

percentage of Rebar discredited $= 20.4\%$.

$$l_d \text{ (Revised)} = 7.42 \times \frac{1}{1-0.204}$$

$$= 9.32'$$

But, never less than 12".

l_d provided = 42"

Safety margin = 3.50 O.K.

FLOOR

a) l_d AT East Wall End.

From page 13-10 OF analysis report, it can be seen that the Floor does not crack along the reinforcement. Therefore, no revision is needed

b) l_d at West Wall End

The floor cracks along the reinforcement at elements 4, 5 and 6. Floor slab thickness is 72".

crack spacing $= 1.165 \times 72 = 83.8"$

For top bars : #7@12" + #7@12"

percentage of discredited rebars :

$$\frac{6"}{83.8} \times 100\% = 7.2\%$$

$$l_d \text{ (Revised)} = 19.14 \times \frac{1}{1-0.072} = 20.63"$$

FLOOR

l_d provided = 36"

Safety Margin = 1.74 O.K.

For bottom bars #11 @ 12"

percentage of discredited rebars = $\frac{12}{83.8} \times 100\% = 14.3\%$

l_d (Revised) = $35.55 \times \frac{1}{1-0.143} = 41.5$"

l_d (provided) = 42"

Safety Margin = 1.01 O.K.

c) l_d at South Wall End

The floor cracks at element 26. Same percentages of discredited rebars as b) will be applied.

For top Bars:

l_d (revised) = $.053 \times \frac{1}{1-0.072} = .06$"

FLOOR

But never less than 12".

l_d (provided) = 36"

Safety margin = 3

For bottom bars =

$$l_d \text{ (Revised)} = 0.41 \times \frac{}{1-0.143} = 0.48"$$

But never less than 12".

l_d provided = 18"

Safety margin = 1.5 o.k.

d) l_d at North Wall End

The floor cracks at element 12. This case is the same as c). Same Safety Margins apply.

IN SUMMARY, THE REVISED SAFETY MARGINS OF DEVELOPMENT LENGTH TAKING INTO ACCOUNT THE EFFECTS OF CRACKS ALONG THE MAIN REBARS AT EACH LOCATION IS TABULATED BELOW.

WEST WALL		NORTH WALL		EAST WALL		SOUTH WALL		POOL FLOOR	
LOCATION	SAFETY MARGIN	LOCATION	SAFETY MARGIN	LOCATION	SAFETY MARGIN	LOCATION	SAFETY MARGIN	LOCATION	SAFETY MARGIN
a)	5.5	a)	1.92 1.47	a)	4.39 1.69	a)	1.66 1.27	a)	1.88 1.97
b)	1.16	b)	N/A	b)	1.21	b)	N/A	b)	1.74 1.01
c)	N/A	c)	1.88	c)	2.5	c)	2.5	c)	3.0 1.5
d)	2.82	d)	1.69	d)	1.46	d)	1.27	d)	3.0 1.5
e)	1.04	e)	3.5	e)	1.50 2.0	e)	1.5 1.81		
		f)	1.50 1.12	f)	3.5 1.17	f)	0.93*		
						g)	1.69		
						h)	3.50		

* SEE P. 25 FOR DISCUSSION

Ref 1: Raymond E. Untraner, George E. WARREN, "stress Development of Tension Steel in Beams", ACI Journal, August 1977

Ref 2: R. Park and T. Paulay, "Reinforced Concrete Structures," John Wiley & Sons, 1975

Ref. 3: Chu-kia Wang and Charles G. Salmon, "Reinforced Concrete Design," 3rd Ed. Harper & Row Publisher.

Ref 4: Saeed M. Mirza and Jules Houde, "Study of Bond Stress-Slip Relationships in Reinforced Concrete", ACI Journal, January 1979.

Ref 5: R. Park and Gamble, "Reinforced Concrete Slabs" John Wiley & Sons, 1980

Consumers Power Company
Big Rock Point Plant
Docket 50-155

3. ORTHOTROPIC PLATE ASSUMPTIONS
June 8, 1983

10 pages

3. Orthotropic Plate Assumptions:

The strain-stress relations for an orthotropic plate can be written as: [Ref: J.E. Aston and J.M. Whitney, "Theory of Laminated Plates," Technomic Publishing Co., 1970; and R.M. Jones, "Mechanics of Composite Materials", McGraw Hill, 1975]

$$\varepsilon_x = \frac{\sigma_x}{E_x} - \frac{\nu_y \sigma_y}{E_y}$$

$$\varepsilon_y = -\frac{\nu_x \sigma_x}{E_x} + \frac{\sigma_y}{E_y}$$

$$\gamma_{xy} = \frac{\tau_{xy}}{G_{xy}}$$

or

$$\begin{bmatrix} \varepsilon_x \\ \varepsilon_y \\ \gamma_{xy} \end{bmatrix} = \begin{bmatrix} \frac{1}{E_x} & -\frac{\nu_y}{E_y} & 0 \\ -\frac{\nu_x}{E_x} & \frac{1}{E_y} & 0 \\ 0 & 0 & \frac{1}{G_{xy}} \end{bmatrix} \begin{bmatrix} \sigma_x \\ \sigma_y \\ \tau_{xy} \end{bmatrix} \quad \text{— Eq.(1)}$$

Where, ε_x, ε_y, γ_{xy} are the strain components,

σ_x, σ_y, τ_{xy} are the stress components

E_x is the elastic modulus in x-direction

E_y is the elastic modulus in the Y-direction

ν_y is the Poisson's ratio relating the strain ε_x with the stress σ_y

ν_x is the Poisson's ratio relating the strain ε_y with the stress σ_x

G_{xy} is the shear modulus for x-Y directions.

The relation between ν_x and ν_y is given by

$$\frac{\nu_x}{E_x} = \frac{\nu_y}{E_y}$$

Therefore, the relations expressed in Eq. (1) can also be written as

$$\begin{bmatrix} \varepsilon_x \\ \varepsilon_y \\ \gamma_{xy} \end{bmatrix} = \begin{bmatrix} \frac{1}{E_x} & -\frac{\nu_y}{E_y} & 0 \\ -\frac{\nu_y}{E_y} & \frac{1}{E_y} & 0 \\ 0 & 0 & \frac{1}{G_{xy}} \end{bmatrix} \begin{bmatrix} \sigma_x \\ \sigma_y \\ \tau_{xy} \end{bmatrix} \qquad \text{Eq. (1a)}$$

which is the form used in ANSYS.

The shear modulus G_{xy} for isotropic case is given by

$$G_{xy} = \frac{E}{2(1+\nu)} \qquad \text{Eq. (2)}$$

For orthotropic materials no such relation exists. Some form of empirical relation between G_{xy}, E_x, E_y, ν_x and ν_y has to be used for the computation purposes. Based on an analogy with the Eq. (2), ANSYS uses an empirical relation of the form

$$G_{xy} = \frac{E_x E_y}{E_x + E_y + \nu_y E_x + \nu_x E_y}$$

or

$$G_{xy} = \frac{E_x E_y}{E_x + E_y + 2\nu_y E_x}$$

The degree of accuracy with this expression is as good as that obtained with any other empirical relation since the actual value for G_{xy} for cracked concrete is not known exactly.

The ANSYS input consists of E_x, E_y and ν_y which are read as EX, EY and NUXY.

The relations between stresses and strains, from inverting Eq. 1, can be written as

$$\begin{bmatrix} \sigma_x \\ \sigma_y \\ \tau_{xy} \end{bmatrix} = \frac{1}{(1-\nu_x \nu_y)} \begin{bmatrix} E_x & \nu_y E_x & 0 \\ \nu_x E_y & E_y & 0 \\ 0 & 0 & (1-\nu_x \nu_y) G_{xy} \end{bmatrix} \begin{bmatrix} \varepsilon_x \\ \varepsilon_y \\ \gamma_{xy} \end{bmatrix}$$

Extending these equations to plate theory, the relation

between moments, curvatures and twist can be written as

$$\begin{bmatrix} M_x \\ M_y \\ M_{xy} \end{bmatrix} = \frac{h^3}{12(1-\nu_x\nu_y)} \begin{bmatrix} E_x & \nu_y E_x & 0 \\ \nu_x E_y & E_y & 0 \\ 0 & 0 & (1-\nu_x\nu_y)\,G_{xy} \end{bmatrix} \begin{bmatrix} -\partial^2 W/\partial x^2 \\ -\partial^2 W/\partial y^2 \\ 2\,\dfrac{\partial^2 W}{\partial x \partial y} \end{bmatrix}$$

Substituting M_x, M_y and M_{xy} into the plate equilibrium equation

$$\frac{\partial^2 M_x}{\partial x^2} + \frac{\partial^2 M_x}{\partial y^2} - 2\,\frac{\partial^2 M_{xy}}{\partial x \partial y} = -q$$

gives

$$D_x \frac{\partial^4 w}{\partial x^4} + D_y \frac{\partial^4 w}{\partial y^4} + \frac{\partial^4 w}{\partial x^2 \partial y^2}\left(\nu_y D_x + \nu_x D_y + 4 D_{xy}\right) = q$$

where $D_{xy} = \dfrac{G_{xy} h^3}{12}$, $D_x = \dfrac{E_x h^3}{12(1-\nu_x\nu_y)}$, $D_y = \dfrac{E_y h^3}{12(1-\nu_x\nu_y)}$

Considering that $\nu_x D_y = \nu_y D_x$, the orthotropic plate equation can be written as

$$D_x \frac{\partial^4 w}{\partial x^4} + 2\left(\nu_y D_x + 2 D_{xy}\right) \frac{\partial^4 w}{\partial x^2 \partial y^2} + D_y \frac{\partial^4 w}{\partial y^4} = q$$

For application to the present case, for a section that is not cracked in the x and Y directions, E_x and E_y are equal to .. E_c and $\nu_c = 0.17$. For a section cracked only in the x direction, $E_x = E_c I_{cr}/I_g$, $E_y = E_c$ and $\nu_y = \nu_c$ in this case ν_x will be very small and given by $\nu_x = \nu_c E_x / E_c$. For a section cracked only in the Y direction, $E_x = E_c$, $E_y = E_c I_{cr}/I_g$ and $\nu_x = \nu_c$. For this case $\nu_y = E_y \nu_c / E_c$ is a very small number. For a section cracked both in the x and Y directions, $E_x = E_c I_{crx}/I_g$, $E_y = E_c I_{cry}/I_g$ and ν_x and ν_y are very small numbers and the values (which may approximately be) given by $\nu_x = E_x \nu_c / E_c$ and $\nu_y = E_y \nu_c / E_c$ can be used. The relationship $\nu_x E_y = \nu_y E_x$ will still be maintained. The manner in which the material properties were input into ANSYS overestimates ν_x (and hence '$\nu_x D_y + 2D_{xy}$' term) for elements cracked in Y-direction only. The effect of this approximation is discussed in the following.

Consider a simply supported rectangular plate

under uniform loading. The deflection at the center of the plate is given by (only one term solution is used):

$$w_o = \frac{16 q_o}{\pi^6} \left[\frac{1}{\frac{D_x}{a^4} + \frac{2(\nu_y D_x + 2D_{xy})}{a^2 b^2} + \frac{D_y}{b^4}} \right]$$

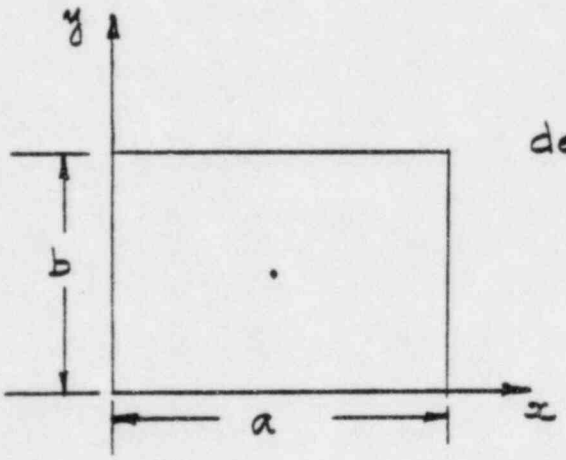

The values of w_o (central deflection) calculated for all the cases and compared with the value based on correct input for Poisson's ratio are summarized in the tables on the following pages. The value of q is taken as 1 psi, a as 312 in. and b as 240 in.

The deflection using the material property input to ANSYS is the same as the correct value for elements that are either uncracked or cracked due to bending moment M_x. For elements cracked in both

Element Description and ANSYS Material Property Number	Central Deflection (in.)	
	From ANSYS Input	Actual Value
West Wall Cracked - X (2)	0.1406×10^{-2}	0.1406×10^{-2}
West Wall Cracked - Y (3)	0.1714×10^{-2}	0.3095×10^{-2}
West Wall Cracked - XY (4)	0.7178×10^{-2}	0.7609×10^{-2}
North Wall top portion Cracked-X (5)	0.1557×10^{-2}	0.1557×10^{-2}
North Wall top portion Cracked-Y (6)	0.1714×10^{-2}	0.3095×10^{-2}
North wall top portion Cracked - XY (7)	0.8887×10^{-2}	0.9169×10^{-2}
N. Wall Bottom Portion Cracked - X (8)	0.3177×10^{-3}	0.3177×10^{-3}
N. Wall Bottom Portion Cracked - Y (9)	0.2854×10^{-3}	0.7477×10^{-3}
N. Wall Bottom Portion Cracked - XY (10)	0.2226×10^{-3}	0.2362×10^{-2}
E. Wall top portion Cracked - X (11)	0.1039×10^{-1}	0.1039×10^{-1}
E. Wall top portion Cracked - Y (12)	0.1422×10^{-1}	0.2059×10^{-1}
E. Wall top portion Cracked - XY (13)	0.3975×10^{-1}	0.4181×10^{-1}
E. Wall Bottom Portion Cracked - X (14)	0.3520×10^{-3}	0.3520×10^{-3}
E. Wall Bottom Portion Cracked - Y (15)	0.3286×10^{-3}	0.8288×10^{-3}
E. Wall Bottom Portion Cracked - XY (16)	0.2389×10^{-2}	0.2541×10^{-2}
S. Wall top Portion Cracked - X (17)	0.1039×10^{-1}	0.1039×10^{-1}

Element Description and ANSYS Material Property Number	Central Deflection (in.)	
	From ANSYS input	Actual Value
S. Wall top portion Cracked-Y (18)	0.1422×10^{-1}	0.2059×10^{-1}
S. Wall top portion Cracked-XY (19)	0.3975×10^{-1}	0.4181×10^{-1}
S. Wall bottom portion (h = 69 in.) Cracked-X (20)	0.5028×10^{-3}	0.5028×10^{-3}
S. Wall bottom portion (h = 69 in.) Cracked-Y (21)	0.5113×10^{-3}	0.1157×10^{-2}
S. Wall bottom portion (h = 69 in.) Cracked-XY (22)	0.3186×10^{-2}	0.3377×10^{-2}
S. Wall bottom portion (Avg. h = 65.63 in.) Cracked-X (23)	0.5761×10^{-3}	0.5761×10^{-3}
S. Wall bottom portion (Avg. h = 65.63 in.) Cracked-Y (24)	0.6226×10^{-3}	0.1306×10^{-2}
S. Wall bottom portion (Avg. h = 65.63 in.) Cracked-XY (25)	0.3433×10^{-2}	0.3635×10^{-2}
S. Wall bottom portion (Avg. h = 58.88 in.) Cracked-X (26)	0.7854×10^{-3}	0.7854×10^{-3}
S. Wall bottom portion (Avg. h = 58.88 in.) Cracked-Y (27)	0.8970×10^{-3}	0.1749×10^{-2}
S. Wall bottom portion (Avg. h = 58.88 in.) Cracked-XY (28)	0.4383×10^{-2}	0.4637×10^{-2}
S. Wall bottom portion (Avg. h = 52.13 in.) Cracked-X (29)	0.1113×10^{-2}	0.1113×10^{-2}
S. Wall bottom portion (Avg. h = 52.13 in.) Cracked-Y (30)	0.1335×10^{-2}	0.2428×10^{-2}
S. Wall bottom portion (Avg. h = 52.13 in.) Cracked-XY (31)	0.5793×10^{-2}	0.6118×10^{-2}
S. Wall bottom portion (Avg. h = 45.38 in.) Cracked-X (32)	0.1656×10^{-2}	0.1656×10^{-2}
S. Wall bottom portion (Avg. h = 45.38 in.) Cracked-Y (33)	0.2071×10^{-2}	0.3523×10^{-2}

Element Description and ANSYS Material Property Number	Central Deflection (in.)	
	From ANSYS input	Actual Value
S. Wall bottom portion (Avg. h = 45.38 in) Cracked-XY (34)	0.7995×10^{-2}	0.8429×10^{-2}
S. Wall bottom portion (h = 42 in.) Cracked-X (35)	0.2088×10^{-2}	0.2088×10^{-2}
S. Wall bottom portion (h = 42 in.) Cracked-Y (36)	0.2612×10^{-2}	0.4443×10^{-2}
S. Wall bottom portion (h = 42 in.) Cracked-XY (37)	0.1009×10^{-2}	0.1063×10^{-1}
Pool Floor, Cracked-X (38)	0.4300×10^{-3}	0.4300×10^{-3}
Pool Floor, Cracked-Y (39)	0.5232×10^{-3}	0.7337×10^{-3}
Pool Floor, Cracked-XY (40)	0.1700×10^{-2}	0.1746×10^{-2}

x and Y directions the deflections calculated for ANSYS material property are slightly smaller than the actual values. For elements cracked due to moment My ~~only~~ the deflections calculated for ANSYS material property are considerably smaller than the actual values. Therefore, the stiffnesses of cracked elements are exactly calculated for elements cracked due to bending moment Mx, and are overestimated for elements cracked due to bending moment My and ~~also~~ for elements cracked in both directions. The thermal bending moments are overestimated for the elements cracked in the y-direction or for the element cracked in both x and Y directions. The bending moments for the dead load case is performed using the Uncracked model of the pool structure and are, therefore, not affected by the approximation used in the material properties input into ANSYS. In general there is an overestimation of the bending moments in the cracked elements and this is conservative.

Consumers Power Company
Big Rock Point Plant
Docket 50-155

4. POTENTIAL CRACK AT EAST WALL
June 8, 1983

7 pages

4. Potential Crack at East Wall

The potential crack at East Wall due to Dead weight can be investigated by studying the stress condition of a cut-out element in this region. A perspective view is prepared on next page to understand the stress condition of the cut-out element. Note that the stress condition of the cut-out element can be studied by inferring the stress conditions of the differential elements. One is near the outer face of east wall and one is near the bottom face of the floor; one is from the support wall. The stress condition of those differential elements are readily available from

the computer output of the "Dead Load Run". They are tabulated on next page.

It is noted that S_x of the cut-out element will be in the order of S_x of the east wall differential elements. S_y of the cut-out element will be in the order of S_x of the floor differential elements. And S_z of the cut-out element will be in the order S_z of the east support wall elements.

It is found that S_y, S_z of the cut-out element is significantly under compression, with small shearing stress S_{yz}. The possibility of resolving into a tension principal stress is very unlikely, so is the crack.

However, this stress condition of the cut-out element is not unexpected, because of the heavy dead load of the east pool wall on top of the support wall. The typical potential crack will develop if no heavy dead load on top of it. A good representing picture is taken from "PCI design handbook" PCI, 1971, and is attached here. Note that there is no heavy load on top of the end of the precast, prestressed beam.

NUS CORPORATION

Page ___ of ___

DATE 5-19-83

CLIENT CPCO FILE NO. 5148-FA-08 BY M. Li

SUBJECT NRC Discussion Items Checked By TKG

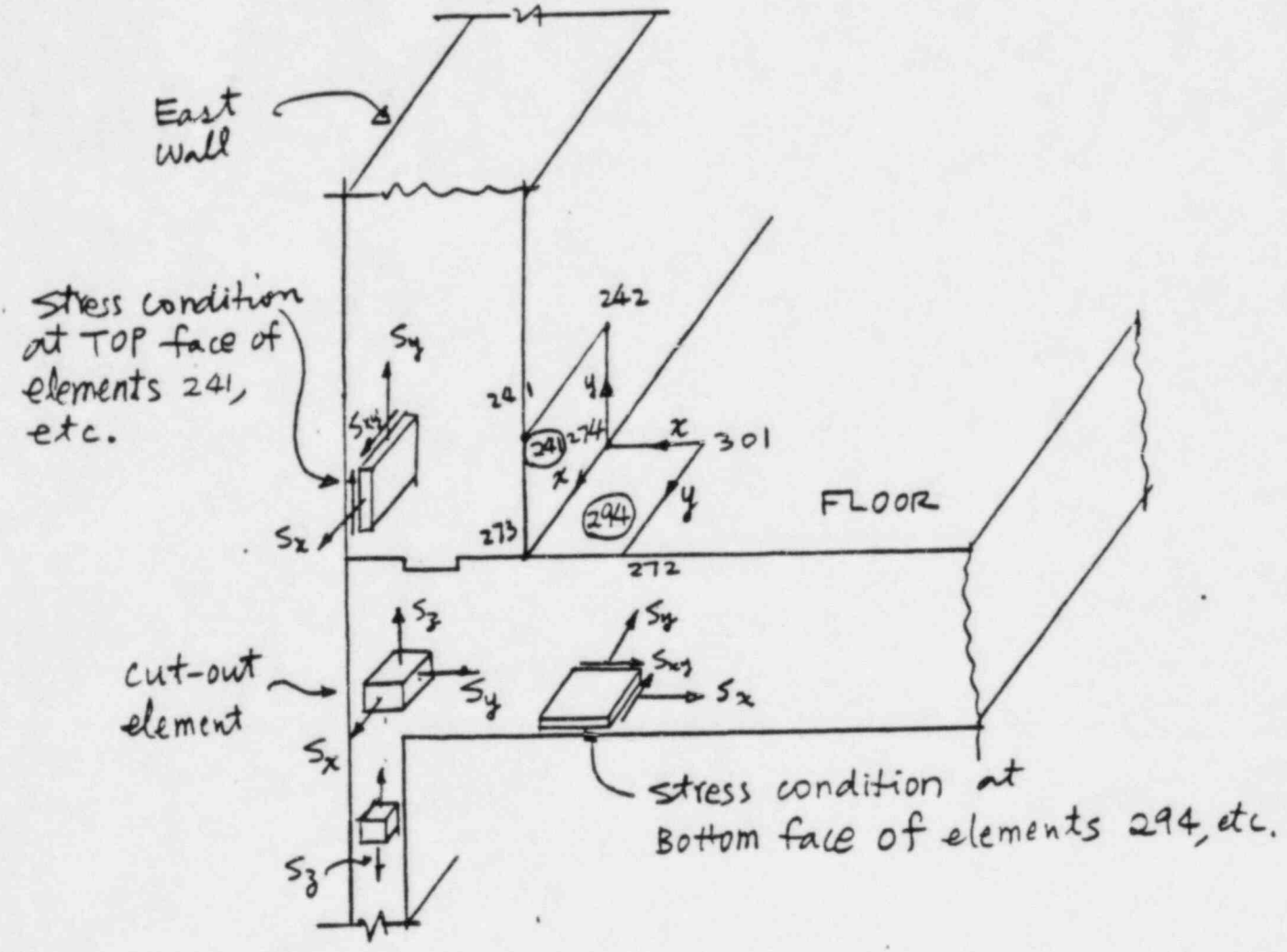

stress condition at outer face of East Wall

Element no.	$S_{x_{(PSI)}}$	$S_{y_{(PSI)}}$	$S_{xy_{(PSI)}}$
241	-11.7	-41.1	-2.4
242	-9.4	-40.8	-0.9
243	-7.3	-42.9	-0.9
244	-6.4	-44.8	-1.3
245	-7.3	-45.8	-1.5
246	-9.9	-45.8	-1.4
247	-12.9	-45.6	-0.6
248	-14.1	-47.9	2.5

Stress Condition at Bottom face of Floor.

Element no.	Sx (PSI)	Sy (PSI)	Sxy (PSI)
294	-12.7	-8.0	-12.4
298	-17.9	-4.4	-16.1
299	-24.8	2.3	-12.6
300	-29.2	5.8	-5.6
301	-29.8	5.1	2.6
302	-26.4	.1	9.9
303	-20.0	-8.3	14.1
318	-15.6	-12.8	11.2

NUS CORPORATION

DATE 5-19-83

CLIENT CPCO FILE NO. 5148-FA-08 BY M. L.

SUBJECT NRC Discussion Items Checked By TKG

Compressive Stress at East Support Wall

Element no.	F_z (#)	dead wt. of Wall (#)	Total F_z (#)	Area (b×d)	S_z (psi)
297	-39984	-30615	-70599	15×18	-261
305	-78956	-61230	-140,186	30×18	-260
307	-81109	-61230	-142339	30×18	-264
309	-84549	-61230	-145 779	30×18	-270
311	-87046	-61230	-148276	30×18	-275
313	-87962	-61230	-149192	30×18	-276
315	-88 414	-61230	-149 644	30×18	-277
317	-91269	-61230	-152 499	30×18	-282
320	-49451	-30615	-80066	15×18	-297

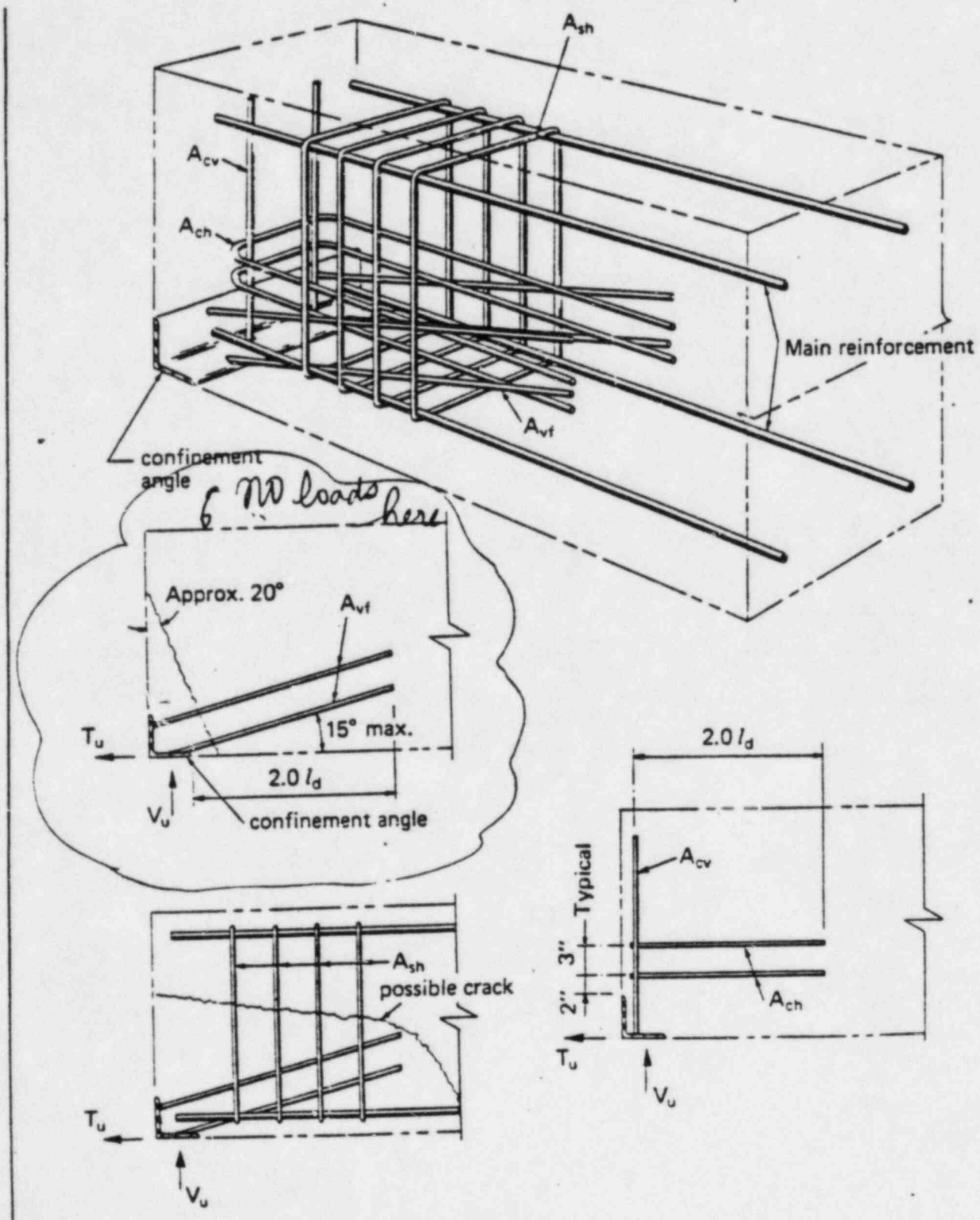
A_{sh}
A_{cv}
A_{ch}
Main reinforcement
A_{vf}
confinement angle
6 NO loads here
Approx. 20°
A_{vf}
15° max.
T_u
$2.0\,l_d$
V_u
confinement angle
$2.0\,l_d$
A_{cv}
Typical
3"
2"
A_{ch}
T_u
V_u
A_{sh}
possible crack
T_u
V_u

Consumers Power Company
Big Rock Point Plant
Docket 50-155

5. KEY AT THE POOL SOUTH WALL
June 8, 1983

4 pages

5. Key at the Pool South Wall:

Reference: Drwg No. 0T40G20113-Rev A

Key exists at a distance of 18'6" from the face of the east wall and is 3'6" Wide. The nodal points in the finite element model corresponding to this region of the South Wall are: 30, 31, 62, 63, 94, 95, 126, 127, 158, 159, 190, 191, 222, 223, 254 and 255. The transverse displacements, Uy, for these nodal points are given in the following table.

Node No.	Uy (inches)	
	Dead Weight	Thermal
30	-0.0074	-0.1353
62	-0.0071	-0.0961
94	-0.0067	-0.0707
126	-0.0065	-0.0625
158	-0.0061	-0.0512
190	-0.0054	-0.0492
222	-0.0040	-0.0326
254	-0.0018	-0.0176

Node No.	Uy (inches)	
	Dead Weight	Thermal
31	-0.0054	-0.1126
63	-0.0054	-0.0879
95	-0.0054	-0.0747
127	-0.0053	-0.0680
159	-0.0051	-0.0633
191	-0.0047	-0.0603
223	-0.0035	-0.0402
255	-0.0016	-0.0209

The largest total deflection of 0.1427 inches occurs at the top of the wall and is directed outwards from the pool. There is a 0.75 inch Fesco board expansion joint between the Vertical Key and the south wall. Therefore, the lateral deflection of 0.1427 inches is insufficient to involve the Vertical Key into structural interaction with the pool.

In-plane (membrane) displacements:

Node No.	Ux (inches)			Node No.	Ux (inches)		
	Dead Load	Thermal Load	Total		Dead Load	Thermal Load	Total
30	0.00106	-0.02352	-0.02246	31	0.00110	-0.03812	-0.03702
62	0.00080	-0.02505	-0.02585	63	0.0008	-0.03818	-0.03738
94	0.0006	-0.02424	-0.02364	95	0.0005	-0.03411	-0.03361
126	0.00049	-0.02409	-0.02360	127	0.00038	-0.03336	-0.03298
158	0.00023	-0.02541	-0.02518	159	0.00009	-0.03289	-0.03280
190	0.00012	-0.02947	-0.02935	191	-0.00012	-0.03795	-0.03807
222	-0.00018	-0.03095	-0.03113	223	-0.00027	-0.04067	-0.04094
254	-0.00038	-0.03004	-0.03042	255	-0.00049	-0.03840	-0.03889

The largest in-plane displacement in the south wall at the vertical key occurs at a height of 54 inches from the pool flair and is equal to 0.041 inches. This is very small to involve the key into any structural interaction with the south wall.

Transverse displacement along the horizontal Key in the west wall:

Node No	Displacement (inches) U_x		
	Dead Load	Thermal	Total
225	-0.00078	-0.06126	-0.06204
226	-0.00072	-0.06400	-0.06472
227	-0.00082	-0.06327	-0.06409
228	-0.00094	-0.06289	-0.06383
229	-0.00097	-0.06757	-0.06854
230	-0.00089	-0.07088	-0.07177
231	-0.00071	-0.06782	-0.06853
232	-0.00053	-0.06029	-0.06082
233	-0.00050	-0.04808	-0.04858

The largest transverse displacement is about 0.072 inch. The Fesco board expansion joint at the key between the West wall and the adjacent reactor concrete block is 0.75 inch. Therefore, no structural interaction at the key between the West wall and the adjacent reactor concrete block is possible.

Consumers Power Company

General Offices: 1945 West Parnall Road, Jackson, MI 49201 • (517) 788-0550

COPY

June 10, 1983

Dennis M Crutchfield, Chief
Operating Reactor Branch No 5
Nuclear Reactor Regulation
US Nuclear Regulatory Commission
Washington, DC 20555

DOCKET 50-155 - LICENSE DPR-6 -BIG ROCK POINT PLANT - RESPONSE TO NRC STAFF CONCERNS - AMENDMENT 2 TO SPENT FUEL RACK ADDITION - "CONSOLIDATED APPLICATION"

Consumers Power Company on June 8, 1983 submitted information on five unresolved items from the NRC Safety Evaluation Report (SER) of May 16, 1983 on the above subject. In that letter of June 8, 1983, Consumers Power Company committed to provide documentation of the basis for resolution of concerns identified by two items. Those two items were: 3. Orthotropic Plate assumptions; and 6. Transient Time. Attached is our technical justification of the basis for resolution of concerns for those items.

We feel that the information attached to this letter completes Consumers Power Company's response to the questions rasied by the NRC Staff during its review of the structural analysis in Amendment 2. Consumers Power Company believes the analysis, as amplified by the additional information furnished in response to Staff questions, adequately addresses the pertinent and significant technical issues. We trust that the Staff will also concur with this judgment and issue a SER promptly.

Thomas C Bordine (Signed/wgf)

Thomas C Bordine
Staff Licensing Engineer

CC Administrator, Region III, USNRC
NRC Resident Inspector - Big Rock Point Plant

Attachments

OC0683-0004A-NL02

Consumer Power Company
Big Rock Point Plant
Docket 50-155

1. OVERVIEW OF DISCUSSION ITEMS
June 10, 1983

During the CP Co/NRC/NUS June 2 meeting, six issues relative to the NUS analysis of the Big Rock Point spent fuel pool were discuseed. Four of the issues were tentatively resolved. The two remaining items were determined to be more appropriately addressed by a written summary to be provided the NRC at a later date. It is not the purpose of this attachment to specifically deal with the items associated with the modeling of orthotropic plate behavior or the method of applying thermal loads to the pool. It is the purpose of the discussion below to cast the analysis into its proper prospective.

The purpose of the analyses which have been conducted is to provide assurance that the pool can sustain the postulated loadings while maintaining overall structural stability. The analysis was not performed to provide a new analysis procedure or to confirm the adequacy of existing ones. The analysis is merely a vehicle by which one is enabled to make the structural stability assessment. Should experience and engineering judgment imply that the pool structure is adequate, the analysis is secondary or, perhaps, unnecessary. The incremental method employed in the Big Rock Point spent fuel pool analysis was not contemplated in the original scope. It was done in order to provide assurance that concrete cracking distributions which generate stiffness mismatches do not in turn result in unacceptable shear distributions. The incremental process resulted in vast amounts of data, data processing routines and model manipulations. The analytical complexities tended to introduce as many questions as were answered. The bulk of detail tended to obscure the obvious conclusion of the process which were that:

- Joint stiffness assumptions made thermal loadings appear much more severe than they actually would be.
- The self-limiting nature of thermal loads applied to lightly reinforced concrete structure make even "analytical" failure essentially impossible at such small thermal gradients.
- The incremental methodology should not be recommended for similar structures because of its complexity. Nonetheless, that approach as used in this application does appear does appear to confirm the appropriateness of certain quasi-linear types of analysis which have been performed in the past on similar structures.

Experience with reinforced concrete clearly indicates that non-cyclic applications of thermal gradients simply do not constitute a failure mechanism. None of the consultants with which Consumer Power Company has discussed this issue can identify such a failure as ever having occurred. Recent analysis performed on lightly reinforced, relatively thick walls in the Midland Plant diesel generator building clearly indicate that for walls cracked by 70°F thermal gradients, the out-of-plane moment capacity with respect to primary loads for a given axial load is unaffected. Visual inspection of the fuel pool and on inspection of drawings give insight as to why intuition and analysis both indicate that the pool is structurally adequate to sustain the postulated thermal load. The box-like nature of the pool and the support condition indicate significant redundancy. The light reinforcement has an almost ironic benefit in that it provides for a flexible structure which will not be likely to develop the moments the analysis assumptions allow to exist. The deadweight stresses are extremely small and the thermal gradients are also small. Such gradients are relatively typical in certain thick structural walls due to weather conditions.

The analysis which has been performed on the Big Rock Point spent fuel pool has been encumbered somewhat by the lack of appropriate industry standards. It is suggested that analysis procedures and appropriate allowable loads are somewhat limited because detailed thermal analysis of concrete structures with modest gradients, such as 70°F, simply are not generally performed. Since thermal gradient failures do not constitute a failure mechanism in reinforced concrete, rigorous design/analysis procedures are limited. Lack of appropriate code allowables have resulted in the use of primary load allowables for secondary loads in the fuel pool analysis which has been performed. This restriction is most apparent in the use of very restrictive beam-diagonal tension shear allowables for thick wall slabs where diagonal tension cannot even be developed.

It is not appropriate to imply that analysis details are not important. However, it is important that such details be considered in the proper context. That context is associated with an analysis which:

- For simplicity and conservatism posed a much more severe loading environment than exists by assuming rigid structural joints in locations of significance.

- Conducted and extremely complicated non-linear process to propose an approximate yet viable load dissipation and redistribution scheme to evaluate structural sections and joints with respect to a loading generally understood not to cause structural failure.

- Compared resulting loads to very conservative code allowables typically applied to primary loads.

The conclusion of the analysis was that the structure is stable under the imposed loading. That conclusion is consistent with intuition and past design and field experience.

Consumers Power Company
Big Rock Point Plant
Docket 50-155

2. DISCUSSION OF MODELING OF ORTHOTROPIC BEHAVIOR AND METHOD OF APPLICATION OF THERMAL LOAD

June 10, 1983

In order to analyze complex structures, the experienced engineer must make assumptions and approximations. The ultimate goal is to produce results which depict the responses of the structure to the imposed loading conditions. To further assist the engineer, design code allowables contain generous margins with respect to structural failure. This is done to account for the uncertainties associated with (the need to make) assumptions and approximations.

During the CPCo/NRC/NUS June 2 meeting, two of the approximations made by NUS during the analysis of the spent fuel pool structure were reviewed in detail. These were the methods used to model orthotropic plate behavior and the method used to apply the thermal load incrementally. To finalize the record, NRC requested that CPCo/NUS submit a written summary of the technical justification (presented at the meeting) for these assumptions which demonstrated the subsequent results were not only acceptable but in fact, conservative.

In the thermal stress analysis of the spent fuel pool the thermal gradients were applied so that all the structural elements (i.e., the walls and the floor) of the pool reached their maximum thermal gradient at the same time. Although the peak thermal gradients occur at different times for the walls of different thicknesses, the value of the thermal gradient does not vary significantly from wall to wall during the time interval chosen for the analysis, namely 190 hours, except for the 24 inch thick portion at the top of the south and east walls. This results in a slightly delayed cracking of the thinner walls and, therefore, in a slight artificial increase in the effective stiffness and moment generating capability of these walls during the early part of the transient. Since the thinner walls are already relatively flexible, this slight increase in the effective stiffness (which will get adjusted at the end of the transient) has little effect on moments and shears generated in the adjacent walls.

The values of Poisson's ratio and modulus of elasticity input to the ANSYS computer code lead to an approximation in the orthotropic behavior of the floor and wall slabs. The stiffnesses of certain cracked elements are overestimated which in turn results in an overestimation of the thermal bending moments. The effect of all of this is simply a small change in the predicted cracked regions of the structure with an associated small change in calculated shears and moments.

It is very important to note that the moments and shears calculated from the thermal stress analysis are very conservative. The thermal moments in the slabs, as predicted by the thermal stress analysis, due to the application of the thermal gradients develop due to the assumed rigid nature of the joints between the adjacent walls of the pool and between the west wall and floor of the pool. If these joints are permitted relative rotation between the adjacent structural slabs they join, the magnitude of the thermal moments developed will be significantly decreased. The rigid nature of these joints to closing-type moments (these moments are similar to the thermal moments and create tension on the outer surfaces of the pool walls and floor) depends on the continuity across the corner of the joint of the reinforcement at the outer surfaces of the wall and floor slabs.

According to Park and Paulay (Reinforced Concrete Structures, John Wiley, 1975, pages 717-720 and Figure 13.52) adequate strength of joints for the assumption of rigidity between slabs can be expected only under the following conditions:

(i) The tension steel is continuous around the corner (i.e., it is not lapped within the joint).

(ii) Bars at right angles to the potential cracks should be provided to prevent the growth and widening of the cracks.

(iii) Rectangular ties should surround the tension steel within the joint and should prevent widening of the splitting cracks.

The type of joint that provides the rigid connection between adjacent slabs and the typical joints in the Big Rock Point pool structure are shown in Figure 1. In all the joints of the spent fuel pool the reinforcements at the outer faces of the walls and the floor are not continuous around the corner of the adjacent slabs. These joints are not close to the ideal or theoretical rigid joint shown in Figure 1. The splices, wherever used, appear to be just temperature and shrinkage reinforcement. Therefore, the joints between adjacent walls and between the walls and floor of the pool are in fact closer to pinned joints than rigid joints for thermal bending moments. The assumption of total rigidity of the joints between adjacent walls and between the west wall and the pool floor has resulted in a large overestimation of the thermal moments. In fact, had an analysis been performed assuming pinned conditions at these joints, the thermal

bending moments would be so small that the pool structure would not even crack. For the Big Rock spent fuel pool such an analysis is closer to reality. Because the evaluation of the degree of rigidity of the joints in an exact manner is extremely difficult to carry out and incorporate in a complicated analysis such as the one performed, the conservative analysis assuming total rigidity at the various joints described earlier was performed. The overestimation of the thermal moment more than compensates for the assumptions involved in the orthotropic property input as well as the manner in which the thermal gradient increments were applied during the analysis.

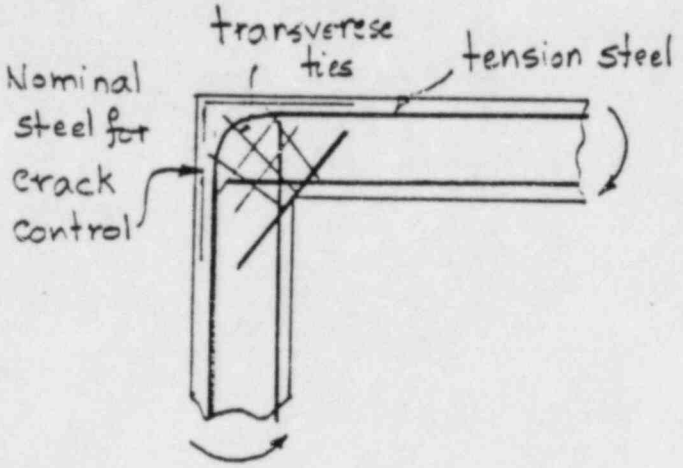

Theoretically rigid joint
(Park and Paulay)

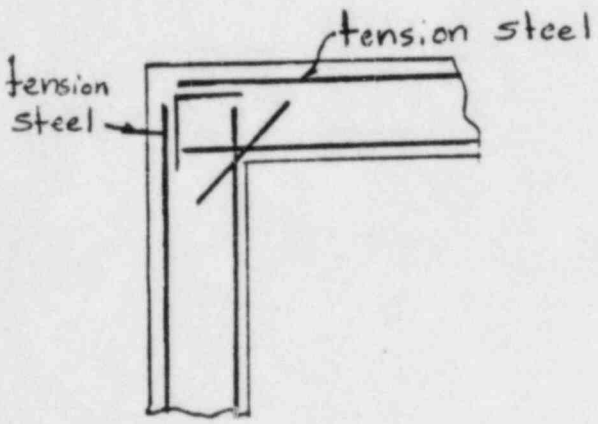

Typical wall-to-wall joint. (BRP spent Fuel Pool)

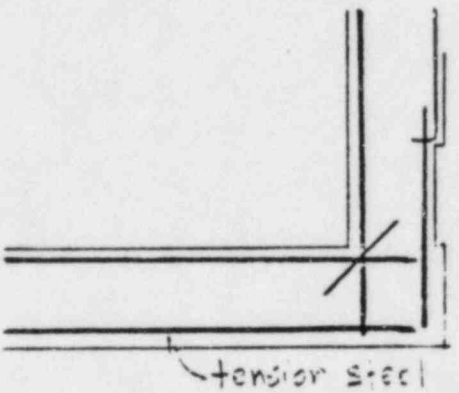

West-Wall to floor joint
(BRP spent Fuel Pool)

FIGURE 1.

Consumers Power Company
Big Rock Point Plant
Docket 50-155

3. MODELING OF FUEL POOL BEHAVIOR DUE TO THERMAL TRANSIENT

Consumers Power Company

OPERATING SERVICES DEPARTMENT

Subject: DISCUSSION ITEM : MODELING OF FUEL POOL BEHAVIOR DUE TO THERMAL TRANSIENT

Sketch No____ Cal No____
Project No____
Originator E.T. Wong
Reviewed by RBJ
Approved by____
Date 6-9-83 Page 1 of 17

A. INTRODUCTION

PROBLEM DEFINITION

IN ADDRESSING THE STRUCTURAL INTEGRITY OF THE BRP FUEL POOL DURING A HYPOTHETICAL LOCA TRANSIENT, IT WAS FELT DESIRABLE TO ANALYTICALLY MONITOR THE STRUCTURAL EFFECTS THROUGH THIS TRANSIENT. THE CONCERN WAS THAT AS THE STRUCTURE CRACKS AND SELF-RELIEVES DUE TO THERMAL MOMENT, THE RESULTING SHEAR FORCES MAY EXCEED THE ALLOWABLE SECTION CAPACITIES SOMEWHERE IN THE STRUCTURE. THIS CONCERN IMPLIES A TACIT ASSUMPTION THAT SHEAR FAILURE IS BRITTLE AND UNDESIRABLE.

THE APPROACH USED IN THE REPORT FOLLOWS THE GUIDELINE OUTLINED IN ACI 349-APP. A. TO KEEP THIS VERY COMPLEX PROBLEM REASONABLY TRACTABLE, CERTAIN ASSUMPTION WERE MADE :

- ONE DIMENSIONAL 'THROUGH WALL' TRANSIENT CURVES ARE DEVELOPED TO PROVIDE THERMAL INPUTS TO THE STRUCTURE
- SINCE THE POOL IS MADE UP OF WALLS OF VARIOUS THICKNESS WHICH RESULTS IN CURVES WHOSE MAXIMUM RESPONSES OCCUR AT DIFFERENT TIMES, IT IS CONSIDERED ECONOMICALLY INFEASIBLE IF NOT ANALYTICAL IMPOSSIBLE TO USE A TIME HISTORY APPROACH. THIS APPROACH REQUIRES SOME REASONABLE AMOUNT OF TIME INCREMENT STEPS, CAPTURING ALL MAXIMUM THERMAL GRADIENT POINTS & 'STABILIZING' THE CRACK PATTERNS, ETC, EACH OF THESE STEPS REQUIRES SOLUTION TO A NEW STIFFNESS MATRIX. THEREFORE IT IS DECIDED TO APPROXIMATE THIS PROCESS USING EQUAL FRACTIONS OF THE MAXIMUM THERMAL GRADIENT ACROSS EACH INDIVIDUAL WALL, ASSUMING THAT THEY OCCUR SIMULTANEOUSLY.

A CONCERN WAS RAISED REGARDING THE VALIDITY OF

THE CONCLUSIONS OF THE ANALYSIS BASED ON THIS APPROXIMATION. SPECIFICALLY, THE CONCERN WAS THAT BY IGNORING THE TIME EFFECT, THE SHEAR DISTRIBUTION OBTAINED IS NOT REALISTIC. THEREFORE, STRUCTURAL INTEGRITY AGAINST A BRITTLE SHEAR FAILURE CANNOT BE ASSURED. IT WAS OBSERVED THAT THE LEAST SHEAR MARGIN WAS ONLY 1.4.

B. OBJECTIVE

THIS DISCUSSION WILL ADDRESS THE MAGNITUDE OF THE ERROR IN PREDICTING THE THERMAL MOMENTS (RELATED TO ΔT). IT WILL ALSO EVALUATE THE POSSIBLE IMPACTS OF THE ERROR ON THE BEHAVIOR OF THE POOL STRUCTURE.

C. ERROR EVALUATION

METHOD

TO NARROW DOWN THE SCOPE OF THE EVALUATION, THE FOLLOWING ASSUMPTIONS ARE MADE:

1. THERMAL MOMENT IS A FUNCTION OF LINEARIZED ΔT.
2. THE ERRORS WITH THE APPROXIMATION METHOD ARE DUE TO THE FACT THAT WALLS OF DIFFERING THICKNESSES HAVE MAXIMUM THERMAL RESPONSES THAT OCCUR AT DIFFERENT TIMES. IT IS ASSUMED THAT THE ERRORS ARE INTRODUCED MAINLY AT THE JUNCTURE BETWEEN TWO WALLS OF DIFFERING THICKNESSES, AND THAT IT IS LOCAL IN NATURE, AND BY SAINT-VENANT PRINCIPLE, PROBABLY HAVE NO INFLUENCE BEYOND A FEW ELEMENTS. FOR INSTANCE, ANY ERROR IN THE N.W. CORNER OF THE POOL IS UNLIKELY TO AFFECT THE CRACK PATTERN AT THE N.E. OR S.E CORNERS, ETC.

SINCE THE ERROR IS ASSUMED TO BE LOCAL, IT IS POSSIBLE TO NARROW DOWN THE REGION OF INTEREST TO THE JUNCTURE BETWEEN TWO WALLS WITH LARGE TIME LAGS BETWEEN THEIR RESPECTIVE "ΔT VS. TIME CURVES" GENERALLY THIS IS AT THE JUNCTURE BETWEEN TWO WALLS WITH LARGE DIFFERENCES IN THICKNESS.

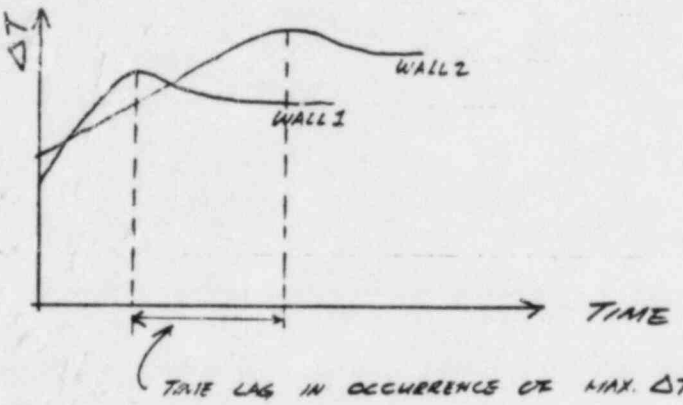

FIG. 1 (Rg.13) IS A PLOT OF THE FUEL POOL WITH ITS WALLS LAID FLAT IN THE PLANE OF POOL FLOOR. THE PROCEDURE FOR THIS ERROR ANALYSIS IS AS FOLLOWS:

1. IDENTIFY THE WALL JUNCTURE OF CONCERN, e.g., BETWEEN THE W. (48") AND THE N. (81") WALLS.
2. PICK A WALL AS A 'BENCHMARK' WALL AND IDENTIFY THE TIME WHEN $i(0.1\Delta T_{max})$ (WHERE $i = 4, \ldots, 10$) OCCURS. CALL THIS t_i ($i = 4, \ldots, 10$)
3. FROM THE ΔT CURVE OF THE <u>OTHER</u> WALL, IDENTIFY THE <u>ΔT</u> VALUES THAT CORRESPOND TO THE t_i FROM THE LAST STEP.
4. CALCULATE THE % ERROR OF EACH TIME STEP i AS FOLLOWS:

$$\text{ERROR} = \left(\frac{\Delta T_{i,\text{USED}} - \Delta T_{i,\text{ACTUAL}}}{\Delta T_{i,\text{ACTUAL}}} \right) \times 100\%$$

WHERE $\Delta T_{i,\text{LIGED}} = i\,(0.1\,\Delta T_{max})$ (FOR THE OTHER WALL IN STEP 3)

$i = 4, \ldots, 10$

$\Delta T_{i,\text{ACTUAL}}$ = ΔT READ FROM THE ΔT VS TIME CURVE FOR THE WALL IN STEP 3.
$i = 4, \ldots, 10$.

5. SINCE THIS ERROR IS ASSUMED TO BE LOCALLY CONFINED, THE SAME PROCEDURE MAY BE APPLIED TO ANOTHER WALL JUNCTURE OF CONCERN WITH A NEW 'BENCHMARK' WALL.

THIS ANALYSIS WILL GIVE AN ERROR OF THE INCREMENTAL ΔT APPROXIMATION COMPARED TO A TIME HISTORY APPROACH. THIS TIME HISTORY TIME INCREMENT POINTS (t_i's) ARE NOT OF EQUAL DURATION THOUGH & ITS CHOICE MAY NOT HAVE BEEN OPTIMAL. NEVERTHELESS, IT PROVIDES AN INSIGHT INTO THE SENSITIVITY OF THIS APPROXIMATION METHOD.

D. RESULTS AND DISCUSSION

I. GENERAL

SEVEN(7) WALL/FLOOR JUNCTURES WERE INVESTIGATED. THESE ARE SELECTED AFTER REVIEWING FIG 3 & TABLE 1. THE FORMER SHOWS THE THICKNESSES OF VARIOUS PORTIONS OF THE POOL. THE LATTER HIGHLIGHTS THE TIME LAG BETWEEN MAXIMUM ΔT's OF SOME WALLS.

THE WALL/FLOOR JUNCTURES SELECTED ARE THOSE BETWEEN THE WEST END OF THE SOUTH WALL & THE FLOOR SLAB (42" ~ 72"); WEST WALL & THE NORTH WALL (48" ~ 81"); SOUTH WALL & POOL FLOOR, SOUTH WALL & EAST WALL, SOUTH WALL AT THE TAPER (69" ~ 72", 69" ~ 78", 68" ~ 58.9" RESPECTIVELY),

AND FINALLY AT THE 24" WALLS JUNCTURES WITH 48" & 78" WALLS. THE RESULTS OF THESE ERROR ANALYSIS ARE SHOWN IN TABLES 2 THROUGH 5.

GENERALLY, BY USING THE APPROXIMATE PROCEDURE (INCREMENTAL ΔT) THE LINEARIZED ΔT ACROSS A THICKER WALL, AT ANY INSTANCE, IS OVERPREDICTED WITH RESPECT TO THAT ACROSS A THINNER WALL. THIS WILL RESULT IN AN OVERPREDICTION OF THERMAL MOMENT IN THE THICKER WALL AT ANY INSTANCE. THIS MAY RESULT IN A PREMATURE INDICATION OF CRACKING IN THE THICKER WALL. CRACKING OF AN ELEMENT WILL, OF COURSE, RELIEVE THE THERMAL MOMENT AND RESULT IN A REDISTRIBUTION OF THE MOMENT DUE TO DEADWEIGHT & THERMAL EFFECT IN THE IMMEDIATE NEIGHBORHOOD. THIS WILL AFFECT THE STRESSES IN THE THIN WALL AT THE JUNCTURE, POSSIBLY DELAYING, IF NOT PREVENTING ALTOGETHER THE CRACKING OF THE NEIGHBORING ELEMENTS ON THE THINNER WALL. THIS EFFECT, HOWEVER, IS LOCAL.

II. MAGNITUDE OF ERROR & INTERPRETATION

AFTER A GENERAL DISCUSSION OF THE EFFECTS OF THE ERROR, IT IS APPROPRIATE TO FOCUS ON THE MAGNITUDE OF THIS ERROR. THE MAXIMUM ERROR BETWEEN WALLS (EXCEPT THE 24" WALLS WHICH WILL BE DISCUSSED LATER), IS OF THE ORDER OF 15% (42" VS. 72" & 48" VS 81").

IT SHOULD BE NOTED THAT THIS ERROR ANALYSIS IS BASED ON READ-OUT OF HAND SKETCHED CURVES. GRAPHICAL READ-OUT ERROR MAY BE OF THE ORDER OF SEVERAL %'s. THEREFORE, THE ERRORS ASSOCIATED WITH A MAJORITY OF

OF WALL JUNCTURES ARE INSIGNIFICANT (eg. 69" PORTION OF S. WALL WITH POOL FLOOR, EAST WALL & TAPERING PORTION OF S. WALL).

ANOTHER RELEVANT FACTOR THAT AFFECTS THE INTERPRETATION OF THIS ERROR IS THAT THE WALL THERMAL TRANSIENT CURVES, & HENCE ΔT CURVES, ARE BASED ON 1-DIMENSIONAL HEAT CONDUCTION MODELS. THE THERMAL CHARACTERISTICS OF THE POOL, IN PARTICULAR AT THE JUNCTURE BETWEEN WALLS & FLOORS ARE 2- OR 3-DIMENSIONAL IN NATURE. THE DIFFERENCES IN THERMAL GRADIENT AT THE JUNCTURE OF WALL/FLOOR OF DIFFERENT THICKNESSES WILL TEND TO BE SMOOTHED OUT. THEREFORE, THE ERROR AS COMPUTED ARE OVERESTIMATED.

THEREFORE, IN VIEW OF THE MAXIMUM ERROR INVOLVED & CONSIDERING THE MAGNITUDE OF OTHERWISE ACCEPTABLE GRAPHICAL READ-OUT ERROR, & THE FACT THAT THESE ERRORS ARE OVERESTIMATED, IT APPEARS THAT THE INCREMENTAL ΔT APPROXIMATION IS NOT UNREASONABLE.

HOWEVER, AS SHOWN IN TABLE 5, THE ERROR BETWEEN THE 24" WALL & THE 78" WALL IS AS HIGH AS 34%. THIS IS PERHAPS A BIT TOO HIGH TO BE EXPLAINED BY GRAPHICAL ERRORS & 2 DIMENSIONAL TRANSIENT FLOW 'SMOOTHING' OUT PROCESS. TO ADDRESS THIS ISSUE, IT IS NECESSARY TO DISCUSS THE IMPACT OF SUCH ERRORS.

III. IMPACT OF ERROR

BEFORE ADDRESSING THE IMPACT, IT IS NECESSARY TO

DIGRESS & DISCUSS THE MAIN CONCERN WITH THE POSSIBLE IMPACT OF THE ERRORS IN THE APPROXIMATION PROCEDURE. THE MAIN CONCERN IS THAT THE CRACK PATTERN THUS OBTAINED DOES NOT REFLECT A REAL PICTURE. THIS WILL RESULT IN AN INDETERMINATE ASSESSMENT OF THE SHEAR FORCES.

TO ADDRESS THIS CONCERN, IT IS NECESSARY TO REITERATE THAT:

1. EXCEPT FOR A FEW LOCATIONS, THE ERRORS ARE SMALL.
2. ONE DIMENSIONAL HEAT CONDUCTION TRANSIENT CURVES OVERESTIMATE THIS VERY LOCALIZED ERRORS.

IT MAY BE CONJECTURED THAT MOST OF THE ORDER OF MAGNITUDE OF THIS ERROR IS NOT INCONSISTENT WITH MOST OTHER STRUCTURAL ANALYSIS PROCEDURES. FURTHERMORE, THE DEGREE OF 'EXACTNESS' OF SHEAR CAPACITY PER CODE SHOULD BE BORNE IN MIND (E.G. Ref. 2 & 3) FINALLY, THE CONSEQUENCES OF A SHEAR FAILURE & THE AVAILABLE MARGINS AS CALCULATED SHOULD BE CONSIDERED.

III. i) SHEAR DISTRIBUTION & MARGINS

SINCE IT IS TACITLY ASSUMED THAT IF THE SHEAR MARGIN ARE LARGE, CERTAIN DEGREES OF APPROXIMATION MAY BE ACCEPTABLE, IT MAY BE USEFUL TO IDENTIFY ALL LOCATIONS WHERE THE AVERAGE SHEAR MARGIN IS LESS THAN 2.50. THERE ARE ALTOGETHER 5 LOCATIONS (SEE FIG.)

THESE LOCATION WILL BE DISCUSSED INDIVIDUALLY.

THE TOP OF THE W. WALL (MARGIN 2.14) IS NOT SENSITIVE TO THE ERRORS. AT THE BOTTOM OF THE E. WALL & AT THE POOL FLOOR (MARGINS 1.42 & 2.10) THE SHEAR DISTRIBUTION IS AGAIN INSENSITIVE TO THIS ERROR BECAUSE THE TRANSIENT CURVES AT THE WALL JUNCTURE ARE VERY SIMILAR. AT THE TOP OF THE N. WALL (MARGIN 1.48) THE ERROR INTRODUCED IS NOT EXCESSIVE (≥ 14% MAX) FOR REASONS SUGGESTED EARLIER.

THE LAST LOCATION IS AT THE TOP OF THE E. WALL (MARGIN 1.62), THE ERROR INTRODUCED BY THE APPROXIMATE INCREMENTAL ΔT PROCEDURE MAY BE OF THE ORDER OF 35%. THERE IS A CONCERN OVER THE ACTUAL MARGIN OF SAFETY HERE. (NOTE THAT THIS ERROR IN ΔT, & HENCE THERMAL MOMENT, DOES NOT NECESSARILY TRANSLATE TO THE SAME ORDER OF ERROR IN PREDICTION OF SHEAR FORCES.)

MARGIN OF SAFETY DEPENDS ON BOTH LOAD AND CAPACITY. THE AVERAGE SHEAR CAPACITY USED IN THE REPORT IS BASED ON ACI 349-80 EQNS. 11-4 & 11-9. THESE TWO EQUATIONS ARE USED BASICALLY FOR BEAM OR ONE-WAY SLABS. THEY ARE USE IN THIS REPORT TO ALLOW ONE MEANINGFUL WAY TO EVALUATE THE DATA. (ANOTHER WAY TO EVALUATE THE DATA, AS ALSO REPORTED, IS THE ELEMENT BY ELEMENT LOCAL SHEAR EVALUATION.) THE WALL/FLOOR OF THE FUEL POOL ACTUALLY ACT AS TWO WAY SLABS. FURTHERMORE, THEY CAN BE CONSIDERED AS 'THICK SLABS'. PRESENTLY, THERE IS NO CODE CRITERIA FOR THICK SLABS. HOWEVER, REF. 1 NOTED THAT 'DEEP BEAM ACTION IS ALWAYS AVAILABLE IN DEEP SLABS'. EQNS. 11-4 & 11-9 OF

OF ACI 349-80 ARE CONSERVATIVE ESTIMATES OF SECTION CAPACITY SUBJECTED TO INTERACTION OF AXIAL FORCES & SHEAR. THEY ARE BASED ON $2\sqrt{f'_c}$ WHICH IS APPROPRIATE FOR A LONG SLENDER BEAM. THIS TENDS TO UNDERESTIMATE THE STRENGTH OF DEEP BEAM ACTION. IN ADDITION, REF. 2 OBSERVES THAT " THE SUDDEN DIAGONAL TENSION FAILURE WHICH IS COMMON IN LONG & SLENDER BEAMS USUALLY DOES NOT TAKE PLACE WHEN SLAB ACTION IS PRESENT. ALSO, SLAB ACTION SEEMS TO PERMIT THE COMPRESSION ZONE OF A SLAB TO ACCEPT REDISTRIBUTION WITH RELIABILITY."

THEREFORE, IT SEEMS THAT THE STRUCTURE IS MORE FORGIVING TO ERROR THAN AT FIRST THOUGHT OF BECAUSE OF

1. A DUCTILE FAILURE BEHAVIOR
2. SHEAR CAPACITY HAS BEEN UNDERESTIMATED.

FURTHERMORE IN ADDRESSING SPECIFICALLY THE TOP OF THE E. WALL, IT IS NOTED THAT

3. CALCULATED MARGIN OF AVERAGE SHEAR IS 1.6
4. THIS IS A ISOLATED PHENOMENON
5. THE CONSEQUENCE OF A FAILURE AT THIS LOCATION IS INSIGNIFICANT, i.e. IT IS UNLIKELY TO COMPROMISE THE POOL'S ABILITY TO RETAIN WATER.

TO SUMMARIZE THE ABOVE, REASONS 1, 2, & 3 ABOVE INDICATES A LOW PROBABILTY OF FAILURE. REASON 1 ALSO MINIMIZES THE IMPACT OF ANALYTICAL ERROR INTRODUCED BY THE APPROXIMATE PROCEDURE. REASONS 4 & 5 DEMONSTRATES THAT THE CONSEQUENCE OF A FAILURE, SHOULD IT OCCUR AT THE LOCATION OF MOST UNCERTAINTY,

IS MINIMAL.

E. SUMMARY OF ERROR SENSITIVITY ANALYSIS

IN ORDER TO ANALYSE A COMPLEX STRUCTURE LOADED UNDER A NON-LINEAR PROCESS, AND FOR ECONOMIC & FEASIBILITY REASONS, CERTAIN APPROXIMATE PROCEDURE WAS USED. THE SENSITIVITY OF THE ERROR ASSOCIATED WITH THIS APPROXIMATION IS ANALYSED BOTH OBJECTIVELY & SUBJECTIVELY. THE FOLLOWING IS A SUMMARY:

1. EXCEPT FOR SOME LOCAL AREAS WHERE THE ERROR IS OF THE ORDER OF 15 OR 35 %, MOST OF THE ERROR ARE SMALL AND ARE CLOSE TO OR WITHIN THE RANGE OF GRAPHICAL READ-OUT ERROR.

2. IF ONE CONSIDERS MULTI-DIMENSIONAL HEAT FLOW MODEL AS IS TRUE IN REAL LIFE, ONE CAN CONCLUDE QUALITATIVELY THAT THESE CALCULATED ERRORS ARE OVERESTIMATED.

3. IF BASED ON THE REASONING OF 1 & 2 ABOVE, ONE CAN ACCEPT AN ERROR OF THE ORDER OF 15 % AS BEING REASONABLE, THEN THERE IS ONLY ONE LOCATION OF CONCERN (W.R.T. MODEL ACCURACY) WHERE THE MARGIN AGAINST AVERAGE SHEAR IS LESS THAN 2.50.

4. IT IS OBSERVED THAT STRUCTURAL INTEGRITY OF THE POOL IS NOT AS SENSITIVE TO THE ERROR IN THE PREDICTION OF SHEAR DISTRIBUTION AS ASSUME DUE TO DUCTILE SHEAR BEHAVIOR IN SLABS.

5. THE SHEAR MARGINS ARE ACTUALLY MUCH HIGHER THAN CALCULATED, THIS IS DUE TO THE USE OF A VERY CONSERVATIVE ESTIMATE OF CAPACITY (FOR LACK OF A BETTER PUBLISHED CRITERIA)

6. THE CONSEQUENCE OF A POTENTIAL SHEAR FAILURE AT THE ONE LOCATION OF CONCERN IS INSIGNIFICANT.

F. CONCLUSION

IT IS CONCLUDED THAT

1. EXCEPT FOR ISOLATED LOCATION, THE ERRORS INCURRED ARE GENERALLY SMALL & OVERESTIMATED.

2. MARGINS OF SAFETY W.R.T. AVERAGE SHEAR IS MUCH HIGHER THAN CALCULATED.

3. THE STRUCTURAL INTEGRITY OF OF THE POOL IS NOT SENSITIVE TO ERRORS IN PREDICTION OF SHEAR DISTRIBUTION

4. AT THE ONE SINGLE AREA OF POSSIBLE CONCERN DUE TO MODEL UNCERTAINTY, THE CONSEQUENCE OF A SHEAR FAILURE IS INSIGNIFICANT.

THEREFORE, IN CAN BE CONCLUDED THAT THE APPROXIMATE PROCEDURE USED IN THE REPORT IS REASONABLE & ITS CONCLUSIONS VALID.

G. REFERENCES

1. KAR, A.K, " DESIGN OF CONTAINMENT BASE MATS", REPORT OF SPECIALTY CONFERENCE ON STRUCTURAL DESIGN OF NUCLEAR PLANT FACILITIES. DEC, 1973

2 ACI- ASCE COMMITTEE 326 , " SHEAR AND DIAGONAL TENSION, ", ACI JOURNAL VOL 59 , JAN, FEB, AND. 1962.

3. ACI- ASCE COMMITTEE 426, " THE SHEAR STRENGTH OF REINFORCED CONCRETE MEMBERS," JOURNAL OF THE STRUCTURAL DIVISION, ASCE Vol. 99 NO. ST 6 JUNE 1973.

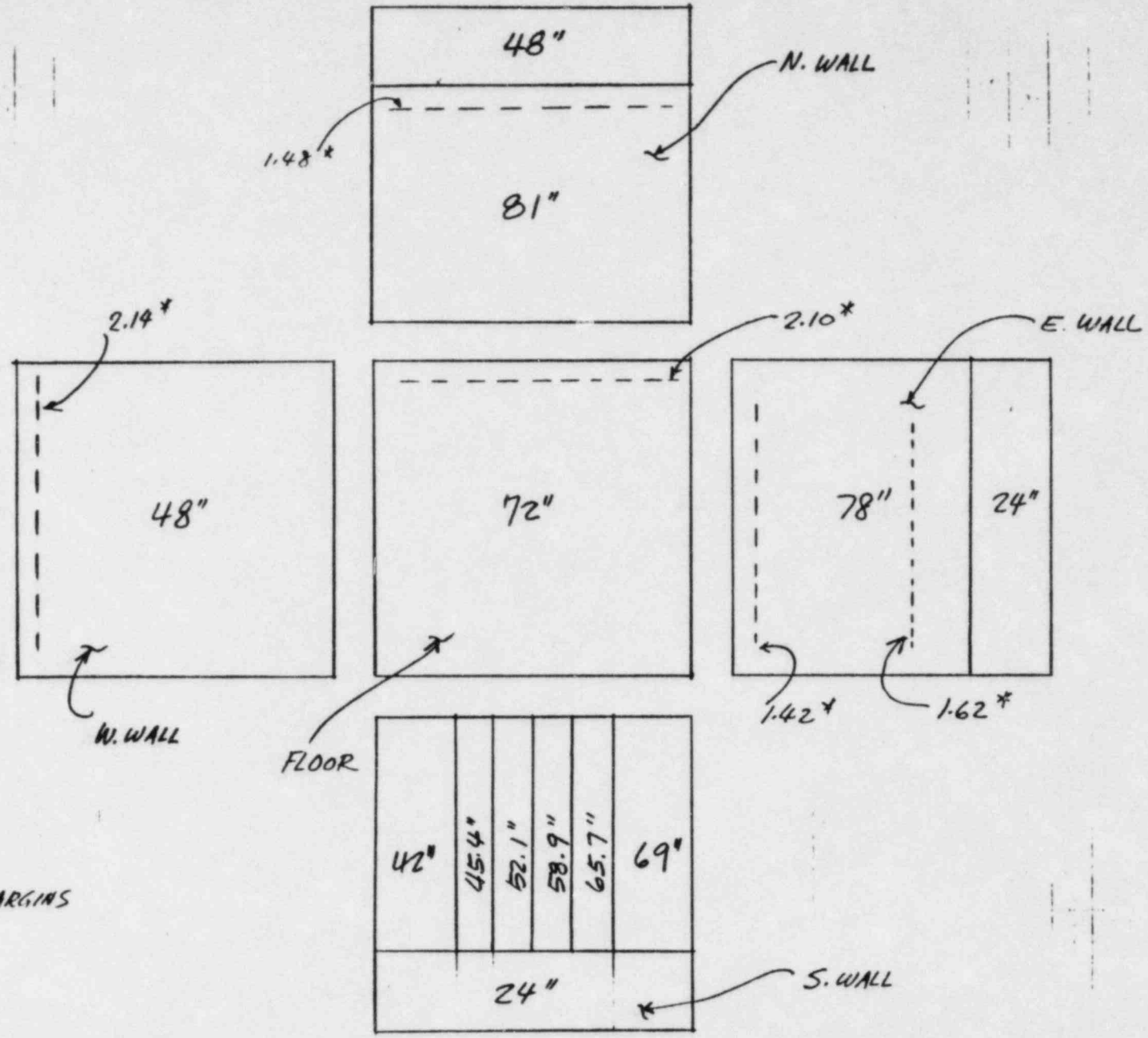

* AVG. SHEAR MARGINS

FIG. 1 WALLS LAID FLAT IN THE PLANE OF THE FLOOR

Floor & WALL – TIME (hrs after loss of cooling)

Δt increment	58.8"	65.6"	72"	69"	52.12"	48"	42"	45.4"	81"	78"	24"
.4 ΔT_{max}	12	11	11	11	10	11	11	11	10	11	10
.5 ΔT_{max}	24	25	24	23	20	20	20	20	24	24	15
.6 ΔT_{max}	30	31	31	31	27	29	27	27	34	33	21
.7 ΔT_{max}	37	37	40	40	34	36	33	34	43	43	27
.8 ΔT_{max}	45	46	50	50	40	43	40	40	55	55	32
.9 ΔT_{max}	61	61	70	64	46	53	46	50	80	73	40
1.0 ΔT_{max}	108	115	150	150	105	85	85	100	~~140~~ 180	185	55

TABLE 1

TIME OF OCCURRENCE OF $i(\Delta T_{max})$ FOR EACH INDIVIDUAL WALL/FLOOR

'BENCHMARK' WALL

WALL ID & THICKNESS	42"		72"		
ΔT_{max}	66°F		71°		
i	$i(0.1\Delta T_{max})$	t_i (HR)	$\Delta T_{i,USED} = i(0.1\Delta T_{max})$	$\Delta T_{i,ACTUAL}$	ERROR %
4	26.4	12	28.4	28.5	0%
5	33.0	20	35.5	33	8%
6	39.6	27	42.6	38	12%
7	46.2	33	49.7	43	16%
8	52.8	40	56.8	50	14%
9	59.4	46	63.9	55	16%
10	66.0	85	71.0	67.5	5%

TABLE 2

'BENCHMARK' WALL

WALL ID & THICKNESS	48"		81"		
ΔT_{max}	69°F		72°F		
i	$i(0.1\,\Delta T_{max})$	Σ_i (HR.)	$\Delta T_{i,USED} = i(0.1\,\Delta T_{max})$	$\Delta T_{i,ACTUAL}$	ERROR %
4	27.6	13	28.8	31.5	-9%
5	34.5	21	36.0	34.5	4%
6	41.4	30	43.2	41.5	4%
7	48.3	36	50.4	45	12%
8	55.2	44	57.6	51	13%
9	62.1	54	64.8	57	14%
10	69.0	86	72	67	7%

TABLE 3

'BENCHMARK' WALL

WALL THICKNESS	69"		58.9"			72"			78"		
ΔT_{max}	71°F		70°F			71°F			72°F		
i	$i(0.1\Delta T_{max})$	t_i (hr)	$\Delta T_{i,USED}$	$\Delta T_{i,ACTUAL}$	ERROR	$\Delta T_{i,USED}$	$\Delta T_{i,ACTUAL}$	ERROR	$\Delta T_{i,USED}$	$\Delta T_{i,ACTUAL}$	ERROR
4	28.4	12	28.0	27.5	2%	28.4	28.5	0%	28.8	29.0	-1%
5	35.5	23	35.0	35.5	-1%	35.5	35.5	0%	36.0	36.0	0%
6	42.6	32	42.0	44.0	-5%	42.6	42.5	0%	43.2	41.5	4%
7	49.7	39	49.0	51.0	-4%	49.7	48.5	2%	50.4	47.5	6%
8	568	50	56.0	58.5	-4%	56.8	56.5	1%	57.6	55	5%
9	63.9	64	63.0	64.0	-2%	63.8	62.0	3%	64.8	61.5	5%
10	71.0	150	70.0	68*	+3%	71.0	71.0**	0%	72.0	71.0	1%

* ACTUALLY @ 150° ΔT WAS ALREADY PEAKED

** T_{max}

TABLE 4

BENCHMARK WALL

WALL THICKNESS	24"		48"			78"		
ΔT_{max}	59°F		69.0°F			72°F		
i	$i(0.1\Delta T_{max})$	t_i (HR)	$\Delta T_{i,USED} = i(0.1\Delta T_{max})$	$\Delta T_{i,ACTUAL}$	ERROR%	$\Delta T_{i,USED}$	$\Delta T_{i,ACTUAL}$	ERROR%
4	23.6	10	27.6	26.2	5%	28.8	28.5	1%
5	29.5	15	34.5	29.5	17%	36.0	31.0	16%
6	35.4	22	41.4	34.5	20%	43.2	34.5	25%
7	41.3	29	48.3	41.5	16%	50.4	38.5	31%
8	47.2	33	55.2	46	20%	57.6	43.5	32%
9	53.1	41	62.1	51.2	21%	64.8	48.5	34%
10	59.0	55	69.0	62.5	10%	72.0	57.0	26%

TABLE 5

CRACK SPACING OF TWO WAY SLABS

Ref. 2 and Ref. 3 were cited in Ref. 1 as the exploring study of crack phenomenon of two way concrete slab. The main interest of Ref. 2 and Ref. 3 were to control the crack width so that it remains within the code limit and deteriorating of reinforcing steel is not likely to happen. Governing equation was developed and verified with test results to predict the the crack width. Not too much attention was paid to the spacing between cracks. No equation was developed to calculate the crack spacing. It is very difficult to evaluate the crack spacing of two way slabs. However, by studying the contents of Ref. 2 and Ref. 3, it is found that :

(1) The slab thickness varied from 3.2 in. to 4.1 in.,

(2) the wire mesh spacing varies from 3"x3", 4"x4", 6"x6", 8"x8", to 6"x12".

(3) for grid index, $I = \phi_1 S_2 / f_{x_1}$, less than 160, an orthogonal cracking pattern will develop. The spacing of the cracks was generally approximately 4 inch.

(4) for grid index greated than 160, the dominant cracks were diagonal yield line cracks which developed fully early in the loading history of the specimens.

For the purpose of qualitative comparison, 4"x4" wire mesh used in a 4" thick slab is considered closely spacing reinforcement and will cause orthogonal cracking pattern, the #11 & 12" reinforcement

used in the Big Rock Point spent fuel pool floor slab of 72" thick should be considered as closely spacing reinforcement and will cause orthogonal cracking pattern. Since the crack width of orthogonal crack pattern is narrower than that of diagonal crack pattern, the orthogonal pattern was to be preferred, which is the case of Big Rock Point. And it is the opinion of Ref 1 that the aim of crack control is to ensure that fine, closely spaced cracks form, rather than a few wider cracks. It seems the spacing between cracks is not as important an issue as the crack width.

All in all, the evaluation of crack spacing is not readily available, but the floor or wall slabs

of the BRP spent fuel pool will develop some closely spaced fire cracks orthogonally. And this kind of crack pattern is desired.

References

1. Park and Gramble, "Reinforced Concrete Slabs" John Wiley & Son, 1980

2. E. G. Nawy and G. S. Orenstein, "Crack Width Control in Reinforced Concrete Two-way Slabs," J. Struct. Div., ASCE, Vol. 96, No. ST. 3, March, 1970, pp 701-721

3. E. G. Nawy and K. W. Blair, "Further Studies on Flexural Crack Control in Structural Slab Systems," ACI SP-30, ACI, Detroit, 1971, pp 1-41.

Solution. Consider a 10-in-wide strip of slab containing one bar.

$$\frac{A_s}{b} = \frac{0.31}{10} = 0.031 \text{ in}^2/\text{in} \qquad d = 10 - 0.75 - 0.31 = 8.94 \text{ in}$$

$$\rho = \frac{A_s}{bd} = \frac{0.031}{8.94} = 0.00347 \qquad \rho n = 0.00347 \times 9 = 0.0312$$

From elastic theory,[9.21]

$$k = \sqrt{\rho^2 n^2 + 2\rho n} - \rho n$$
$$= \sqrt{0.0312^2 + 2 \times 0.0312} - 0.0312 = 0.221$$

$$kd = 0.221 \times 8.94 = 1.98 \text{ in}$$

$h_1 = d - kd = 8.94 - 1.98 = 6.96$ in
$h_2 = h - kd = 10 - 1.98 = 8.02$ in

From the Gergely–Lutz equation (Eq. 9.9),

$$t_b = 0.75 + 0.31 = 1.06 \text{ in} \qquad A = 2t_b b = 2 \times 1.06 \times 10 = 21.2 \text{ in}^2/\text{bar}$$

$$w_{max} = 0.076 \sqrt[3]{1.06 \times 21.2} \frac{8.02}{6.96} (52{,}000 \times 10^{-6})$$
$$= 0.0129 \text{ in (0.33 mm)}$$

From the Beeby equations (Eqs. 9.14 and 9.15),

$$\varepsilon_s = \frac{52{,}000}{29{,}000{,}000} = 0.00179$$

$$\varepsilon_m = \left[0.00179 - \left(\frac{2.5 \times 10}{0.031} \times 10^{-6}\right)\right] \frac{8.02}{6.96} = 0.000984 \times \frac{8.02}{6.96} = 0.00113$$

$c_0 = 0.75$ in

For maximum crack width, c is the distance from the bar surface to a point on the concrete surface midway between bars; that is,

$$c = \sqrt{t_b^2 + (0.5 \text{ bar spacing})^2} - 0.5 \times \text{bar diameter}$$
$$= \sqrt{1.06^2 + 5^2} - 0.31 = 4.80 \text{ in}$$

$$w_{max} = \frac{3 \times 4.80 \times 0.00113}{1 + [2(4.80 - 0.75)/8.02]}$$
$$= 0.0081 \text{ in (0.21 mm)}$$

Note. The maximum crack width calculated from the Beeby equation is 37% less than that calculated from the Gergely–Lutz equation. For lightly reinforced members, the term in Eq. 9.15 which accounts for the stiffening effect of concrete between cracks reduces the average longitudinal steel strain to significantly less than the steel strain at the crack (average longitudinal steel strain = $0.55\varepsilon_s$ in this example), and hence Beeby's equations ca be expected to give lower w_{max} values than the Gergely–Lutz equation i lightly reinforced slabs.

Ref. 1

9.3.4 Computation of Width of Flexural Cracks in Two-Way Slabs

Much less attention has been given in past investigations to the determinatio of the width of flexural cracks in reinforced concrete floors under two-wa bending. The major work conducted in the United States is that by Nawy e al.,[9.26, 9.27] whereas in the United Kingdom it is that by Clark.[9.28]

Approach by Nawy et al. Nawy et al.[9.26, 9.27] have reported the results of test on two-way concrete slabs reinforced by high-strength welded mesh rei forcement. Two distinct types of cracking were observed: an orthogon pattern of cracks which followed the lines of the reinforcement, and a d gonal pattern which at higher loads eventually developed into the yield lin pattern. Nawy et al. explained this behavior by assuming that the steel forc was transferred mainly to the concrete at the node points of the crossin steel. The use of closely spaced small-diameter wires was found to result i the orthogonal crack pattern, whereas the use of widely spaced large diam ter wires led to the diagonal crack pattern. The width of cracks in the ortho onal pattern was found to be smaller than the width of cracks in the diagon pattern, and thus the orthogonal pattern was to be preferred. A "grid index factor was introduced to determine the effect of reinforcing steel spacin diameter and content, and concrete cover thickness, on the crack widt Regression analysis was performed on the results of a range of two-way sl tests, and empirical equations for maximum crack width were proposed. Th equations were also checked against crack widths measured by other inve tigators, including slabs reinforced by deformed bars rather than mesh rei forcement, and it was concluded that the equations gave good agreeme with the experimental crack widths.[9.27] For two-way slabs, flat slabs, an plates, the Nawy–Orenstein equations for maximum crack width may b written as

$$w_{max} = K \beta f_s \sqrt{M_I} \text{ in} \qquad (9.1$$

where K depends on the loading and boundary conditions and can be take as 2.8×10^{-5} for uniformly loaded slabs and plates, $\beta = h_2/h_1$ = ratio distances to the neutral axis from the extreme tension fiber and from th centroid of reinforcing steel, f_s is the steel stress (ksi), and M_I is the gr index, given by

$$M_I = \frac{d_{b1} s_2}{\rho_1} \qquad (9.1$$

where direction 1 is the direction in which the crack width is measure (normal to the crack direction), direction 2 the direction perpendicular t

direction 1, d_{b1} the diameter of bar running in direction 1 (in), s_2 the spacing of bars running in direction 2 (in), and ρ_{t1} the area A_{b1} of bars running in direction 1 divided by the effective area of concrete in tension perpendicular to those bars (1 in = 25.4 mm and 1 ksi = 6.89 N/mm²). The effective area of concrete in tension is the rectangular area extending across the slab which has the same centroid as the reinforcement, and is equal to $2t_{b1}s_1$ for the direction 1 bars, where t_{b1} is the distance from direction 1 bar centroid to extreme tension fiber and s_1 the spacing of direction 1 bars. Therefore, the grid index given by Eq. 9.17 can also be written as

$$M_t = \frac{d_{b1}s_2}{A_{b1}/2t_{b1}s_1} = \frac{2t_{b1}s_1s_2d_{b1}}{A_{b1}} \tag{9.18}$$

Most of the notation is illustrated in Fig. 9.5.

Comparison of the Gergely–Lutz Eq. 9.9 and the Nawy Eq. 9.16 shows them to be quite different in form apart from the linear dependence on the steel stress f_s and position of the steel with respect to the neutral axis and the extreme tension fiber. Nawy and Blair[9.27] claim that Eq. 9.9 considerably underestimates the crack widths in one-way and two-way slabs. However, an alternative view could be that Eq. 9.16 is unduly conservative in some cases. For example, in tests on eight reinforced concrete slabs supported on rectangular columns conducted by Hawkins et al.,[9.29] the average strain in the slab steel over the column face was measured when the crack width there was 0.016 in (0.41 mm).

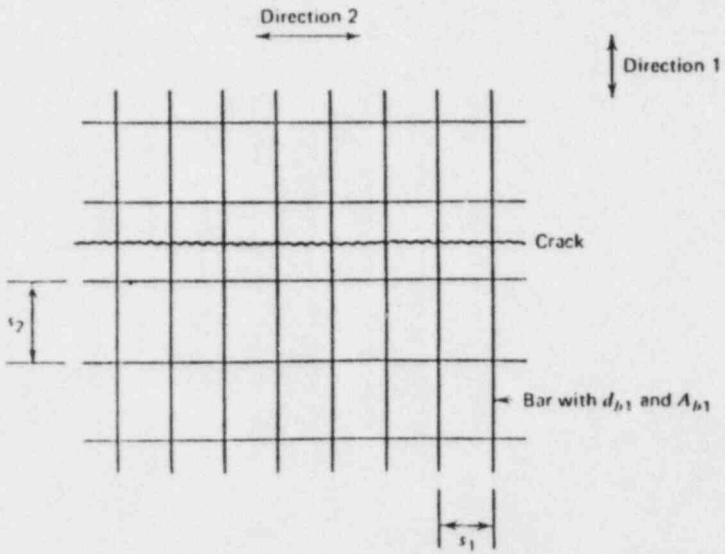

Figure 9.5 Steel arrangement for the determination of the grid index for the Nawy–Orenstein equation.

From these measured steel strains and the slab properties, the maximum crack widths were calculated for each specimen using the Gergely–Lutz Eq. 9.9 and the Nawy–Orenstein Eq. 9.16 (with $K\beta = 3.0 \times 10^{-5}$). The maximum crack widths from the Gergely–Lutz equation ranged between 0.011 and 0.016 in, with a mean of 0.014 in, and from the Nawy–Orenstein equation ranged between 0.010 and 0.023 in, with a mean of 0.018 in. It could be considered that Eq. 9.9 was as adequate as Eq. 9.16 as a design equation in this case. Also, it needs to be borne in mind that tests on multipanel floor systems have shown that the critical cracking takes place principally in negative-moment regions above the faces of the beams in slab and beam floors, and near the columns in flat slab and flat plate floors, whereas the studies of two-way slabs reported by Nawy et al. have principally dealt with positive-moment regions. Certainly, it would appear reasonable to use the Gergely–Lutz equation in regions of slabs where one-way bending was predominant, for example in negative-moment regions when slabs are supported on stiff beams and in slabs at column faces, and in the critical positive-moment regions of rectangular panels. The Nawy–Orenstein equation may be unusable in some of these cases, since the grid index M_t defined by Eq. 9.18 breaks down if s_2 becomes large or if the direction 2 bars are not present (i.e., $s_2 \to \infty$), as can be the case in the negative-moment regions in the middle strips of most slabs.

Example 9.2

If the critical negative-moment section of the slab in Example 9.1 is part of a two-way slab and the reinforcement in each direction is identical, calculate the maximum crack width at the extreme tension fiber using the Nawy–Orenstein equation.

Solution

$$\beta = \frac{h_2}{h_1} = \frac{8.02}{6.96} = 1.15 \qquad K = 2.8 \times 10^{-5}$$

$$f_s = 52 \text{ ksi} \qquad d_{b1} = 0.625 \text{ in} \qquad s_2 = 10 \text{ in}$$

$$\rho_{t1} = \frac{0.31}{10 \times 2 \times 1.06} = 0.0146$$

Therefore, from Eq. 9.16,

$$w_{max} = 2.8 \times 10^{-5} \times 1.15 \times 52 \sqrt{0.625 \times \frac{10}{0.0146}}$$

$$= 0.0346 \text{ in (0.88 mm)}$$

Note that this calculated crack width is 2.7 times the width calculated by the Gergely–Lutz equation and 4.3 times the width calculated by the Beeby equation in Example 9.1. The crack width calculated by the Nawy–Orenstein equation in this example is difficult to understand because it is so high that it implies that the steel is not bonded to the concrete. That is, if the reinforce-

ACI 318-77 Method for One-Way Slabs. The ACI 318-77 method for beams and one-way slabs is based on the Gergely–Lutz equation (Eq. 9.9) with h_2/h_1 put equal to 1.2. The requirement may be written as permissible maximum crack width $\geq 0.076\sqrt[3]{t_b A} \times 1.2 f_s \times 10^{-6}$ in, with t_b in inches, A in square inches, and f_s in psi (1 in = 25.4 mm, 1 psi = 0.00689 N/mm²). Substituting the permissible values for crack widths (0.013 in for interior exposure and 0.016 in for exterior exposure) into the equation gives

$$f_s \sqrt[3]{t_b A} \leq 175{,}000 \text{ lb/in} \qquad \text{for interior exposure} \qquad (9.20a)$$

and

$$f_s \sqrt[3]{t_b A} \leq 145{,}000 \text{ lb/in} \qquad \text{for exterior exposure} \qquad (9.20b)$$

where again the units are inches and pounds. ACI 318-77 requires the section to be proportioned so that either Eq. 9.20a or 9.20b is satisfied. This check need only be carried out when the design yield strength for the reinforcement exceeds 40,000 psi (276 N/mm²). In structures subjected to very aggressive environment or designed to be watertight, Eq. 9.20b does not apply, since a smaller maximum allowable crack width needs to be adopted.

To use Eq. 9.20a or 9.20b, the steel stress f_s at the service load is required. This steel stress may be found from $f_s = M/(jdA_s)$, where M is the service load bending moment, jd the level arm of the internal moment, and A_s the steel area. Alternatively, f_s may be taken as 60% of the specified yield strength of the steel, provided that the moment redistribution from the elastic bending moment diagram assumed in design is not greater than that allowed in ACI 318-77.

The Commentary to the ACI Code[9.2] indicates that the average value for h_2/h_1 is about 1.35 for floor slabs rather than the value of 1.2, which really applies to beams, used to determine Eqs. 9.20a and 9.20b. Accordingly, it would be consistent for thin one-way slabs to reduce the limiting values on the right-hand side of Eqs. 9.20a and 9.20b to 156,000 lb/in for interior exposure and 129,000 lb/in for exterior exposure.

Example 9.3

Check the adequacy of the reinforcement arrangement at the critical negative moment section of the slab in Example 9.1 using the ACI 318-77 approach.

Solution. With reference to Example 9.1, $f_s = 52{,}000$ psi, $t_b = 1.06$ in, and $A = 21.2$ in²/bar. Therefore,

$$f_s \sqrt[3]{t_b A} = 52{,}000 \sqrt[3]{1.06 \times 21.2} = 146{,}700 \text{ lb/in}$$

which, according to Eqs. 9.20a and 9.20b, is adequate for interior exposure and is almost adequate for exterior exposure.

recommended use of the Nawy–Orenstein equation (Eq. 9.16) for crack control in two-way slabs. However, there is no reference to crack control formulas for two-way slabs in either the 1977 ACI Code[9.1] or its Commentary.[9.2] In the absence of such code recommendations it would appear necessary to use an approximate equation, such as the Gergely–Lutz expression, if checks on two-way slabs are necessary.

It is evident that crack widths will not normally be a problem in design unless the steel stresses at service load are very high or the crack widths are to be kept very small. In view of the wide scatter of measured crack widths on structural elements, great accuracy in calculations for crack control cannot be justified. The best crack control is obtained when the reinforcing bars are well distributed over the zone of concrete tension. The aim is to ensure that fine, closely spaced cracks form, rather than a few wide cracks. The ACI Code[9.1] requires the spacing of the reinforcement at critical sections of solid slabs not to exceed two times the slab thickness in order to ensure that bars are not spaced widely apart.

9.4 REFERENCES

9.1 "Building Code Requirements for Reinforced Concrete (ACI 318-77)," American Concrete Institute, Detroit, 1977, 102 pp.

9.2 "Commentary on Building Code Requirements for Reinforced Concrete (ACI 318-77)," American Concrete Institute, Detroit, 1977, 132 pp.

9.3 W. G. Corley, J. M. Hanson, and T. Helgason, "Design of Reinforced Concrete for Fatigue," *J. Struct. Div., ASCE*, Vol. 104, No. ST6, June 1978, pp. 921–932.

9.4 A. R. Lord, "Extensometer Measurements in a Reinforced Concrete Building over a Period of One Year," *Proc. ACI*, Vol. 13, 1917, pp. 45–60.

9.5 P. J. Taylor and J. L. Heiman, "Long-Term Deflection of Reinforced Concrete Flat Slabs and Plates," *Proc. ACI*, Vol. 74, November 1977, pp. 556–561.

9.6 P. J. Taylor, "Initial and Long-Term Deflections of a Reinforced Concrete Flat Plate Structure," *Civ. Eng. Trans., Inst. Eng. Aust.*, Vol. CE12, No. 1, April 1970, pp. 14–20.

9.7 F. A. Blakey, "Deformations of an Experimental Lightweight Flat Plate Structure," *Civ. Eng. Trans., Inst. Eng. Aust.*, Vol. CE3, No. 1, March 1961, pp. 18–22.

9.8 F. A. Blakey, "Deflection as a Design Criterion in Concrete Buildings," *Civ. Eng. Trans., Inst. Eng. Aust.*, Vol. CE5, No. 2, September 1963, pp. 55–58.

9.9 R. K. Agarwal and N. J. Gardner, "Form and Shore Requirements for Multistorey Flat Slab Type Buildings," *Proc. ACI*, Vol. 71, November 1974, pp. 559–569.

9.10 P. Grundy and A. Kabaila, "Construction Loads on Slabs with Propped Formwork in Multistorey Buildings," *Proc. ACI*, Vol. 60, December 1963, pp. 1729–1738.

9.11 P. J. Taylor, "Effects of Formwork Stripping Time on Deflections of Flat Slabs and Plates," *Aust. Civ. Eng. Constr.*, Vol. 8, No. 2, February 1967, pp. 31–35.

9.12 F. D. Beresford, Discussion of "Effects of Formwork Stripping Time on Deflections of Flat Slabs and Plates," *Aust. Civ. Eng. Constr.*, Vol. 8, No. 5, May 1967, p. 61.

9.13 "Collapse Blamed on Premature Shore Removal," *Eng. News-Rec.*, Vol. 190, No. 16, April 19, 1973, p. 11. Also March 8, 1973, p. 12; March 15, 1973, p. 12.

9.14 E. V. Leyendecker and S. G. Fattal, "Investigation of the Skyline Plaza Collapse in Fairfax County, Virginia," National Bureau of Standards, U.S. Dept. of Commerce, Building Science Series No. 94, February 1977, 95 pp.

ment is not bonded to the concrete, the calculated crack width at the level of the steel would be $w_{max}\, h_1/h_2 = 0.0346 \times 6.96/8.02 = 0.0300$ in (0.76 mm), which is equal to the extension of steel uniformly stressed to 52 ksi (359 N/mm²) over a length of 0.0300/(52/29,000) = 16.7 in (424 mm). The maximum crack spacing for unbonded reinforcement tends toward $2h_0 = 2 \times 8.02 = 16.0$ in (406 mm) for this slab, according to Beeby's work outlined in Section 9.3.3. However, the bars are not unbonded, and therefore crack spacing should be smaller than calculated above. In fact, the transverse steel spacing s_2 is implicitly assumed by Nawy et al. to be the crack spacing. Therefore, the maximum crack width should be much smaller than calculated above. Hence, it would seem that the Nawy–Orenstein equation can very greatly overestimate the maximum crack widths under some common conditions.

Approach by Clark. Clark[9.28] has reported the results of theoretical and experimental studies of one-way spanning slabs with bars at various angles to the direction of moment, this simulating regions of two-way slabs with bending predominantly in one direction. In the proposed method of crack width prediction, the equivalent area of steel normal to the crack direction was found using the following relationship determined by Lenschow[9.30] for slabs cracked in one direction:

$$A_n = \sum_{i=1}^{m} A_i \cos^4 \alpha_i \tag{9.19}$$

where A_i is the area of the ith layer of steel, α_i the angle between the normal to the crack and the direction of the ith steel layer, and m the number of steel layers. Once the equivalent area of steel normal to the crack is found using Eq. 9.19, the neutral-axis depth and steel stress can be found from elastic theory, and then Beeby's equation used to predict the maximum crack width. Reasonable agreement with experimentally obtained crack widths was obtained by Clark. An interesting result from the tests was that for slabs with bars in various directions there was apparently little interaction between the bars apart from contributing to the equivalent area of steel normal to the crack. For example, the crack control obtained from a slab reinforced only perpendicular to the cracks was little different from that obtained when bars were also placed parallel to the cracks.

Calculation of Steel Stress. To apply the crack-width equations to two-way slabs, the bending moment at the cracked sections is required so that the steel stresses may be calculated. Elastic theory for slabs may be used to determine the bending moment in the service load range, but it should be kept in mind that cracking will cause some redistribution of moments from that calculated for an uncracked slab even though the slab is in the elastic range.

9.3.5 Code Provisions for Crack Control

Permissible Crack Widths. The permissible values for the width of flexural cracks in practice depend mainly on the environment in which the structure has to serve, particularly from the point of view of the possibility of corrosion of the reinforcement. The permissible values recommended by ACI Committee 224[9.31] are listed in Table 9.4.

In comparison with these values the crack control equations of ACI 318-77[9.1] are based on only two maximum allowable crack widths, 0.016 in (0.41 mm) for interior exposure and 0.013 in (0.33 mm) for exterior exposure. According to the Commentary[9.2] these limiting crack widths were chosen primarily to give reasonable reinforcing details in terms of practical experience with existing structures. However, the Code does warn that these limiting values may not be sufficient for structures subjected to aggressive exposure or designed to be watertight, and that for such structures special investigations and precautions are required. Although clear experimental evidence is not available regarding the maximum crack widths beyond which danger of corrosion exists, it is evident that Table 9.4 could be taken as a guide. However, as is evident from the discussion in Section 9.3.1, protection against corrosion is not just a matter of limiting the surface crack width in the concrete. A reasonable thickness of good-quality, well-compacted concrete is also essential for durable structures.

It is also worth noting that the British code of practice CP 110:1972[9.32] requires in general that the surface crack widths at service load not exceed 0.3 mm (0.012 in) except where members are subjected to particularly aggressive environment. The recommendations of the European Concrete Committee–International Federation of Prestressing[9.33] require that the surface crack widths at the service load not exceed 0.1 mm (0.004 in) in a very exposed (particularly aggressive) environment, 0.2 mm (0.008 in) in an unprotected environment (external member in bad weather conditions or internal member in a damp or aggressive environment), or 0.3 mm (0.012 in) in a protected environment (internal member in normal surroundings).

Table 9.4 Permissible Crack Widths in Reinforced Concrete[a]

Exposure Condition	Maximum Allowable Crack Width [in (mm)]
Dry air or protective membrane	0.016 (0.41)
Humidity, moist air, soil	0.012 (0.30)
Deicing chemicals	0.007 (0.18)
Seawater and seawater spray, wetting and drying	0.006 (0.15)
Water-retaining structures	0.004 (0.10)

[a] From Ref. 9.31.

15 M. D. Vanderbilt, "Deflections of Reinforced Concrete Floor Slabs," Ph.D. Thesis, University of Illinois at Urbana-Champaign, 1963, 287 pp. Also issued as Civil Engineering Studies, Structural Research Series No. 263, Department of Civil Engineering, University of Illinois, Urbana, Ill.

16 M. D. Vanderbilt, M. A. Sozen, and C. P. Siess, "Deflections of Multiple-Panel Reinforced Concrete Floor Slabs," *J. Struct. Div., ASCE*, Vol. 91, No. ST4, August 1965, pp. 77–101.

17 J. C. Jofriet, "Short Term Deflections of Concrete Flat Plates," *J. Struct. Div., ASCE*, Vol. 99, No. ST1, January 1973, pp. 167–182.

18 S. Timoshenko and S. Woinowsky-Krieger, *Theory of Plates and Shells*, 2nd ed., McGraw-Hill, New York, 1959, 580 pp.

19 J. F. Brotchie and A. J. Wynn, "Elastic Deflections and Moments in an Internal Panel of a Flat Plate Structure—Design Information," Division of Building Research Technical Paper (Second Series) No. 4, Commonwealth Scientific and Industrial Research Organization, Melbourne, Australia, 1975, 168 pp.

20 ACI Committee 435, "Deflection of Two Way Reinforced Concrete Floor Systems, State-of-the-Art," *Deflections of Concrete Structures*, ACI Special Publication 43, American Concrete Institute, Detroit, 1974, pp. 55–81.

9.21 R. Park and T. Paulay, *Reinforced Concrete Structures*, Wiley, New York, 1975, 769 pp.

9.22 P. Gergely and L. A. Lutz, "Maximum Crack Width in Reinforced Flexural Members," *Causes, Mechanism and Control of Cracking in Concrete*, ACI Special Publication 20, American Concrete Institute, Detroit, 1968, pp. 87–117.

9.23 J. P. Lloyd, H. M. Rejali, and C. E. Kesler, "Crack Control in One-Way Slabs Reinforced with Deformed Welded Wire Fabric," *Proc. ACI*, Vol. 66, May 1969, pp. 366–376.

9.24 A. W. Beeby, "An Investigation of Cracking in Slabs Spanning One Way," Technical Report TRA 433, Cement and Concrete Association, London, April 1970, 33 pp.

9.25 A. W. Beeby, "Prediction and Control of Flexural Cracking in Reinforced Concrete Members," *Cracking, Deflection and Ultimate Load of Concrete Slab Systems*, ACI Special Publication 30, American Concrete Institute, Detroit, 1971, pp. 55–75.

9.26 E. G. Nawy and G. S. Orenstein, "Crack Width Control in Reinforced Concrete Two-Way Slabs," *J. Struct. Div., ASCE*, Vol. 96, No. ST3, March 1970, pp. 701–721.

9.27 E. G. Nawy and K. W. Blair, "Further Studies on Flexural Crack Control in Structural Slab Systems," *Cracking, Deflection and Ultimate Load of Concrete Slab Systems*, ACI Special Publication 30, American Concrete Institute, Detroit, 1971, pp. 1–41.

9.28 L. A. Clark, "Flexural Cracking in Slab Bridges," Technical Report 42.479, Cement and Concrete Association, London, May 1973, 12 pp.

9.29 N. M. Hawkins, H. B. Fallsen, and R. C. Hinojosa, "Influence of Column Rectangularity on the Behaviour of Flat Plate Structures," *Cracking, Deflection and Ultimate Load of Concrete Slab Systems*, ACI Special Publication 30, American Concrete Institute, Detroit, 1971, pp. 127–146.

9.30 R. J. Lenschow, "A Yield Criterion for Reinforced Concrete under Biaxial Moments and Forces," Ph.D. Thesis, University of Illinois at Urbana Champaign, 1966, 527 pp. Also issued as Civil Engineering Studies, Structural Research Series No. No. 311, Department of Civil Engineering, University of Illinois, Urbana, Ill.

9.31 ACI Committee 224, "Control of Cracking in Concrete Structures," *Proc. ACI*, Vol. 69, December 1972, pp. 717–753.

9.32 BSI, "Code of Practice for the Structural Use of Concrete, CP110: Part 1: 1972," British Standards Institution, London, 1972, 154 pp.

9.33 CEB-FIP, "CEB-FIP Model Code for Concrete Structures," International System of Unified Standard Codes of Practice for Structures, Vol. II, Comité Euro-International du Béton/Federation International de la Précontrainte, Paris (English translation), April 1978, 348 pp.

9.34 "Commentary on Building Code Requirements for Reinforced Concrete (ACI 318-71)," American Concrete Institute, Detroit, 1971, 96 pp.

Chapter Ten

SHEAR STRENGTH OF SLABS

10.1 INTRODUCTION

In previous chapters only the flexural behavior of reinforced concrete slabs has been considered. Shear is generally not critical when slabs carry distributed loads or line loads and are supported by beams or walls, because in such cases the maximum shear force per unit length of slab is relatively small. However, shear can be critical in slabs in the vicinity of concentrated loads, because the maximum shear force per unit length of slab is relatively high around such loads. Concentrated loads can be applied to slabs by the transfer of forces: (1) from slab to columns in flat plate and flat slab floors, (2) from columns to footings, and (3) from applied loads such as wheel loads. The moments induced by concentrated loads on slabs in the elastic range were considered in Chapters 2 and 3. The flexural strength of slabs carrying concentrated loads was considered in Chapters 6, 7, and 8.

In many cases the shear stresses in slabs around concentrated loads can be more critical than the flexural stresses, and shear then governs the design. This is particularly true of slab–column connections in flat plate and flat slab floors where the size of the column, or column capital, and the slab thickness, may be governed by the magnitude of the shear force to be transferred.

The shear strength of slabs (or footings) in the vicinity of concentrated loads is governed by the more severe of two conditions, either beam action or two-way action.

Beam Action. In beam action the slab fails as a wide beam with the critical section for shear extending along a section in a plane across the entire width of the slab (or footing). In this case the slab should be treated as a wide beam and the shear strength equations for beams of the ACI Code[10.1] apply. It is to be noted that the Code assumes that the critical section for shear in beam action is located at d from the face of the column or applied load (or from the face of a line load or supporting beam or wall), where d is the distance from the extreme compression fiber to the centroid of the longitudinal tension reinforcement. In fact, the critical section passes through the critical diagonal tension crack across which failure is considered to occur. Therefore, for this type of shear failure conventional theory for beam shear applies (see, e.g., Ref. 10.2) and the theory will not be discussed further here.

d = distance between members;
E = Youngs modulus of elasticity;
E_s = secant modulus based upon the axial stress in the members;
I = member moment of inertia;
L = member lengths;
M_p = plastic moment capacity of the joint;
M_ϕ = Meridional bending moment;
N_θ, N_ϕ, $N_{\theta\phi}$ = shell membrane stresses per unit length of shell;
$N_{\phi s}$ = primary membrane meridional stress at the springline;
$N_{\theta s}$ = primary membrane circumferential stress at the springline;
n = the number of members meeting at the joint;
P = concentrated load applied at a joint;
P_1, P_2, P_3 = member forces;
p_{cr} = critical buckling pressure;
Q_ϕ = shearing force at the shell boundary;
R = shell radius of curvature;
r = base ring radius;
t_B = effective shell bending thickness;
t_m = effective shell membrane thicknesses;
V = rotation of a tangent to the meridian at the shell boundary;
α = $\phi_s - \phi$;
δ = secondary deflection;
Δ = deflection from a perfect surface;
ΔT = change in tension of the base ring;
ϕ = angle enclosed by the shell axis of rotation, the spherical center and any point on the surface;
ϕ_s = ϕ at the springline; and
σ_{cr} = $p_{cr}R/2\ t_m$.

Journal of the
STRUCTURAL DIVISION
Proceedings of the American Society of Civil Engineers

CRACK WIDTH CONTROL IN REINFORCED CONCRETE TWO-WAY SLABS

By Edward G. Nawy,[1] F. ASCE, and Glenn S. Orenstein,[2] A. M. ASCE

INTRODUCTION

Most existing research (2,6,9,10)[3] deals with the crack width studies in beams and one-way members. This investigation covers the effect of two-way action on crack width development in reinforced concrete slabs. It also determines the manner in which such behavior is affected by varying to extremes the diameter and spacing of the mesh reinforcement and the pattern of the welded joints of the mesh. Accordingly, a criterion is developed for limiting the crack width of the critical, namely, controlling cracks to levels acceptable for permissible reinforcement protection, deflection and esthetics.

Both experimental and analytical studies of the cracking problem in two-dimensional members have been made. The principal factors considered were the diameter and spacing of the wire and its welded joints, and the concrete stretched area which is a function of the concrete cover. The experimental part covers two series of tests to destruction. The first series involved tests of 22 slabs of 5-ft 8-in. × 5-ft 8-in. clear span and loaded centrally on an area 6 in. × 6 in. Twelve of the slabs tested were simply supported and 10 were clamped on all boundaries. The second series involved tests to destruction of 32 slabs 6-ft 0-in. × 6-ft 0-in. clear span uniformly loaded and fully clamped at all edges. The first series was reinforced with plain high strength welded mesh reinforcement of diameter varying from 0.192 in. to 0.331 in., and spacings of welded joints from 4 in. × 4 in. to 8 in. × 8 in. to 6 in. × 12 in., while most of the slabs in the second series were reinforced with deformed mesh reinforcement of comparable size and spacing.

The analytical part of the investigation was based on formulating a hypoth-

Note.—Discussion open until August 1, 1970. To extend the closing date one month, a written request must be filed with the Executive Secretary, ASCE. This paper is part of the copyrighted Journal of the Structural Division, Proceedings of the American Society of Civil Engineers, Vol. 96, No. ST3, March, 1970. Manuscript was submitted for review for possible publication on March 21, 1969.

[1] Prof. of Civ. Engrg., Rutgers Univ., New Brunswick, N.J.
[2] Engr., U.S. Army Waterways Experiment Sta., Vicksburg, Miss.

[3] Numerals in parentheses refer to corresponding items in the Appendix I.—References.

esis on the cracking pattern development in two-dimensional concrete structural members. A mathematical model resulted, which was subjected to reasonable experimental verification and proved valid. The analytical work resulted in cracking equations suitable for crack control in two-way slabs both centrally and uniformly loaded and of varying degree of restraint at the supporting boundaries. A grid index has been proposed as a guide for governing the primary failure pattern which controls the crack width.

FRACTURE HYPOTHESIS IN TWO-WAY SLABS

On the basis of the crack pattern developed in this research program, it was proposed by the senior writer that stress concentration develops initially at the welded joints of the wire fabric. The welded joints are being termed as nodal points, such as A_1, B_1, A_2, B_2 in Fig. 1. The stress concentration causes plastic deformation of the concrete in the zone of the welds. The bond between the wire and the concrete at these locations is destroyed, and active cleavages start to generate fracture lines towards paths of least resistance, in the slab zones between C_1C_1 and C_2C_2.

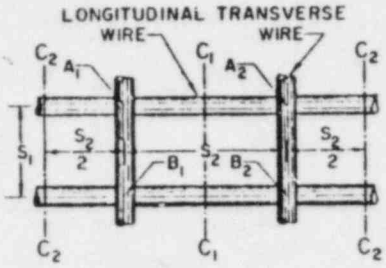

FIG. 1.—ONE UNIT OF WELDED REINFORCEMENT GRID

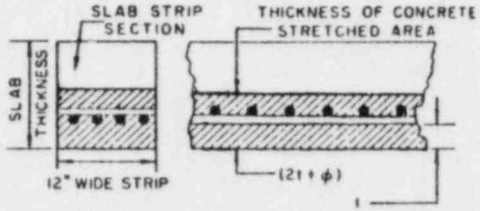

FIG. 2.—CONCRETE TENSILE STRETCHED AREA

Active cleavages develop (1,5) at points A_1, B_1, A_2, B_2 and propagate from these centers along the planes of discontinuity. The planes of discontinuity which are paths of least resistance are the interaction surfaces between the mesh lines and the surrounding gel, namely, A_1B_1, A_1A_2, A_2B_2 and B_2B_1. The result is a total cracking grid of repetitive or frequency lattice on the tensile face of the two-way slab generated from the central portion of the specimen.

If the spacing of the nodal points, namely the fabric welded joints, is large and the active steel ratio, p_t, is low, the magnitude of stress concentration at the welds would be low, no active cleavages form, the bond is not destroyed and the principal cracks follow diagonal yield line cracking early in the loading history, with fewer, but wider cracks. Consequently, proper choice of size and spacing of the fabric can produce a forced cracking grid spacing thereby controlling the width of the cracks.

If the intersecting longitudinal and transverse reinforcing wires are free or tied instead of being welded, as in the case when bars are used, crack control would not be as effective. Stress concentration would be lower at such intersections, and pronounced localized destruction of the concrete at these intersections is less likely. Thus a forced fracture grid under these conditions is more difficult to accomplish.

This hypothesis also leads to the conclusion that deformations on the surface of the wire between the nodal points for small size wire have little effect in arresting or resisting the generation of the cracks from the nodal points, and even less so in the case of primary yield line cracks.

In relating the orthogonal cracks to the yield line cracks, remember that regardless of the pattern of crack generation in two-way slabs, the failure of the slab follows ultimately the generally accepted rigid-plastic failure proposed by Johansen and extended by others. Crack width, however, particularly at service load conditions, is governed by the crack pattern and spacing resulting from the stress distribution in the planner structure, which is in the semi-elastic state. With a larger number and more extensive pattern of orthogonal cracking which can potentially form, the yield line cracks would tend to be finer in width when they form. The energy required to cause the slab to reach its capacity would be higher, and failure would consequently be more ductile and delayed. Therefore, with a proper reinforcement grid pattern and proper distribution of nodal points, the final yield line mechanisms of slab collapse can be made to spread into wide hinge fields of finer cracks.

MATHEMATICAL MODEL AND CRACKING EQUATIONS FOR TWO-WAY SLABS

Fundamental Formulation of Model.—If the distance between two adjacent cracks is a_c, the width of each of the two cracks would be a function of the difference in elongation between the reinforcement and the surrounding stretched concrete over length a_c. From a practical viewpoint, elongation of the concrete and shrinkage strain can be neglected (see Thomas in Ref. 10). Thus

$$w = \propto a_c^{\beta} \epsilon_s^{\gamma} \quad \ldots\ldots\ldots\ldots\ldots\ldots\ldots\ldots\ldots\ldots\ldots\ldots\ldots\ldots\ldots\ldots\ldots\ldots (1)$$

The value of γ depends partly on whether the reinforced member is one or two-dimensional. Previous investigators (10) have shown that a_c varies as $1/k_u$; $k_2 f_t'$; and $\phi_1/(k_3 p_{t_1})$; in which p_t = active steel ratio = A_s/A_t and A_t = concrete stretched area, as defined by Odman in Ref. 2, and as shown in Fig. 2, which is reasonably applicable to two-way slabs. Therefore, $A_t = 12(2t_1 + \phi_1)$ is used in this investigation for a 12-in. strip of the slab. In the orthogonal direction, concrete stretched area $A_{t_2} = 12(2t_2 + \phi_2)$. Table 1 gives test data of the concrete stretched areas, active steel ratios, and grid indexes of all the slabs tested.

It may be assumed from the fracture hypothesis previously outlined that a_c varies as $(k_4 s_2)^{\beta}$. Consequently, the crack spacing, a_c, of flexural cracks can vary as $k_5/k_1 u\ k_2 f_t'\ (k_4\phi_1 s_2/k_3 p_{t_1})^{\beta}$, in which the k terms are constants, subscript 1 denotes the longitudinal direction, the subscript 2 denotes the transverse direction at right angles to 1. Also $u = k_c \sqrt{f_c'}$ as given by the ACI Code 318-63. The ratio $f_t'/\sqrt{f_c'}$ varied in this investigation from 5.57 to 7.80 with a mean of 6.08. Since simplification for the purpose of using the expression by the design engineer warrant considering this ratio of $f_t'/\sqrt{f_c'}$ as constant, Eq. 1 can therefore be rewritten, lumping all the previous parameters to get

$$w = k_6 \left(\frac{\phi_1 s_2}{p_{t_1}}\right)^{\beta} f_{s_1}^{\gamma} \quad \ldots\ldots\ldots\ldots\ldots\ldots\ldots\ldots\ldots\ldots\ldots\ldots\ldots\ldots\ldots\ldots\ldots\ldots (2)$$

TABLE 1.—PROPERTIES OF CONCRETE STRETCHED CRACKED ZONES

Slab designation (1)	Failure load, P_u, in pounds (2)	Concrete stretched area, A_{t_1}, in square inches (3)	Concrete stretched area, A_{t_2}, in square inches (4)	Cover factor, R (5)	Active steel ratio, p_{t_1}, as a percentage (6)	Active steel ratio, p_{t_2}, as a percentage (7)	Grid index, $I_1 = \phi_1 s_2 / p_{t_1}$ (8)	Grid index, $I_2 = \phi_2 s_1 / p_{t_2}$ (9)	Flexural failure load divided by theoretical load (10)	Controlling initial cracking pattern[a] (11)
SA1	25,000	18.52	21.45	1.20	0.755	0.652	129.1	150.0	1.03	O
SA2	23,900	18.52	21.45	1.20	0.755	0.652	129.1	149.4	1.09	O
SA3	27,000	18.52	21.45	1.20	0.755	0.652	129.1	149.4	1.36	O
SB1	18,000	29.17	33.14	1.50	0.442	0.389	508.6	740.7	1.22	YL
SB2	22,000	26.77	24.74	1.20	0.621	0.521	432.4	508.3	1.11	YL
SC1	13,000	28.12	31.05	1.40	0.249	0.225	783.6	865.0	1.28	YL
SC2	12,200	26.92	29.85	1.40	0.260	0.234	750.1	831.7	1.38	YL
SD1	12,000	16.70	18.16	1.20	0.648	0.159	486.1	722.7	1.16	YL
SD2	14,300	16.41	19.85	1.20	0.588	0.146	535.9	790.1	1.30	YL
SE1	27,800	25.61	29.59	2.60	1.008	0.873	131.4	151.8	1.23	O
SE2	53,500	12.37	16.34	1.10	2.087	1.579	83.5	83.8	1.27	O
SE3	41,000	19.57	23.54	1.20	1.319	1.006	108.9	131.0	1.02	O
CSF1	49,700	18.38	22.36	1.50	1.407	1.155	94.1	114.7	0.78	O
CSF2	57,600	18.49	22.34	1.40	1.433	1.189	92.4	112.6	1.01	O
CSG1	43,400	17.67	21.84	1.20	0.730	0.598	358.2	445.2	1.31	YL
CSG2	40,600	12.15	16.20	1.10	1.073	0.808	248.1	329.6	1.22	YL
CSH1	41,500	15.65	18.29	1.20	0.881	0.755	110.3	128.9	1.15	O
CSH2	41,000	14.68	17.61	1.20	0.940	0.770	110.1	126.6	1.16	O
CSI1	37,000	12.50	15.41	1.10	0.556	0.452	347.9	427.6	1.68	YL
CSJ1	41,300	13.72	16.63	1.10	0.993	0.413	106.1	235.7	1.28	O-YL
CSJ2	41,000	19.72	22.44	1.30	0.706	0.303	257.1	321.1	1.36	YL- O
CSK1	30,900	11.90	15.05	1.10	0.902	0.191	340.7	603.1	1.21	YL
WS1	119,600	13.20	18.96	1.30	1.05	0.73	92.4	132.8	1.32	O
WS2	104,100	13.20	18.96	1.30	1.05	0.73	92.4	132.8	1.15	O
WS3	98,600	10.56	7.44	1.20	0.57	0.81	111.6	78.4	2.10	O
WS4	79,600	7.44	10.56	1.20	0.81	0.57	78.4	111.6	1.70	O
WS5	104,800	22.80	26.40	1.50	0.26	0.23	244.8	276.8	2.00	O-YL
WS6	105,000	26.40	22.80	1.50	0.23	0.26	276.8	244.8	2.62	O-YL
WS7	81,200	10.56	15.12	1.20	1.17	0.58	65.2	131.6	1.12	O
WS8	84,000	10.56	10.56	1.20	1.17	0.58	65.2	131.6	1.15	O
WS9	73,700	18.00	24.00	1.40	0.48	0.36	159.2	212.4	1.14	O-YL
WS10	82,900	18.00	24.00	1.85	0.48	0.36	159.2	212.4	1.28	O-YL
WS11	85,400	9.00	13.51	1.20	0.77	0.51	251.2	379.2	2.32	YL
WS12	81,000	9.00	13.51	1.10	0.77	0.51	251.2	379.2	2.21	YL
WS13	105,900	30.00	36.00	2.00	0.43	0.36	610.0	736.0	1.40	YL
WS14	109,500	24.00	30.00	1.90	0.54	0.43	480.6	610.0	1.35	YL
WS15	74,100	25.51	30.00	1.80	0.25	0.21	260.2	308.8	2.24	YL- O
WS16	63,100	16.30	18.00	1.30	0.39	0.36	186.4	185.2	1.88	O-YL
WS17	65,300	16.30	18.00	1.30	0.39	0.36	186.4	185.2	1.74	O-YL
WS18	65,300	27.00	31.49	1.70	0.23	0.20	281.8	324.0	2.02	YL
WS19	68,300	28.49	33.00	1.80	0.30	0.24	160.0	188.9	1.28	YL
WS20	73,000	18.00	15.00	1.30	0.44	0.53	108.6	90.0	1.40	O
WS21	73,000	18.00	15.00	1.30	0.44	0.53	108.6	90.0	1.26	O
WS22	71,900	25.51	22.46	1.60	0.31	0.36	153.9	132.6	1.26	O
WS23	68,300	18.00	24.00	1.40	0.33	0.25	192.8	264.4	1.63	YL
WS24	62,700	30.00	33.00	1.80	0.20	0.22	318.0	298.2	1.76	YL
WS25	84,700	27.00	21.00	1.20	0.26	0.66	372.4	290.4	1.25	YL
WS26	74,500	27.00	24.00	1.60	0.26	0.58	372.4	333.6	1.54	YL
WS27	79,200	21.00	18.00	1.40	0.32	0.78	268.0	231.0	1.73	YL
WS28	84,000	24.00	18.00	1.40	0.20	0.74	339.6	261.6	1.48	YL
WS29	73,000	30.00	27.00	1.80	0.31	0.34	468.6	427.2	1.80	YL
WS30	70,800	33.00	30.00	1.90	0.28	0.31	518.4	468.6	1.81	YL
WS31	68,300	18.00	15.00	1.30	0.51	0.61	285.0	238.2	1.24	YL
WS32	77,600	18.00	15.00	1.30	0.51	0.61	285.0	238.2	1.40	YL
							Mean		1.445	
							SD		0.390	

[a] O = Orthogonal; YL = Yield Line.

The steel strain in Eq. 1 was converted to steel stress f_s in Eq. 2. If the term defining wire spacing and the active steel ratio, namely $\phi_1 s_2 / p_{t_1}$, is called the grid index, because it describes numerically and conveniently the mesh pattern and the concrete stretched area, then it can be considered herein that there are two stochastically independent parameters; the steel stress and the grid index.

TESTING PROGRAM

Control Tests.—High early-strength cement was used in the mix. Graded crushed stone of maximum size 3/4 in. and local graded sand were used. The water content varied between 4.9 gal and 6.6 gal of total water per bag of cement. The mix was vibrated with electric vibrators in the forms and the specimens were cured for a period varying between 3 days and 86 days in the different specimens, as shown in Table 2. Six control cylinders 6 in. in diam and 12 in. high were taken from each slab mix, cured under the same curing conditions as the test slabs, and tested the same day that the corresponding slab was tested. Half the cylinders were tested in compression and the other half in tensile splitting.

Control specimens were also taken from the wire reinforcement of each slab and instrumented with SR-4 electric strain gages. Three control specimens were then tested for tensile strength for each wire size and slab, and the stress-strain diagrams for the different wire sizes were plotted. The yield strength varied from 67,500 psi to 96,600 psi. The ultimate strength varied from 80,000 psi to 101,630 psi. Shear reinforcement was also provided in the form of horizontal mats and vertical cages for the centrally loaded slabs series. They were used to prevent any premature failure in these slabs by punching shear.

TESTING SETUP

Simply Supported Centrally Loaded Slabs.—The slabs were simply supported on all four sides on a 2-in. wide strip. The clear span in each direction was 5 ft 8 in. and the overall dimensions were 6 ft 2 in. × 6 ft 2 in. Corners were not held down. Load was applied through a hydraulic pressure ram system through hydraulic jacks to a ram 5 in. in diam and having a travel of 6 in. The load was transmitted to the slab through a steel rigid platten having an area of 6 in × 6 in.

Twelve slabs were tested in this group. The total thickness varied from 3.6 in to 4.1 in. The effective depth varied from 1.8 in. to 3.75 in. All specimens in this series were reinforced with plain high strength wire mesh welded at the joints. The mesh in each slab was instrumented with SR-4 electric gages at all critical locations. One layer of mesh was used in the bottom of each slab, and shear reinforcement was also provided over an area 24 in. × 24 in. at the center.

Clamped Centrally Loaded Slabs.—The clamped slabs in this series were 7 ft 10 in. × 7 ft 10 in. in overall area, while the clear span was 5 ft 8 in. × 5 ft 8 in. Each slab contained three holes equally spaced at each of the four sides outside the support area, so that 12 holes were provided in each slab. These holes permitted clamping rods to pass through to the testing frame for an-

TABLE 2.—GENERAL PROPERTIES OF SLABS TEST SPECIMENS[a]

Slab designation (1)	Water cement ratio, in U.S. gallons per sack (2)	Average slump, in inches (3)	Age at test, in days (4)	Cylinder compressive strength, f'_c, in pounds per square inch (5)	Cylinder tensile splitting strength, f_t, in pounds per square inch (6)
SA1	5.9	1-3/4	7	4420	365
SA2	6.1	9-1/2	14	4060	360
SA3	5.8	1-3/4	13-1/2	5275	515
SB1	6.0	2-1/4	11	5660	450
SB2	6.6	3-1/2	12	4470	370
SC1	6.2	3-3/4	9-1/2	4270	470
SC2	6.5	5-1/3	12	4500	470
SD1	5.9	2-1/2	11	5340	515
SD2	5.8	3	13	5300	540
SE1	5.6	3	12	5530	510
SE2	6.3	7-1/2	11	3810	410
SE3	6.3	6-1/2	11	4340	505
CSF1	5.1	5-1/4	6-1/2 m	5770	540
CSF2	5.8	3-3/4	12	5000	535
CSG1	5.3	3	12	4520	425
CSG2	6.3	3-1/4	9	4060	390
CSH1	4.9	2-1/2	9	3980	470
CSH2	5.7	1-3/4	10	5360	570
CSI1	6.1	2-1/2	17	5010	550
CSJ1	6.2	1-7/8	17	5710	560
CSJ2	6.5	1-1/2	17	5100	560
CSK1	5.9	2	16	4990	530
WS1	8.2	8	86	3300	280
WS2	8.2	8	80	3360	280
WS3	6.6	3-1/2	42	4870	535
WS4	6.6	3-1/2	50	4870	535
WS5	4.2	2	32	5840	570
WS6	4.2	2	41	5880	570
WS7	6.1	8	64	2830	335
WS8	6.1	8	64	2830	335
WS9	7.5	7	53	4170	450
WS10	7.5	7	53	4170	450
WS11	8.6	7	55	4400	470
WS12	8.6	7	55	4400	470
WS13	7.5	7	55	4070	410
WS14	7.5	7	55	4070	410
WS15	7.6	7-1/2	40	3930	420
WS16	7.5	7	48	4530	420
WS17	7.5	7	48	4530	420
WS18	7.6	7-1/2	40	3930	420
WS19	6.5	6	49	4850	500
WS20	7.5	7	44	4420	440
WS21	7.5	7	45	4420	440

Total center thickness, in inches (7)	Central d_1, in inches (8)	Wire gage (9)	Wire diameters, ϕ_1/ϕ_2, in inch per inch (10)	Wire spacing $S_1 \times S_2$, in inches (11)	Wire yield strength, 0.2% offset, in pounds per square inch (12)	Center-line deflection at ultimate load, in inches (13)
3.85	3.20	#3	0.2437	4 × 4	96000	1.62
3.75	3.10	#3	0.2437	4 × 4	88100	1.95
3.65	3.00	#3	0.2437	4 × 4	80500	1.34
3.60	2.55	#2-0	0.3310	8 × 8	75900	1.42
3.95	3.25	#2-0	0.3310	8 × 8	78400	1.63
3.95	2.90	#3	0.2437	8 × 8	80600	2.16
3.60	2.60	#3	0.2437	8 × 8	82700	2.31
4.10	3.50	#2/#6	0.2625/ 0.1920	6 × 12	94200	1.46
4.00	3.40	#2/#6	0.2625/ 0.1920	6 × 12	95700	1.50
4.10	1.80	#2-0	0.3310	4 × 4	84200	1.95
4.10	3.75	#2-0	0.3310	4 × 4	77600	1.38
4.10	3.45	#2-0	0.3310	4 × 4	82100	1.22
3.45	2.85	#2-0	0.3310	4 × 4	86700	0.29
3.64	2.67	#2-0	0.3310	4 × 4	86850	0.33
3.45	2.88	#2-0	0.3327	8 × 8	85100	0.76
3.30	2.96	#2-0	0.3325	8 × 8	78440	0.86
3.45	2.93	#3	0.2437	4 × 4	83120	0.65
3.45	2.96	#3	0.2437	4 × 4	82050	0.68
3.50	3.20	#3	0.2420	8 × 8	80950	1.11
3.40	2.95	#3	0.2430	4 × 8	81900	0.70
3.40	2.70	#3	0.2432	4 × 8	83550	0.80
3.20	2.80	#2/#6	0.2624/ 0.1920	6 × 12	88500	1.18
3.00	2.45	D4.6	0.242	4 × 4	83500	1.40
3.00	2.45	D4.6	0.242	4 × 4	83500	1.48
3.00	2.56	D2.0	0.159	4 × 4	86500	1.18
3.00	2.69	D2.0	0.159	4 × 4	86300	1.52
3.00	2.05	D2.0	0.159	4 × 4	86300	1.94
3.00	1.90	D2.0	0.159	4 × 4	86300	1.50
3.00	2.56	D2.9	0.191	4 × 4	92000	1.16
3.00	2.56	D2.9	0.191	4 × 4	93000	1.38
3.00	2.25	D2.9	0.191	4 × 4	93000	1.53
3.00	2.26	D2.9	0.191	4 × 4	93000	1.68
3.00	2.62	D4.6	0.242	8 × 8	67500	1.34
3.00	2.62	D4.6	0.242	8 × 8	67500	1.42
3.00	1.75	#00	0.331	8 × 8	83500	2.52
3.00	2.00	#00	0.331	8 × 8	83500	2.60
3.00	1.94	#8	0.162	4 × 4	72000	2.54
3.00	2.32	#8	0.162	4 × 4	72000	1.72
3.00	2.32	#8	0.162	4 × 4	72000	1.48
3.00	1.87	#8	0.162	4 × 4	72000	1.96
3.00	1.81	D2.0	0.159	3 × 3	81900	1.54
3.00	2.25	D2.0	0.159	3 × 3	81900	1.58
3.00	2.25	D2.0	0.159	3 × 3	81900	1.37

TABLE 2.–

Slab designation (1)	Water cement ratio, in U.S. gallons per sack (2)	Average slump, in inches (3)	Age at test, in days (4)	Cylinder compressive strength, f'_c, in pounds per square inch (5)	Cylinder tensile splitting strength, f'_t, in pounds per square inch (6)
WS22	6.5	6	49	4850	500
WS23	7.6	7	45	4190	430
WS24	7.6	7	45	4190	430
WS25	7.7	6 1/2	33	3800	360
WS26	7.7	6 1/2	32	2800	360
WS27	8.3	10	34	3550	390
WS28	8.3	10	34	3550	390
WS29	7.7	8	26	3800	425
WS30	7.7	8	27	3800	420
WS31	8.3	9	28	3780	390
WS32	8.3	9	65	3780	390

[a] In the clamped slabs series CSF1 through CSK1 and WS1 through WS32, the same also used at the top for the negative moment.

chorage. The supports were also 2-in. wide flat edged. To insure uniformity of clamping stress along all the four sides of each slab, the clamping force was transmitted through a wooden frame 5 in. × 5 in. in cross section as seen in Fig. 3. The external load applied to the clamped slabs was also centrally imposed on a 6-in. × 6-in. area through the same hydraulic loading system.

Ten slabs were tested in this series. All specimens were reinforced with two similar layers of smooth high strength mesh reinforcement welded at the joints, one on top and one at the bottom in order to provide for the positive moment at the center and the negative moment of equal magnitude at the support. The total thickness of each slab was kept almost constant, with a variation from 3.20 in. to 3.50 in. at the center. The mesh spacing was also varied from 4 in. × 4 in. to 8 in. × 8 in. to 6 in. × 12 in. Shear reinforcement was also provided in this series. SR-4 electric strain gages were placed both on the positive and the negative steel at the critical locations.

Clamped Uniformly Loaded Slabs.—The clamped slabs in this series were 7 ft 0 in. × 7 ft 0 in. in overall area, while the clear span was 5 ft 0 in. × 5 ft 0 in. A 12-in. peripheral strip was provided as shown in Fig. 3. Seventy-two holes were evenly spaced in two rows in the clamping peripheral strip outside the 5-ft 0-in. × 5-ft 0-in. area and load was transmitted to the slabs through the use of a rubber pressure bag filled with nitrogen. Load was applied in an inverted position as seen in the detail in Fig. 3. Ideally complete fixity at all the four boundaries of the slabs in this series was achieved, and no rotation or lateral movement of the boundaries was possible.

Thirty-two slabs were tested in this series. Most of them were reinforced with deformed welded wire mesh and the total thickness of each slab was constant at 3 in. The average effective depth varied from 1.63 in. to 2.63 in.

CONTINUED

Total center thickness, in inches (7)	Central d_1, in inches (8)	Wire gage (9)	Wire diameters, ϕ_1/ϕ_2, in inch per inch (10)	Wire spacing $S_1 \times S_2$, in inches (11)	Wire yield strength, 0.2% offset, in pounds per square inch (12)	Center-line deflection at ultimate load, in inches (13)
3.00	1.94	D2.0	0.159	3 × 3	81900	1.42
3.00	2.25	D2.0	0.159	4 × 4	81900	1.55
3.00	1.75	D2.0	0.159	4 × 4	81900	1.92
3.00	1.87	D4.6	0.242	4 × 8	67500	2.46
3.00	1.87	D4.6	0.242	4 × 8	67500	1.94
3.00	2.12	D4.6	0.242	4 × 8	67500	1.92
3.00	2.00	D4.6	0.242	4 × 8	67500	1.80
3.00	1.75	D4.6	0.242	6 × 6	67500	2.24
3.00	1.62	D4.6	0.242	6 × 6	67500	1.76
3.00	1.25	D4.6	0.242	6 × 6	67500	1.84
3.00	1.25	D4.6	0.242	6 × 6	67500	1.76

pattern and amount of reinforcement used at the bottom for the positive moment was

The reinforcement was in two equal layers and instrumented with SR-4 gages at all critical locations both in the positive and negative regions. Some difficulty was encountered in placing the SR-4 gages in the deformed reinforcement due to the small space between the deformations in the mesh. It was possible, however, through maximum trimming of the gage to ensure that the gage grid covered the undeformed portion of the reinforcing wire. The mesh spacing was varied from 3 in. × 3 in. to 4 in. × 4 in., 6 in. × 6 in., 4 in. × 8 in. and 8 in. × 8 in. No shear reinforcement was necessary in this series.

All the slabs in this research program were whitewashed at the tensile face in order to facilitate accurate and prompt reading of the crack width.

Testing Procedure.—Load was applied in at least 10 increments at intervals of approximately 8 min between each two increments of load. Three min were allowed for the hydraulic pressure to stabilize itself before the readings were taken. Deflection was measured with 4-in. travel dials located at the center of each slab and at quarter points both on the principal axes and the diagonals. Corner lift in those specimens which were simply supported was also measured. The deflection dials had an accuracy of 0.001 in.

The crack widths were observed with powerful illuminated microscopes of 0.001-in. accuracy. Maximum and minimum crack widths were read at 6-in. space intervals on the path of the major crack lines. In the centrally loaded series, crack width was read outside the central 6-in. × 6-in. loading area and at each increment of load up to failure. A minimum crack width in this investigation was considered to be such, if it showed the least width within a 12-in. distance from the maximum crack width reading.

Strain in the wire mesh reinforcement and in the compressive surface of the concrete was recorded both by an electronic automatic multichannel

scanner recorder and by manual strain indicators. The automatic recorder used has 48-channel capacity and operates at a speed of one channel per sec. The strain output was also monitored directly on IBM 526 Card Punch for prompt evaluation by the Computer Center.

It was important to locate precisely the position of each gage in the finished slab so that direct correlation between crack width and steel stress could be effected. This was achieved by keeping a record of the accurate coordinates of each gage and maintaining these coordinates while placing the concrete.

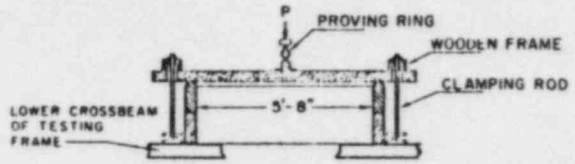

SECTIONAL ELEVATION
CENTRALLY LOADED SLABS

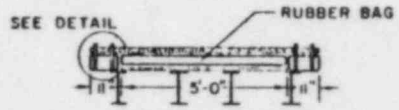

SECTIONAL ELEVATION
UNIFORMLY LOADED SLABS

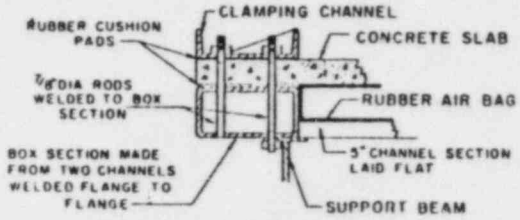

BOUNDARY CLAMPING DETAIL
UNIFORMLY LOADED SLABS

FIG. 3.—SLAB TESTING SETUPS

The major properties of the 54 slabs tested and analyzed in the program are listed in Table 2.

TEST RESULTS

Simply Supported Centrally Loaded Slabs Series SA *and* SE.—Wire spacing was 4 in. × 4 in. and active steel ratio p_t varied between 0.75% and 2.0% as seen in Table 1. Crack pattern followed closely the mesh reinforcement pattern. The yield line mechanism developed drastically when the load was 80% to 85% of the slab collapse load. Only relatively narrow cracks developed, forming a uniform square grid of orthogonal cracks at the tensile side. The width of the yield line cracks was also relatively very narrow as compared to the crack widths in Series SB, SC, and SD. Spacing of the cracks was generally approximately 4 in. The grid index, $I = \phi s/p_t$ varied between 83 and 150.

Simply-Supported Centrally-Loaded Slabs Series SB, SC, *and* SD.—Wire spacing was either 8 in. × 8 in. or 6 in. × 12 in. The active steel ratio, p_t, was 0.5% as seen in Table 1. The yield line mechanism developed early in the loading history of each slab, namely at about 35% to 50% of the ultimate load. Very few orthogonal cracks developed, and the width of all the cracks was appreciably larger than the cracks developed in Series SA and SE. Their spacing was diagonal following the yield line mechanism. The grid index, varied in value between 508 and 865 for the different tests.

Clamped Slabs Series CSF *and* CSH.—The wire spacing was 4 in. × 4 in. and the active steel ratio p_t varied between 1.4% and 0.77%. It is noted that p_t in these series of tests was comparable in value to those of the simply-supported slabs. The crack widths were considerably smaller than any of the other series and followed the same square grid of orthogonal pattern as the mesh reinforcement. The spacing of the cracks was generally very close to 4 in., and the yield line cracks developed fully only very late in the loading history of the specimens at about 85% of the failure load. The grid index value varied between 113 and 129.

Clamped Centrally Loaded Slabs Series CSG, CSI, CSJ *and* CSK.—Spacing of the mesh grid was 8 in. × 8 in. in series CSG and CSI, while the spacing in CSJ was 4 in. × 8 in. and in CSK 6 in. × 12 in. The active steel ratio, p_t, varied between 0.19% and 0.90%. The dominant cracks were diagonal yield line cracks which developed fully early in the loading history of the specimens. The spacing of the few orthogonal cracks which formed was approximately 7 in. to 8 in. The grid index value varied between 235 and 603.

Clamped Uniformly Loaded Series WS1 *through* WS10 *and* WS21, WS22 *and* WS23.—Spacing of the mesh grid was 4 in. × 4 in. The active steel ratio p_t varied between 0.48% and 1.05%. The dominant cracks were orthogonal except in WS5 and WS6 where p_t was 0.26% and 0.23%, respectively. In WS5 and WS6, yield line cracks developed earlier than the others in this series, dominant cracks were also orthogonal and narrower than most of those discussed later. The grid index varied from 92 to 159 except in WS5 and WS6 where its value was 244.

Clamped Uniformly Loaded Series WS11 *through* WS32.—The rest of the uniformly loaded slabs series, WS11 through WS32, not presented in the previous paragraph, developed dominant yield lines of considerably wide cracks early in their loading history. The spacing of the cross wires varied between 3 in. × 3 in., 4 in. × 4 in., 4 in. × 8 in., 6 in. × 6 in. and 8 in. × 8 in. as given in Table 2. The grid index value varied between 251 and 736 as tabulated in Table 1. p_t values between 0.20% and 2.11%.

It must be emphasized that the final collapse mechanism in all the slabs tested in this program was by complete development of the yield lines. What is considered as governing the behavior of the slabs tested is whether few diagonal yield line cracks or numerous narrow orthogonal cracks dominated early in the loading history up to 75% of the collapse load.

ANALYSIS

Crack Width Regression Equations.—The fracture hypothesis and the mathematical model proposed in Eq. 2 were applied previously by the senior writer

to experimental results from 22 centrally-loaded slabs (1,3,5). A regression equation in the form

$$W_{max} = 2.75 \times 10^{-6} \frac{f_t'}{(f_c')^{1/3}} \left[\frac{\phi_1 s_2}{p_{t_1}}\right]^{0.27} f_s^{1.42} \quad \ldots\ldots\ldots\ldots (3)$$

for fully clamped centrally loaded slabs was found as best fit for the data. This is a nonlinear power function both for steel stress f_s and grid index, $\phi_1 s_2/p_{t_1}$.

It was also indicated by the author in Ref. 1 that simplification of Eq. 3 can be achieved with some acceptable loss of accuracy of crack width evaluation. Such acceptance is based upon the natural large random scatter in cracking behavior. Ratio $f_t'/(f_c')^{1/2}$ can be assumed as constant. Steel stress f_s can be linearized to fit data closely at certain levels of stress rather than the whole range covered by $f_s^{1.42}$.

On this basis a statistical analysis of the data (6) resulted in the following equations pertaining to the various loading and boundary conditions applied in this investigation: Clamped slabs, uniformly loaded (8)

$$W_{max} = 2.8 \times 10^{-6} R\sqrt{I}\, f_s \quad \ldots\ldots\ldots\ldots (4)$$

clamped slabs, centrally loaded

$$W_{max} = 2.1 \times 10^{-6} R\sqrt{I}\, f_s \quad \ldots\ldots\ldots\ldots (5)$$

and simply supported slabs, centrally loaded

$$W_{max} = 3.1 \times 10^{-6} R\sqrt{I}\, f_s \quad \ldots\ldots\ldots\ldots (6)$$

in which R = the cover ratio; I = the grid index; and f_s = the steel reinforcement stress, in kips per square inch. Note that Eqs. 4, 5, and 6 are dimensionally correct.

Data plots of measured steel stress f_s versus crack width for the three previous boundary conditions are given in Figs. 4, 5, and 6. The data seem to fit the equations best in the stress range of 30 ksi to 50 ksi as demonstrated by the 45% scatter band shown in these plots. Normality of the data was established statistically.

Theoretical Versus Experimental Values of Crack Width.—Eqs. 4, 5, and 6 have been applied to stress levels of 20 ksi, 30 ksi, 35 ksi, 50 ksi, and 60 ksi steel reinforcement stress. These stress levels were chosen as they represent terminal design stages.

Table 3 lists the observed and the theoretical values of crack width at the five stress levels indicated based on the proposed simplified equations. It is seen that the mean value of this ratio W_D/W_C is very close to 1.0 while the standard deviation is closest at stress level of 30 ksi. The largest deviation is 0.332 at a stress level of 60 ksi which is expected in the random process of cracking behavior.

Yield Line Cracks Versus Orthogonal Cracks.—A study of the behavior of each of the 54 slabs tested in this program substantiates the cracking hypothesis presented. Definite diagonal yield line cracks developed in the early

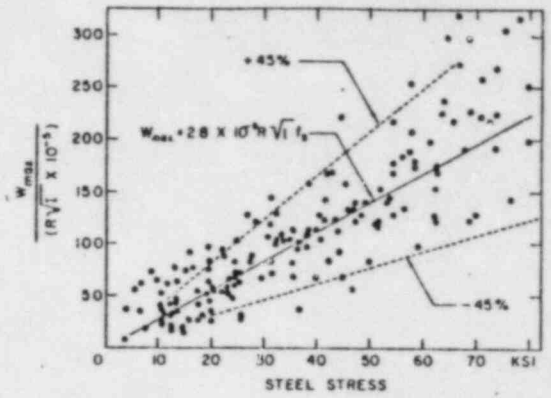

FIG. 4.—CRACK WIDTH VERSUS REINFORCEMENT STEEL STRESS IN CLAMPED UNIFORMLY LOADED SLABS

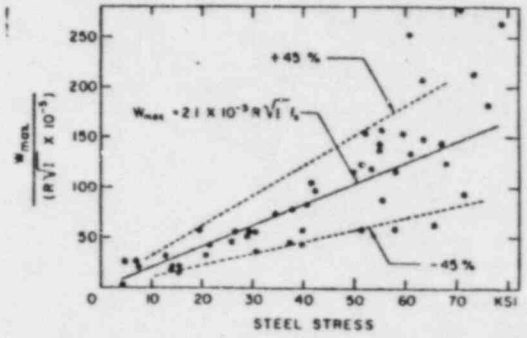

FIG. 5.—CRACK WIDTH VERSUS REINFORCEMENT STEEL STRESS IN CLAMPED CENTRALLY LOADED SLABS

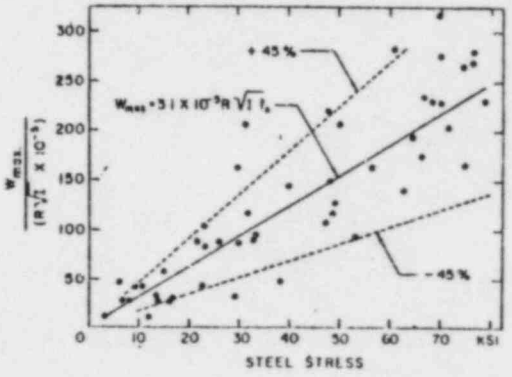

FIG. 6.—CRACK WIDTH VERSUS REINFORCEMENT STEEL STRESS IN SIMPLY SUPPORTED CENTRALLY LOADED SLABS

TABLE 3.—CORRELATION OF OBSERVED AND COMPUTED MAXIMUM CRACK WIDTHS

Slab number	20 ksi			30 ksi			35 ksi	35 ksi			50 ksi			60 ksi		
	w_o	w_c	w_o/w_c	w_o	w_c	w_o/w_c	w_o	w_c	w_o/w_c	w_o	w_c	w_o/w_c	w_o	w_c	w_o/w_c
SA1	0.012	0.0085	1.41	0.019	0.0127	1.50	0.024	0.0148	1.62	0.033	0.0211	1.56	0.039	0.0225	1.73
SA2	0.006	0.0085	0.71	0.010	0.0127	0.79	0.012	0.0148	0.81	0.019	0.0211	0.90	0.032	0.0225	1.42
SA3	0.009	0.0085	1.06	0.013	0.0127	1.02	0.016	0.0148	1.08	0.023	0.0211	1.09	0.034	0.0225	1.51
SB1	0.013	0.0228	0.57	0.023	0.0342	0.67	0.028	0.0398	0.70	0.044	0.0569	0.77	0.058	0.0684	0.85
SB2	0.007	0.0155	0.45	0.013	0.0232	0.56	0.015	0.0271	0.55	0.024	0.0387	0.62	0.036	0.0465	0.77
SC1	0.021	0.0248	0.85	0.032	0.0365	0.88	0.038	0.0425	0.89	0.053	0.0608	0.87	0.064	0.0744	0.86
SC2	0.029	0.0238	1.24	0.044	0.0357	1.23	0.056	0.0416	1.35	0.077	0.0595	1.29	0.093	0.0714	1.30
SD1	0.020	0.0164	1.22	0.026	0.0246	1.06	0.029	0.0287	1.01	0.041	0.0410	1.00	0.051	0.0492	1.04
SD2	0.017	0.0170	1.00	0.025	0.0258	0.98	0.029	0.0301	0.96	0.040	0.0431	0.93	0.050	0.0510	0.98
SE1	0.013	0.0185	0.70	0.020	0.0277	0.72	0.024	0.0323	0.74	0.035	0.0462	0.76	0.051	0.0555	0.92
SE2	0.006	0.0054	1.11	0.009	0.0081	1.11	0.012	0.0095	1.26	0.019	0.0136	1.40	0.026	0.0162	1.61
SE3	0.006	0.0077	0.78	0.009	0.0116	0.78	0.012	0.0135	0.89	0.018	0.0193	0.93	0.025	0.0231	1.08
CSF1	0.005	0.0061	0.82	0.008	0.0092	0.88	0.010	0.0109	0.92	0.022	0.0153	1.44	0.036	0.0183	1.97
CSF2	0.004	0.0056	0.71	0.007	0.0085	0.82	0.009	0.0099	0.91	0.014	0.0141	1.00	0.019	0.0168	1.13
CSG1	0.007	0.0095	0.74	0.012	0.0143	0.84	0.015	0.0167	0.90	0.028	0.0238	1.18	0.037	0.0285	1.30
CSG2	0.006	0.0073	0.82	0.010	0.0109	0.92	0.013	0.0127	1.02	0.021	0.0182	1.15	0.027	0.0219	1.23
CSH1	0.005	0.0053	0.94	0.009	0.0079	1.14	0.010	0.0093	1.07	0.016	0.0132	1.21	0.023	0.0159	1.45
CSH2	0.003	0.0053	0.57	0.004	0.0079	0.51	0.005	0.0093	0.54	0.007	0.0132	0.53	0.009	0.0159	0.57
CSI1	0.009	0.0086	1.05	0.014	0.0129	1.09	0.020	0.0151	1.33	0.044	0.0215	2.05	0.052	0.0258	2.02
CSJ1	0.006	0.0065	0.92	0.010	0.0097	1.03	0.013	0.0113	1.16	0.022	0.0162	1.36	0.035	0.0195	1.80
CSJ2	0.007	0.0088	0.80	0.011	0.0131	0.84	0.014	0.0153	0.91	0.022	0.0219	1.01	0.028	0.0264	1.06
CSK1	0.009	0.0086	1.05	0.013	0.0129	1.01	0.015	0.0151	0.99	0.023	0.0216	1.11	0.029	0.0258	1.12
WS1	0.009	0.0070	1.28	0.013	0.0105	1.24	0.016	0.0122	1.31	0.024	0.0175	1.37	0.036	0.0210	1.72
WS2	0.007	0.0070	1.00	0.010	0.0105	0.95	0.012	0.0122	0.98	0.017	0.0175	0.97	0.028	0.0210	1.33
WS3	0.006	0.0071	0.85	0.009	0.0106	0.85	0.011	0.0124	0.89	0.016	0.0177	0.91	0.033	0.0213	1.55
WS4	0.005	0.0071	0.70	0.009	0.0106	0.85	0.013	0.0124	1.05	0.021	0.0177	1.20	0.032	0.0213	1.50
WS5	0.009	0.0133	0.68	0.013	0.0201	0.65	0.015	0.0234	0.64	0.021	0.0334	0.63	0.028	0.0400	0.70
WS6	0.007	0.0133	0.53	0.009	0.0201	0.45	0.010	0.0234	0.43	0.019	0.0334	0.57	0.022	0.0400	0.55
WS7	0.008	0.0067	1.20	0.011	0.0099	1.11	0.013	0.0116	1.12	0.019	0.0166	1.15	0.027	0.0201	1.35
WS8	0.006	0.0054	1.11	0.009	0.0814	1.11	0.010	0.0095	1.05	0.014	0.0136	1.03	0.020	0.0162	1.24
WS9	0.008	0.0099	0.81	0.011	0.0148	0.74	0.013	0.0173	0.75	0.018	0.0246	0.73	0.027	0.0297	0.91
WS10	0.013	0.0114	1.14	0.019	0.0172	1.10	0.024	0.0200	1.20	0.034	0.0286	1.19	0.042	0.0342	1.23
WS11	0.014	0.0117	1.20	0.016	0.0176	0.91	0.020	0.0211	0.96	0.031	0.0292	1.06	0.035	0.0352	0.99
WS12	0.011	0.0098	1.12	0.017	0.0146	1.17	0.019	0.0171	1.11	0.034	0.0244	1.40	0.045	0.0294	1.53
WS13	0.030	0.0288	1.04	0.046	0.0433	1.04	0.052	0.0506	1.03	0.072	0.0723	0.99	0.092	0.0865	1.06
WS14	0.022	0.0262	0.80	0.031	0.0393	0.79	0.035	0.0461	0.76	0.051	0.0663	0.78	0.059	0.0886	0.67
WS15	0.019	0.0137	1.39	0.023	0.0206	1.12	0.026	0.0240	1.08	0.035	0.0272	1.29	0.042	0.0326	1.29
[a]WS16	0.012	0.0094	1.28	0.014	0.0141	0.99	0.016	0.0164	0.98	0.023	0.0234	0.98	0.028	0.0282	0.99
WS17	0.011	0.0094	1.17	0.013	0.0141	0.92	0.014	0.0164	0.85	0.025	0.0234	1.06	0.033	0.0282	1.17
WS18	0.019	0.0163	1.17	0.028	0.0246	1.04	0.037	0.0286	1.29	0.047	0.0410	1.15	0.065	0.0489	1.33
WS19	0.014	0.0135	1.04	0.022	0.0202	1.09	0.024	0.0236	1.02	0.034	0.0336	1.01	0.044	0.0405	1.09
WS20	0.003	0.0069	0.43	0.006	0.0104	0.58	0.007	0.0121	0.58	0.013	0.0173	0.75	0.015	0.0207	0.72
WS21	0.005	0.0069	0.72	0.010	0.0104	0.96	0.013	0.0121	1.07	0.017	0.0173	0.98	0.020	0.0207	0.97
WS22	0.010	0.0110	0.91	0.017	0.0165	1.03	0.020	0.0192	1.04	0.026	0.0274	0.95	0.031	0.0333	0.93
WS23	0.016	0.0117	1.37	0.022	0.0176	1.26	0.023	0.0206	1.12	0.031	0.0294	1.06	0.037	0.0351	1.06
WS24	0.018	0.0183	0.98	0.026	0.0267	0.92	0.031	0.0312	0.99	0.045	0.0455	0.99	0.055	0.0548	1.00
[a]WS25	0.015	0.0131	1.15	0.021	0.0197	1.07	0.026	0.0229	1.14	0.038	0.0327	1.16	0.045	0.0393	1.15
WS26	0.016	0.0168	0.95	0.025	0.0250	1.00	0.029	0.0294	0.99	0.039	0.0412	0.85	0.047	0.0495	0.95
WS27	0.011	0.0126	0.87	0.017	0.0188	0.90	0.021	0.0220	0.96	0.029	0.0314	0.93	0.036	0.0378	0.96
WS28	0.013	0.0134	0.97	0.021	0.0201	1.00	0.024	0.0234	1.03	0.034	0.0335	1.01	0.046	0.0402	1.14
WS29	0.017	0.0218	0.78	0.026	0.0327	0.80	0.031	0.0381	0.81	0.053	0.0546	0.97	0.076	0.0654	1.18

TABLE 3.—

Slab number	20 ksi			30 ksi			35 ksi
	W_o	W_c	W_o/W_c	W_o	W_c	W_o/W_c	W_o
WS30	0.019	0.0241	0.79	0.029	0.0361	0.80	0.034
WS31	0.012	0.0116	1.03	0.016	0.0176	0.91	0.018
WS32	0.015	0.0116	1.29	0.019	0.0176	1.08	0.021
		Mean	0.939			0.937	
		SD	0.238			0.118	

[a] Not included in analysis.

loading history of these slabs when grid index $I_1 = \phi_1 s_2/p_{t_1}$ was in excess of about 160, and the wire spacing in excess of 4 in.

The yield lines and hinge fields in these cases dominated throughout the loading history, thereby causing less major cracks to develop and very few orthogonal cracks narrow in nature to appear. The few yield line cracks were wider than would otherwise have been the case if more orthogonal cracks had developed. Those slabs can therefore be considered unsatisfactory for crack control reliability criteria since they would not satisfy crack width tolerances acceptable at working stress levels.

In slabs where the grid index was less than about 160, orthogonal cracks dominated throughout the loading history, They generated from the nodal points of the reinforcement and had relatively small crack widths. They are found to satisfy currently acceptable crack reliability criteria at service load levels of codes available on crack control.

Simply supported centrally loaded slabs series SB, SC, and SD and clamped centrally slabs series CSG, CSI, CSS and CSK had a low active steel ratio p_t and a high grid index in excess of 160, with large spacing of wires (Table 1). A forced homogeneous grid crack pattern was not possible even in series SB, where large diameter wires were used. Stress concentration at the welded joints was too low to generate the preferred cracking pattern, causing the yield lines to start developing early in the loading history of the specimens. Thus, no flexural cracks of importance other than the yield lines developed up to failure having a considerably large width. In series CSJ1, the mesh index was 196.1, being somewhat close to the value of 160 proposed as limiting. Orthogonal cracks started to generate initially, but yield line cracks at about 45% of the ultimate load began to develop also. The failure of slab CSJ1, and to a similar extent, CSJ2, can be termed a combination of yield line and orthogonal.

Simply supported slabs series SA and SE and clamped centrally loaded slabs series CSF and CSH, having a grid index value lower than 160 (see Table 1), developed a homogeneous square cracking lattice of narrow cracks even up to collapse. The yield line cracks were in most cases narrower than the cracks of the flexural grid pattern and developed fully only when the collapse load was approached. Compare typical Fig. 7 for CSF2 versus typical Fig. 8 for CSH. The active steel ratio in series CSF was higher than in all the other series, though the concrete stretched area was not too different. This observation points to the higher importance of the active steel ratio than the concrete

CONTINUED

35 ksi		50 ksi			60 ksi		
W_c	W_o/W_c	W_o	W_c	W_o/W_c	W_o	W_c	W_o/W_c
0.0420	0.81	0.049	0.0604	0.81	0.062	0.0723	0.86
0.0204	0.88	0.027	0.0294	0.93	0.036	0.0348	1.03
0.0204	1.03	0.032	0.0294	1.09	0.039	0.0348	1.12
	0.970			1.038			1.17
	0.219			0.265			0.332

stretched area. The spacing of the orthogonal wires was 4 in. in this series and the crack spacing was close to 4 in. The square cracking grid in this series as well as the others with low grid index value infers that such stress concentration existed at the nodal points that the cracking pattern generated followed closely the reinforcement pattern.

Uniformly loaded clamped slabs series WS11 through WS15, WS18, WS19 and WS23 through WS32 had a low active steel ratio, p_t, and a high grid index in excess of 160 as seen in Table 1. The spacing of the cross wire was generally 8 in. × 8 in., 4 in. × 8 in. or 6 in. × 6 in. except in WS18 and WS19 where it was closer spaced though the active steel ratio in the two latter slabs was as low as 0.23%. Thus stress concentration at the welded joints was too low to generate the preferred orthogonal cracking grid early in the loading history of the specimens. The result was wide cracks as compared to the rest of the slabs in the WS series.

The balance of the slabs in the WS series not included in the previous analysis had a grid index value lower than 160 except in the case of WS5, WS6, WS16 and WS17, where it was slightly higher. The active steel ratio, p_t, was in most cases in excess of 0.45% as given in Table 1. Orthogonal narrow cracks dominated early in the loading history of the slabs in this group. Typical Fig. 9(*a*) shows slab WS5 at about 50% of its ultimate load while Fig. 9(*b*) shows it just prior to failure with the orthogonal cracking grid of narrow cracks maintained through its loading history. Typical Figs. 10(*a*) and 10(*b*) show slab WS18 at comparable load level with slab SW5. Yet, because of its high grid index value, dominant wide diagonal yield line cracks controlled early in its loading history.

A comparison is also made between the centrally loaded series CS reinforced with smooth wire mesh with the uniformly loaded series SW, most of which were reinforced with deformed wire mesh. It is interesting to note that the effect of wire deformations on controlling the widths of the cracks is negligible for the steel wire diameter sizes used in this investigation. It is thus noted that crack spacing of the controlling cracks in slabs with grid index values less than of 160 to 180 generally followed closely the reinforcement spacing grid. The slab behavior relating to the effect of deformations of the steel wire surface and the orthogonal spacing of the wires on the crack width further confirms the hypothesis that the nodal points, namely the locations of the reinforcement intersections, control the format of the cracking mechanism.

Grid Index as Guide to Control of Cracking Pattern.—From the previous

analyses both for centrally loaded and uniformly loaded slabs, it is seen that the crack pattern and spacing follows the steel wire spacing up to a certain optimum stage. Beyond such a stage, the crack spacing starts to deviate progressively from the reinforcement spacing and becomes diagonally drawn to-

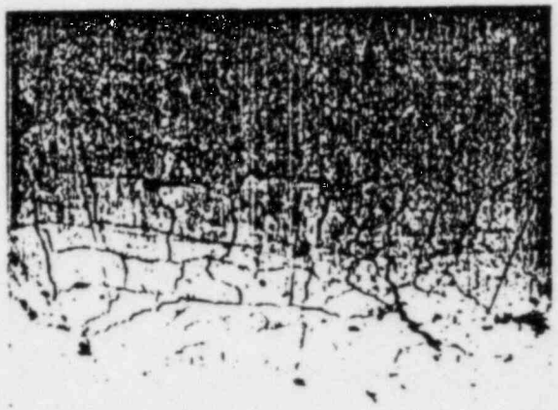

FIG. 7.—TYPICAL ORTHOGONAL CONTROLLING CRACKING PATTERN, CENTRALLY LOADED SLAB CSF2

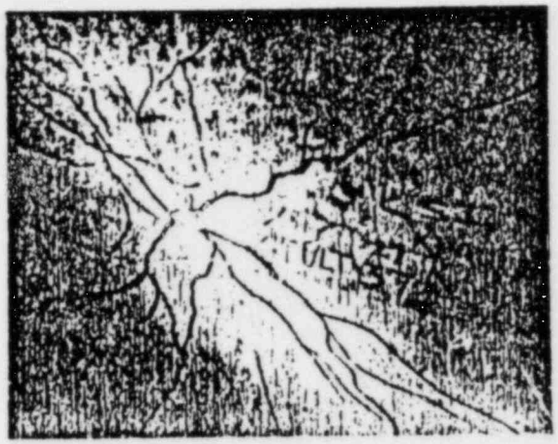

FIG. 8.—TYPICAL YIELD LINE CONTROLLING CRACKING PATTERN, CENTRALLY LOADED SLAB CSI 1

wards the yield lines. A grid index of about 160, with wire spacing of 4 in. to 6 in. seems to be a logical optimum within the limitations of the number of tests in this investigation. It can be deduced that the grid index, which is a function of the active steel ratio and the spacing of the welded joints, is the

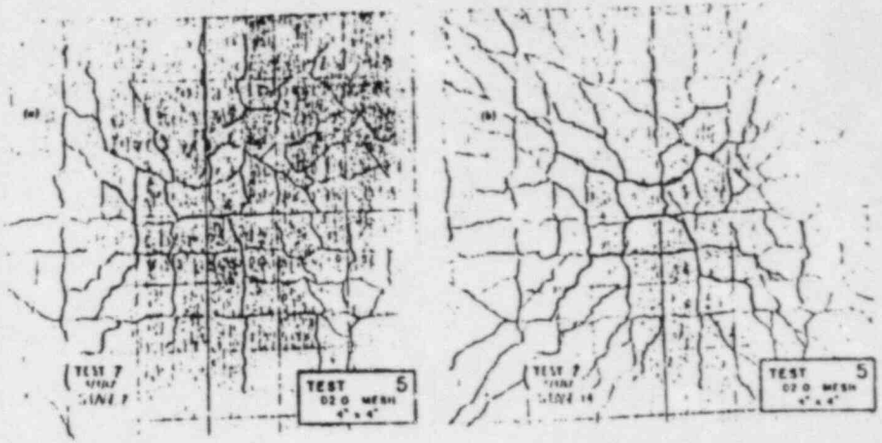

FIG. 9.—TYPICAL UNIFORMLY LOADED SLAB WS5 WITH ORTHOGONAL CRACKS CONTROLLING: (*a*) AT 50% OF ULTIMATE LOAD; (*b*) AT ULTIMATE LOAD

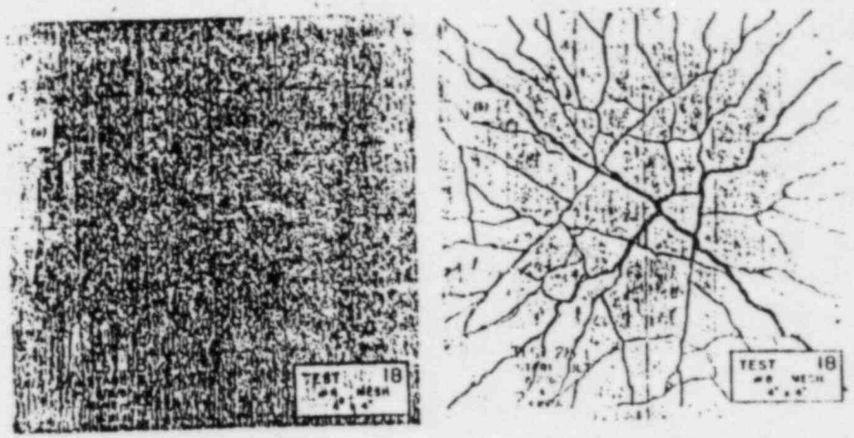

FIG. 10.—TYPICAL UNIFORMLY LOADED SLAB WS18 WITH WIDE YIELD LINE CRACKS CONTROLLING: (*a*) AT 50% OF ULTIMATE LOAD; (*b*) AT ULTIMATE LOAD

primary parameter to be considered in producing a forced cracking grid which can result in limiting the crack width.

CONCLUSIONS

1. Crack width in two-way slabs can be effectively controlled by forcing an orthogonal cracking grid pattern.

2. The difference in effect on crack width control by using deformed versus smooth wire mesh is minor.

3. Orthogonal crack spacing in two-way slabs is a function of the orthogonal spacing of the welded reinforcement only to an optimum reinforcement spacing ranging between 4 in. and 6 in. Cross wires spaced in excess of 6 in. to 8 in., regardless of the diameter of the cross wire, lead to the early development of wide diagonal cracks and no forced fracture grid is possible.

4. Grid index $I = \phi_1 s_2 / p_{t_1}$ is a good indicator in checking whether orthogonal cracking grid patterns or wide diagonal yield line cracks would result. If the index exceeds 160 to 180, pronounced yield line wide cracks develop early in the loading history.

5. Choice of a two-way slab reinforcement geometry which can force an orthogonal cracking grid of narrow cracks is possible through use of the simplified crack control equations developed in this investigation.

ACKNOWLEDGMENT

The writers wish to thank the U.S. Steel Corporation for the welded fabric and other financial support they extended. The second writer's contribution in this paper covered the work on the uniformly loaded slabs series WS. This investigation was initiated and conducted in the Concrete Research Laboratories of the Department of Civil Engineering at Rutgers University, whose Chairman, M.L. Granstrom, is gratefully acknowledged for his continuous support.

APPENDIX I.—REFERENCES

1. American Concrete Institute, "Causes, Mechanism and Control of Cracking in Concrete," Symposium publication *SP-20*, ACI *Committee 224 on Cracking*, pp. 1-240, July, 1968.
2. Comite' European du Beton (CEB), "Recommendations for International Code of Practice for Reinforced Concrete," Joint Translation of A.C.I. and C. & C. A., pp. 156, 1965.
3. Nawy, E. G., "Discussion" of paper by Amos, Seiss and Atlas, "Behavior of One-Way Concrete Floor Slabs Reinforced with Welded Wire Fabric," *Journal of the American Concrete Institute*, December, 1965, pp. 1641-1642.
4. Nawy, E. G., "Discussion" of paper by Taylor and Hayes, "Some Tests on the Effect of Edge Restraint on the Punching Shear in Reinforced Concrete Slabs," *Magazine of Concrete Research*, December, 1965, pp. 225-226.
5. Nawy, E. G., "Crack Width Control in Two-Way Concrete Slabs Reinforced with Welded Wire Fabric, Part I, Centrally Loaded," *Bulletin No. 46*, Bureau of Engineering Research, Rutgers University, November, 1967, pp. 96.
6. Nawy, E. G., "Crack Control in Reinforced Concrete Structures," *American Concrete Institute Journal*, October, 1968, pp. 825-836.
7. Orenstein, G. S., "Flexural Cracking in Two-Way Concrete Slabs Reinforced with Welded Wire Fabric and Subjected to Uniformly Distributed Load," thesis presented to Rutger's University at New Brunswick, N.J., in 1969, in partial fulfillment of the requirements for the degree of Doctor of Philosophy.
8. Orenstein, G. S., and Nawy, E. G., "Crack Width Control in Reinforced Concrete Two-Way Slabs Subjected to Uniformly Distributed Load," published in the *American Concrete Institute Journal*, Jan., 1970.

9. Reis, E. E., Mozer, J. D., Bianchini, A. C., and Kesler, C. E., "Causes and Control of Cracking in Concrete Reinforced with High Strength Steel Bars," *University of Illinois Bulletin, 479*, Urbana, Ill., pp. 66, 1966.
10. Rilem, "Proceedings International Symposium on Bond and Crack Formation in Reinforced Concrete," I-IV, Stockholm, 1957.

APPENDIX II.—NOTATION

The following symbols are used in this paper:

A_s = area of tensile reinforcement in one direction per foot-width of slab;
A_t = concrete stretched area, as shown in Fig. 2;
a_c = crack spacing, in inches;
d = effective depth to center of one layer of reinforcement;
f'_c = cylinder compressive strength of concrete;
f_s = tensile stress in wire reinforcement, in kips per square inch;
f_u = ultimate strength of reinforcement;
f_y = yield strength of reinforcement by 0.2% offset;
f'_t = tensile splitting strength of concrete, ASTM C 496-62T;
$I_1 = \phi_1 s_2 / p_{t_1}$ = grid index in direction 1;
$I_2 = \phi_2 s_1 / p_{t_2}$ = grid index in direction 2;
P = External load at intermediate stage;
P_u = test ultimate load;
P'_u = theoretical ultimate load;
p = steel percentage = $A_s/12d$ in slabs, = A_s/bd in beams;
p_t = active steel ratio = A_s/A_t;
R = cover ratio = ratio of distance from neutral axis to tensile face of concrete to distance from neutral axis to center of gravity of reinforcement;
sd = σ = standard deviation;
s = spacing of reinforcement;
t = thickness of concrete cover, in inches;
u = bond strength in concrete;
w_s = crack width, in inches, at steel level;
w_c = crack width, in inches, at concrete face;
w_{max} = maximum crack width at concrete face;
α, β, γ = coefficients of regression function in slabs;
ϵ_s = tensile unit strain in reinforcement; and
ϕ = diameter of wire reinforcement.

REF. 3

FURTHER STUDIES ON FLEXURAL CRACK CONTROL IN STRUCTURAL SLAB SYSTEMS

By EDWARD G. NAWY and KENNETH W. BLAIR

This paper is a consolidation of almost all available studies on the flexural cracking behavior of two-way action slabs and plates. An analysis is made of the test results of ninety two-way action slabs both rectangular and square and having various boundary conditions. Loads varied from concentrated load simulating column reaction on flat plates, to uniformly distributed load. Reinforcement used varied from smooth to deformed welded wire fabric to rebars. The clear spans of the test slabs ranged from 5 ft 8 in. x 5 ft 8 in. (1.724 x 1.724 m) to 5 ft 0 in. x 5 ft 0 in. (1.524 x 1.524 m) to 5 ft 0 in. x 3 ft 6 in. (1.524 x 1.067 m). Their effective depths ranged from 1.25 in. (3.17 cm) to 3.50 in. (8.89 cm), while the total thickness of the test slabs ranged from 2.5 to 4.0 in.

A fracture hypothesis is presented and a grid index is proposed as an indicator of the controlling flexural cracking pattern to be expected at loads up to 75-80 percent of the ultimate. It is shown that apart from the reinforcement stress level the major controlling parameter is the spacing of the reinforcement in the two orthogonal directions of a two-way action structural slab or plate. The diameter of the reinforcement and the concrete cover were the other parameters that influenced the behavior of slabs, but to a lesser degree.

Criteria are proposed for use by the design engineer in exercising crack control in two-way action slabs, plates, and flat plates of various boundary conditions. The proposed equation is applied to other large scale and full scale tests made by several investigators and found valid. The extent of the work is such that codification of the recommendations is possible for direct application in crack control design of structural slab systems.

Keywords: concrete slabs; cracking (fracturing); flat concrete plates; flexural strength; fracture properties; loads (forces); plates (structural members); reinforced concrete; reinforcing steels; research; restraints; serviceability; two-way slabs; welded wire fabric; yield-line method.

□ Flexural crack control in reinforced concrete floor systems has become vit important. Increased use of high strength reinforcement in concrete and the plication of ultimate load procedures in the design of concrete structures requ more attention to serviceability conditions, of which crack control is a major ment. Since most framed floors are proportioned for two-way action, existin criteria[1] for crack control in beams cannot be safely applied to slabs.

ACI Member EDWARD G. NAWY is a professor of civil engineering at Rutgers, the State University of New Jersey. He is chairman of the ACI 224 Committee on Cracking, chairman of the ACI Board Committee on State Chapters Activities, member of the ACI Committees 115 and 340 and ACI representative to the International Commission on Fracture. He also was Past President (1966) of the New Jersey State Chapter of the ACI.

Dr. Nawy has published numerous papers on topics of research in concrete here and abroad and is also a registered professional engineer in the States of New Jersey, New York, and Pennsylvania. He is a member and founder of the New Jersey Council on Civil Engineering Technology and a consultant to the Industry, and is also a fellow of many professional societies including ASCE, Sigma Xi, Prestressed Concrete Institute, New York Academy of Sciences, etc.

Professor Nawy is also a systems consultant to the Federal Aviation Administration, Washington, D.C., and is listed in "Who's Who in America."

ACI Member KENNETH W. BLAIR is a graduate assistant in the Department of Civil Engineering at Rutgers—The State University of New Jersey. He obtained the BS degree in civil engineering from Rutgers in 1969 and is currently doing graduate work in the area of concrete structures.

This paper is a consolidation of almost all available studies thus far on the flexural cracking behavior of two-way action slabs and plates. An analysis is made of the test results of 90 two-way action slabs, both rectangular and square and having various boundary conditions. The intent is to develop recommendations to the engineering profession for crack control in framed structural floor slabs and plates.

Loads applied to the test slabs varied from concentrated load, simulating column reaction on flat plates, to uniformly distributed load, accomplished by use of pressure rubber bags. The reinforcement in the various test series was varied from smooth to deformed welded wire fabric to rebars. The clear spans of the test slabs ranged from 5 ft 8 in. x 5 ft 8 in. (1.724 x 1.724 m) to 5 ft 0 in. x 5 ft 0 in. (1.524 x 1.524 m) to 5 ft 0 in. x 3 ft 6 in. (1.524 x 1.067 m). Their effective depths ranged from 1.25 in. (3.17 cm) to 3.50 in. (8.89 cm), while the total thickness of the test slabs ranged from 2.5 to 4.0 in.

The analytical part of the investigation was based on the fracture hypothesis previously formulated and tested by the first author,[2,3] giving a mathematical model which can predict the flexural cracking pattern in two-dimensional members. As a result, a basic equation for crack control in two-way action slabs and plates of varying degrees of restraint at the boundaries is proposed.

Through choice of the proper fracture coefficient, the designer can control the flexural crack width in the negative region of reaction zones of flat plates as well as in the negative and positive moment regions of two-way action slabs and flat slabs. A grid index is given as a guide for governing the primary failure pattern which controls the crack width.

CONTROL TESTS

High early-strength cement was used in the concrete mix of all the slabs. Crushed stone of maximum size 3/4 in. and graded local sand were used. The mix was vibrated with electric vibrators in the forms and the specimens were cured for varying periods, as shown in Table 1-A1 of the appendix. Six control cylinders 6 x 12 in. (15.24 x 30.5 cm) were taken from each slab mix, cured under the same curing conditions as the test slabs, and tested the same day that a corresponding slab was tested. Half the number of cylinders was tested in compression and the other half in tensile splitting.

Control specimens were also taken from the wire as well as the rebar steel reinforcement to establish their yield and ultimate strengths. Tables 1-A1 gives the yield strength for the various sizes and types of steel. A typical stress-strain diagram of representative reinforcement is given in Fig. 1-1.

TESTING PROGRAM

Eight series of two-way action slabs (90 slabs) were tested to failure in this research program. Details of their geometrical properties are given in Table 1-A1. The test series comprised the following.

Restrained Centrally Loaded Slabs (Series CSF1—CSK1)

Ten slabs were tested in this series. They were 7 ft 10 in. x 7 ft 10 in. (2.388 x 2.388 m) in over-all area, while the clear span was 5 ft 8 in. (1.724 m) in each direction. They were fully restrained on all four sides and the load was transmitted to the center of each slab through a hydraulic ram system over an area of 6 x 6 in. (15.24 x 15.24 cm). The slabs were reinforced with smooth welded wire fabric in two similar layers at top and bottom to provide for positive and negative moment. The size and spacing of the reinforcement were varied to extremes (see Table 1-A1).

Shear reinforcement was also provided in the form of horizontal mats and vertical cages over an area 24 x 24 in. (61.0 x 61.0 cm) at the center to prevent premature punching failure. The slabs in this series simulated column reaction zones in flat plate structures.

Simply Supported Centrally Loaded Slabs (Series SA1—SE3)

Twelve slabs were tested in this series. They were simply supported on all four sides on 2 in. (5.08 cm) wide supports. Corners were not held down. The over-all

side length in each direction was 6 ft 2 in. (1.88 m) and the clear span was 5 ft 8 in. (1.724 m). They were reinforced with one layer of flexural reinforcement at the bottom whose sizes and spacings were varied to extremes. They were loaded in a manner identical to Series CSF1–CSK1, previously described. Shear reinforcement was also similar.

Uniformly Loaded Square Slabs Restrained on All Sides (Series WS1–WV7)

Thirty-nine slabs were tested in this series. They had an over-all area of 7 ft 0 in. x 7 ft 0 in. (2.134 x 2.134 m) and the clear span was 5 ft 0 in. (1.524 m) in each direction. They were fully restrained on all four boundaries, representing the interior panel of a multi-panel floor system. Uniformly distributed load was applied through a 3/8 in. thick rubber bag of size 5 ft 0 in. x 5 ft 0 in. (1.524 x 1.524 m). In slab tests WS1 through WS32, the bag was filled with nitrogen gas to develop the pressure, while in tests WV1 through WV7 water was used. Pressure was accomplished through a specially designed check-valve system.

Reinforcement was either deformed welded wire fabric of diameter ranging from 0.159 in. (4.0458 mm) to 0.331 in. (8.4074 mm) or #3 rebars (9.53 mm diameter). Two similar layers of two-directional reinforcement, one at the top and one at the bottom, were used in each slab to account for positive and negative bending moments. A central area 24 x 24 in. (61.0 x 61.0 cm) was removed from the negative reinforcement mat to eliminate the possible effect of compression steel on cracking in the positive moment region. The reinforcement diameter and spacing were varied to extremes to observe their effect on the flexural cracking behavior.

Total thickness was either 3 in. (7.62 cm) or 2.5 in. (6.35 cm), and the average effective depth varied between 1.21 in. (3.062 cm) and 2.62 in. (5.237 cm), as given in Table 1-A1. This series of tests could simulate in crack control study the behavior of an interior square panel of a multi-panel floor system.

Uniformly Loaded Square Slabs Restrained on Three Sides and Hinged on One Side (Series WV8–WV12)

Five slabs were tested in this series. They had properties similar to those of the previous uniformly loaded series, except that one side was a hinged support. Total thickness was 2.5 in. (6.35 cm) and the average effective depth was 2.0 in. (6.08 cm). Rubber bag pressure was developed through use of water. This series was intended to simulate a uniformly loaded square end panel of a multi-panel floor system.

Uniformly Loaded Square Slabs Restrained on Two Sides and Hinged on the Other Two (Series WV13–WV17)

Five slabs were tested to failure in this series. Their properties were similar to those of the previous uniformly loaded series (WV8–WV12), except that two adjacent sides were hinged supports. This series was intended to simulate a uniformly loaded square corner panel of a multi-panel floor system.

Uniformly Loaded Rectangular Slabs Restrained on All Sides (Series WV18–WV29)

Twelve slabs were tested to failure in this series. Each slab had a clear span of 5 ft 0 in. x 3 ft 6 in. (1.524 x 1.067 m). The total thickness was 2.5 in. (6.35 cm) and the average effective depth ranged between 1.21 in. (3.07 cm) and 2.0 in. (5.08 cm). Steel reinforcement was either deformed welded wire fabric of diameter ranging from 0.177 in. (4.495 mm) to 0.342 in. (8.687 mm) or #3 rebars (9.53 mm diameter). Reinforcing was in two similar layers on top and bottom, as in the previously described uniformly loaded square slabs. Load was applied through a rubber pressure bag 5 ft 0 in. x 3 ft 6 in. (1.524 x 1.067 m) in area and filled with water under a specially designed pressure control system. This series was intended to simulate an interior rectangular panel of a multi-panel two-way action floor system for crack control study.

Uniformly Loaded Rectangular Slabs Restrained on Three Sides and Hinged on One Side (Series WV30–WV33)

Four slabs were tested to failure in this series. Their size and reinforcement patterns were similar to those of the previous series WV18–WV29, but their total thickness had a constant value of 2.5 in. (6.35 cm) and an effective depth of 2.0 in. (5.08 cm). They also differed in that one of the four sides (the 5 ft 0 in. side) was a hinged support.

Uniformly Loaded Rectangular Slabs Restrained on Two Sides and Hinged on the Other Two (Series WV34–WV36)

Three slabs were tested to failure in this series. Their geometrical properties were generally identical to those of the previous series WV30–WV33 (see Table 1-A1), except that they differed in their boundary conditions. The slabs in this series had two adjacent edges restrained and the other two were hinged supports. They could reasonably simulate the corner panel of a multi-panel two-way action floor system for investigation of crack control behavior.

TESTING PROCEDURE

Load was generally applied in ten increments at intervals of approximately eight minutes between each two increments of load. Three minutes were allowed for the hydraulic pressure to stabilize itself before readings were taken. Deflection was measured with 4 in. travel dials located at the center of each slab and at quarter points both on the principal axes and the diagonals. Corner lift in those specimens which were simply supported was also measured. The deflection dials had an accuracy of 0.001 in.

The crack widths were observed with powerful illuminated microscopes of 0.001 in. accuracy. In the centrally loaded series, crack widths were read outside the 6 x 6 in. loading area and at each increment of load up to failure. Strain in the instrumented steel reinforcement was recorded through electric strain gages via a 96-channel electronic scanner recorder operating at a speed of one channel per

second. The strain output was also monitored directly on a card punch system for prompt evaluation at the Rutgers Center for Computer and Information Services.

It was important to locate precisely the position of each reinforcement gage in the finished slab, so that direct correlation between crack width and steel stress could be made. This was accomplished through keeping an accurate record of the coordinates of each electric gage and maintaining these coordinates while placing the concrete. Accuracy of the applied load was maintained in the centrally loaded test slabs through use of proving rings. In the uniformly loaded slabs, bag pressure was read simultaneously on a mercury manometer and a calibrated pressure gage. Magnitude of restraint at the boundaries was measured through evaluating the degree of rotation of the edges using inclinometers.

FRACTURE HYPOTHESIS IN TWO-WAY ACTION SLABS AND PLATES

As proposed by the first author in References 2 and 3, stress concentration develops initially at the points of intersection of the reinforcement in the rebars and at the welded joints of the wire mesh, namely, at grid nodal points A_1, B_1, A_2, and B_2 in Fig. 1-2. This stress concentration causes plastic deformation of the concrete at these locations as a result of the energy imposed by the external load per *unit area* of slab. The bond between the bar or wire and the concrete at these locations is destroyed and active cleavages start to generate fracture lines towards the paths of least resistance. Planes of discontinuity, which are paths of least resistance, are the interaction surfaces between the reinforcement grid lines and the surrounding concrete gel, namely, A_1B_1, A_1A_2, A_2B_2, and B_2B_1. The resulting fracture pattern is a total repetitive cracking grid, provided the spacing of the nodal points A_1, B_1, A_2, and B_2 is close enough to generate this preferred initial fracture mechanism of orthogonal cracks narrow in width.

If the spacing of the reinforcing grid intersections is too large, the magnitude of the stress concentration and the energy absorbed per unit grid is too low to generate cracks along the reinforcing wires or bars. As a result, the principal cracks follow diagonal yield-line cracking in the plain concrete field (Fig. 1-2) away from the reinforcing bars early in the loading history. These cracks are wide and few.

This hypothesis also leads to the determination that surface deformations of the individual reinforcing elements have little effect in arresting the generation of the cracks or controlling their type or width in a two-way action slab or plate. This conclusion about the effect of surface deformations was also observed by University of Illinois tests.[4,5,6] In a similar manner one can also conclude that scale effect on two-way action cracking behavior is insignificant, since the cracking grid would be a reflection of the reinforcement grid if the preferred orthogonal narrow cracking widths develop.

Therefore, for control of cracking in two-way action floors, the major parameter to be considered is the spacing of the reinforcement in the two perpendicular directions. Concrete cover has only minor effect in such slabs, since it is usually of a constant small value of 3/4 in.

For a constant area of steel determined for moment in one direction, namely, for energy absorption per unit area of slab, the smaller the spacing of the transverse bars or wires, the smaller should be the diameter of the longitudinal bars. The reason is that less energy has to be absorbed by the *individual* longitudinal bars. If one considers that the magnitude of fracture is determined by the energy imposed per specific surface-volume of reinforcement (see Reference 7), then proper choice of the reinforcement grid size, namely, the distribution of the bar or wire intersections, together with the bar size, can control cracking into preferred orthogonal grids.

It must be emphasized that this hypothesis is important for serviceability and reasonable overload conditions. In relating orthogonal cracks to yield-line cracks, the failure of a slab *ultimately* follows the generally accepted rigid-plastic failure mechanism proposed by Johansen and extended by others.

Fig. 1-3a to 1-3f show typical cracking patterns of two-way action slabs. In comparing these slabs, it is seen that early development of extensive, closely spaced orthogonal cracking grids reflects the reinforcement grids whose locations are shown by the straight lines in the pictures. At failure, yield-line rupture mechanisms have to develop as seen in Fig. 1-3f.

As a result of the proposed fracture hypothesis, and on the basis of statistical analysis of the test data of the 90 slabs tested to failure, a basic cracking equation is proposed as follows:

$$w_{max} = K R f_s \sqrt{I} \qquad (1)$$

where

w_{max} = maximum crack width at concrete face, in.

K = fracture coefficient dependent on loading and boundary conditions

R = cover ratio (1.25 on the average) = ratio of distance from neutral axis to tensile face of slab to distance from neutral axis to centroid of reinforcement grid

f_s = reinforcement steel stress (ksi) at service load level, and

I = Grid Index = $(\phi_1 s_2)/p_{t_1}$ (sq. in.), where ϕ_1 is diameter of reinforcing steel in direction "1" closest to concrete outer tension face, s_2 is spacing of reinforcing steel in direction "2" perpendicular to direction "1", and p_{t_1} is active steel ratio in direction "1" (see Notation).

Details of the fundamental formulation of the mathematical model resulting in Eq. (1) are given in Reference 3.

The grid index is proposed as an indirect measure of whether initial orthogonal narrow cracks or wide yield-line cracks control the behavior of a two-way action slab or plate. In summary, the parameters of Eq. (1) are based on the two-way action flexural cracking behavior in directions "1" and "2" as almost all slab systems are subjected to.

ANALYSIS OF TEST RESULTS

eneral

In analyzing the test results of the eight series of test slabs totaling 90 slabs, e geometrical properties of the concrete stretched cracked zones listed in ible 1-A2 of the appendix were applied to Eq. (1). A series of plots was devel- ped in Fig. 1-4a to 1-4h, with the best lines of fit for each loading and boundary ondition as shown. It is noted in all the diagrams that almost all the data fell ithin a 45 percent band of deviation about the best line of fit. It is also noted at the fracture coefficient K is inversely proportional to the degree of restraint the supports.

Table 1-1 lists the values of K for the various loading and boundary conditions. ible 1-2 lists the observed and computed crack widths at reinforcement steel ress levels of 20 ksi (1406 kg/cm^2), 30, 35, 50, and 60 ksi (4219 kg/cm^2). The ean of the ratio of observed to predicted crack widths ranged between 0.844 id 1.088, in most cases less than but close to 1.0 at the 30 ksi stress level. This vel can be generally considered as the upper bound limit of serviceability stress :pected in normally loaded two-way action concrete structural floors, while 24 .i (40 percent f_y = 60 ksi) is the more realistic level at present. The standard :viation ranged between 0.107 and 0.217 at this stress level. Such magnitude of :viation is not unexpected in the random phenomenon of cracking in concrete.[8]

Table 1-2 shows that the proposed cracking equation for two-way action slabs id plates generally overestimates the predicted crack width by 5 to 10 percent the various cases. The ACI 318-71 Code[1] Z equation for crack control in :ams (and one-way slabs) underestimates by considerably more than 62 percent ie predicted crack width, whether in one-way slabs or in two-way action floors[9] standard concrete cover. Hence these Code provisions cannot be safely applied control cracking in two-way slabs, flat slabs, or plates, and could result in un- alistic values of reinforcement spacing in concrete floors. Eq. (1) of this inves- gation, on the other hand, can be equally applicable to one-way slabs using a K lue of 1.6 x 10^{-5} shown in Table 1-1.

ntrally Loaded Slabs Series SA to CSK

In series SA, SE, CSF, and CSH, simulating column reaction zones of flat plates, ie crack pattern followed closely the reinforcement pattern as seen in typical Fig. -3a, with the cracks being spaced at 4 to 4½ in. The Grid Index = $\phi s/p_t$ did not ceed 150 (see Appendix Table 1-A2) and the active steel ratio ranged between .75 and 2.0 percent. The yield mechanism developed drastically when the load as close to 80 percent of the collapse load. The widths of the orthogonal cracks hich controlled up to that load level were narrow (see Table 1-2), and the yield- ne cracks were also narrow as compared to crack widths in the other slabs in the ntrally loaded group which had larger reinforcement spacings.

Series SB, SC, SD, CSG, CSI, CSJ, and CSK had reinforcement spacings vary- ig between 8 x 8 in., 6 x 12 in., and 8 x 4 in. The grid indices ranged in lue from 235 to 865 sq in., and the active steel ratio ranged from 0.19 to 0.5 ercent. The yield-line mechanism in this series developed early in the loading

history of each slab, namely, at about 35 to 50 percent of the ultimate load. Very few orthogonal cracks developed, and the widths of all the cracks were appreciably larger than the cracks developed in the previously discussed slabs (see Table 1-2). Fig. 1-3b is typical for centrally loaded slabs where yield-line cracking controlled throughout the loading range.

Square Uniformly Loaded Slabs Restrained on All Boundaries

Series WS1 through WS10; WS20-23; and WV1, 2, 4, and 5 can simulate an interior square panel of a multi-panel floor system. The reinforcement spacing was either 3 x 3 in. or 4 x 4 in., and their grid indices ranged between 78 and 327 sq in. The active steel ratio ranged between 0.48 and 1.17 percent. The dominant cracks were orthogonal and narrower than most of those discussed later. They were mostly an image of the reinforcing grid pattern. Fig. 1-3c is typical for crack width development in slabs whose grid index falls within this level.

Most of the others in the WS Series were reinforced with deformed welded mesh reinforcement at spacings of 4 x 8 in., 6 x 6 in., and 8 x 8 in., as given in Table 1-A1. Slab WV7 was reinforced with deformed #3 rebar (3/8 in. dia) spaced at 9½ x 9½ in. (24 x 24 cm). All these slabs developed dominant yield lines of considerably wide cracks early in their loading history. The values of the grid indices were generally in the range of 266 to 865 sq in. The use of deformed rebars did not reduce the crack widths, supporting the hypothesis that only the reduction in bar spacing can reduce the crack widths. Fig. 1-3d shows a typical slab in this category at failure, whether square or rectangular.

Uniformly Loaded Square Slabs Partially Restrained

Series WV8, 10, 11, 16, and 17 can simulate the end panels of multi-panel floor systems. The reinforcement spacing of 4 x 4 in. or 6 x 6 in. and their grid indices did not exceed 327 sq in. in value. The active steel ratio did not exceed 0.67 percent. Again, the dominant controlling cracking was orthogonal, narrow flexural cracking even though not all the edges were restrained, but one or two of the edges hinged.

Series WV9, 12, 13, and 15 had reinforcement spacing 8 x 8 in. for deformed welded fabric or 9½ x 9½ in. for deformed rebars (see Table 1-A1). The grid indices were in some cases in excess of 654 sq in. Wide yield-line diagonal cracks controlled early in their loading history and were very few in number, whether in the slabs reinforced with deformed welded fabric or deformed rebars.

Rectangular Uniformly Loaded Slabs Restrained on All Boundaries

Series WV19, 20, 21, 27, and 28 simulating a rectangular interior panel of a multi-panel floor system, had reinforcement spacings 3 x 3 in. or 4 x 4 in., and their grid indices ranged in value between 77 and 168 sq in. The controlling crack widths developed in these slabs and given in Table 1-2 at various stress levels were mainly orthogonal and narrow. A typical slab at failure is shown in Fig. 1-3e, giving a crack pattern reflecting the reinforcing pattern. The other slabs in this series developed wide diagonal yield-line cracks early in their loading history because of the high value of their grid indices.

Rectangular Uniformly Loaded Slabs, Partially Restrained

Series WV18 and WV22-26, simulating end panels of multi-panel floor systems, were reinforced with either deformed wires or 3/8 in. diameter deformed rebars at 8 x 8 in., 9½ x 9½ in., or 12 x 12 in. The grid index in WV23 had a high value of 1086 sq in., while the others in this group ranged between 327 and 653 sq in. It is seen from Table 1-2 that in the case of the widely spaced reinforcement, regardless of type, the crack width at the 20 ksi level was as high as 0.015 to 0.020 in. (0.6 to 0.8 mm). As predicted in the fracture hypothesis previously outlined, few very wide diagonal yield-line cracks developed early in the loading history and their number remained stationary up to failure.

Reinforcement in One Direction Only

Previous studies by the first author[10] included tests on one-way slabs where spacing of transverse reinforcement was up to 16 in. (40 cm). These tests, as well as those in References 4, 5, and 6, have shown that even if the spacing of transverse bars is infinite, cracks would develop at spacings not in excess of 12 in. (30 cm) for rational percentages of longitudinal steels. They have also shown that no significant difference exists in crack spacing whether the reinforcing element were smooth or deformed.

This is in conformity with the hypothesis previously presented, since concrete can withstand a tensile stress not in excess of 400 psi (28.1 kgf/sq cm) before fracture. Hence, in cases where only longitudinal steel is used, such as in the negative region of some flat plates or slabs, or in one-way slabs, a value of s_2 not exceeding 12 in. (30 cm) can be used in Eq. (1). This is also justified because the transverse spacing s_2 in Eq. (1) reflects essentially the spacing of cracks perpendicular to the spacing s_1 of the longitudinal steel closest to the concrete outer tensile fibers.

Comparison with Tests by Others

Limited crack width measurements in test results on two-way action slabs by other investigators are available. Those available involve only a few slabs in any research program, and in most cases either one or two per program. The crack control equation developed as a result of testing 90 slabs in the present investigation was applied to other large-scale and prototype tests listed in Table 1-3. Good agreement is found between the measured and the predicted crack widths, as seen from comparing values in Column 9 to those in Column 12 of Table 1-3 and from the closeness of the data points to the prediction line shown in Fig. 1-5. It can be concluded from this comparison that scale effect is insignificant in crack width evaluation in two-way action slabs and plates, and that the proposed equation gives reasonable prediction of flexural cracking behavior.

DISCUSSION SUMMARY

Summarizing the behavior of the 90 test slabs in this research program, it can be seen from the analysis of the test results that crack width development in

two-way action floors is a function of the grid index

$$I_1 = (\phi_1 s_2)/p_{t_1} \quad \left(\text{or} \quad I_1 = \frac{s_1 s_2 t_b}{\phi_1} \cdot \frac{8}{\pi}\right)$$

in the general crack control Eq. (1), where $w_{max} = KRf_s\sqrt{I}$. The reinforcement spacing in the two perpendicular directions is a major parameter of this proposed index, while the diameter of the reinforcement and the active steel ratio are the two secondary parameters.

Application of the cracking equation to the test results was adequately tested both qualitatively, through observation of behavior as discussed, and quantitatively, through comparison of measured to predicted values, as in Table 1-2. The proposed fracture hypothesis was thus found valid and the proposed cracking equation safe to apply.

Also, for a constant area of steel determined for moment in one direction, the energy hypothesis that smaller spacings of transverse bars require smaller diameter of longitudinal bars was maintained in the design of the experiments. The test results are in conformity with this principle when comparisons are made for the developed crack widths and spacings of the test slabs for various combination of diameter ϕ_1 with spacing s_2, and diameter ϕ_2 with spacing s_1. Bar or wir spacings not exceeding 6 to 8 in. (15-20 cm) force the generation of the preferred grid of numerous narrow orthogonal controlling cracks. To proportion the reinforcement in the two orthogonal directions for achieving this purpose, it is only necessary for the designer to evaluate the predicted possible maximum width w corresponding to a grid index I_1 in direction "1" closest to the concrete tensile outer fibers.

Furthermore, the predicted crack width $w = KRf_s\sqrt{I}$ of Eq. (1) can be presented in tabular as well as graphical form for the various fracture coefficients K describing the load and the boundary conditions applicable to the particular floor. Typical Fig. 1-6 gives a graphical solution of Eq. (1) at reinforcement stre level f_s = 40 percent f_y = 24 ksi for the K values of 1.6 to 4.2 described in Table 1-1.

A stress level of 40 percent of the yield strength of steel is chosen as the upp limit of serviceability stress to which a framed floor slab can be practically subjected at present. Steel of yield 60 ksi is commonly used today as reinforcemen in floor slabs; hence 24 ksi level steel was used for constructing Fig. 1-6, while similar charts for higher stresses can be easily prepared. This diagram can be readily utilized for crack control evaluation with minimal computational effort, once the design engineer determines the maximum width of a flexural crack he can tolerate for the particular exposure condition. Table 1-4 summarizes acceptable permissible crack widths under various exposure conditions, discussed further by the first author in Reference 15 and also in Reference 1.

Eq. (1) was also verified by application to tests of both full-scale floors and smaller-scale models by other investigators. Very close agreement was obtained between the predicted and measured crack width values. Scale effect was found insignificant in two-way action, as predicted in the fracture hypothesis. Design

examples are given in the appendix to illustrate the simple application of the developed crack control hypothesis to structural slabs and plates.

CONCLUSIONS

1) Codification for crack control in two-way action slabs, flat plates and flat slabs is now possible as a result of this investigation. It is also necessary in view of increased use of high strength steel of 60 ksi yield or higher in slabs.

2) Crack control provisions for beams in the ACI Building Code 318-71 are inapplicable and unsafe to apply to two-way action floors. They also result in unrealistic and unsafe reinforcement spacings in one-way slabs having standard 3/4 in. cover.

3) The major parameter controlling the cracking behavior of a two-way system, apart from the reinforcement stress level, is the spacing of the intersecting bars or wires in the two orthogonal directions, while the diameter of the reinforcement and the active steel ratio are the two secondary parameters. Effect of the surface deformations of the steel is negligible.

4) Crack control is accomplished through development of numerous narrow orthogonal cracking grids reflecting the reinforcement grids, rather than through a few wide diagonal yield-line cracks. The grid index I is found to be a good indicator in proportioning the reinforcement spacings. Choice of the proper grid index value $I_1 = (\phi_1 s_2)/p_{t_1}$ from Fig. 1-6 achieves this result.

5) Transverse spacing of the interesting reinforcement in excess of an optimum value up to 8 in. (20 cm) approximately, regardless of the diameter of the reinforcement, leads to early development of wide diagonal cracks and no forced orthogonal fracture patterns are possible. Hence most efficient crack control in two-way action floor design can be achieved only through use of closely spaced small diameter and not through widely spaced large diameter reinforcement.

6) Scale effect is insignificant on crack width development in two-way action floor systems.

7) The proposed equation $w_{max} = K R f_s \sqrt{I}$ predicts as a best fit the probable flexural crack width which can develop in a two-way action floor system. Values of the fracture coefficient K depend on the loading and boundary conditions and the ratio of short to long span, as given in Table 1-1. An average value of R = 1.25 can be used. Reinforcement stress f_s equivalent to 40 percent of the yield strength f_y can be used as a limit for acceptable serviceability conditions at present. The design engineer needs only to evaluate the predicted crack width corresponding to grid index I_1 in direction "1" closest to the concrete outer tensile fibers.

8) In plate regions where reinforcement in only one direction is sometimes used, and in one-way slabs with large spacing of transverse reinforcement, a value of s_2 up to 12 in. (30 cm), but not less than 8 in. (20 cm), can be inserted in the grid index parameter of the cracking equation; the larger the diameter ϕ_1 the larger is the s_2 value applicable within the 12 in. limit.

ACKNOWLEDGMENTS

The writers wish to thank the U.S. Steel Corporation for the welded fabric and other financial support they extended. The second author's contribution is limited to testing and investigating the cracking development in slabs WV1 to WV36 under the direction of the first author. This investigation was initiated and conducted in the Concrete Research Laboratories of the Department of Civil and Environmental Engineering at Rutgers University, The State University of New Jersey.

REFERENCES

1. ACI Committee 318, "Building Code Requirements for Reinforced Concrete (ACI 318-71)," American Concrete Institute, Detroit, 1971.
2. Nawy, E. G., "Crack Width Control in Welded Fabric Reinforced Centrally Loaded Two-Way Concrete Slabs," *Causes, Mechanism, and Control of Cracking in Concrete*, SP-20, American Concrete Institute, Detroit, 1968, pp. 211-235.
3. Nawy, E. G., and Orenstein, G. S., "Crack Width Control in Reinforced Concrete Two-Way Slabs," *Proceedings*, ASCE, V. 93, ST3, Mar. 1970, pp. 701-721.
4. Atlas, A.; Siess, C. P.; and Kesler, C. E., "Control of Cracking in Slabs Reinforced with Welded Wire Fabric," *Causes, Mechanism, and Control of Cracking in Concrete*, SP-20, American Concrete Institute, Detroit, 1968, pp. 205-209.
5. Lloyd, J. P.; Rejali, H. M.; and Kesler, C. E., "Crack Control in One-Way Slabs Reinforced with Deformed Welded Wire Fabric," ACI JOURNAL, *Proceedings* V. 66, No. 5, May 1969, pp. 366-376.
6. Nawy, E. G., Discussion of "Crack Control in One-Way Slabs Reinforced with Deformed Welded Wire Fabric" by J. P. Lloyd, H. M. Rejali, and C. E. Kesler, ACI JOURNAL, *Proceedings* V. 66, No. 11, Nov. 1969, p. 933.
7. Shah, S. P., "Ferro Cement as a New Engineering Material," *Report* No. 70-11, University of Illinois at Chicago, Nov. 1970, pp. 1-37.
8. Hognestad, E., "High Strength Bars as Concrete Reinforcement. Part 2, Control of Flexural Cracking," *Journal*, PCA Research and Development Laboratories, V. 4, No. 1, Jan. 1962, pp. 46-63.
9. ACI Committee 224, Discussion of "Proposed Revision of ACI 318-63: Building Code Requirements for Reinforced Concrete" by ACI Committee 318, Section 10.6, ACI JOURNAL, *Proceedings* V. 67, No. 9, Sept. 1970, pp. 681-683.
10. Nawy, E. G., "Crack Width Control in Two-Way Concrete Slabs Reinforced with Welded Wire Fabric, Part 1, Centrally Loaded," *Engineering Research Bulletin* No. 46, College of Engineering, Rutgers University, 1967, 87 pp.

11. Guralnick, S. A., and LaFraugh, R. W., "Laboratory Study of a 45-Foot Square Flat Plate Structure," ACI JOURNAL, *Proceedings* V. 60, No. 9, Sept. 1963, pp. 1107-1185.

12. Gamble, W. L.; Sozen, M. S.; and Siess, C. P., "An Experimental Study of a Reinforced Concrete Two-Way Slab," *Bulletin* 211, Civil Engineering Studies, Structural Research Series, University of Illinois, 1961, 304 pp.

13. Cardenas, A. E., and Kaar, P. H., "Field Test of a Flat Plate Structure," *Concrete Report*, Portland Cement Association, Skokie, 1970, pp. 1-25.

14. Hopkins, D. C., "Effect of Membrane Action on the Ultimate Strength of Reinforced Concrete Slabs," PhD Thesis, University of Canterbury, Christchurch, New Zealand, 1969, 358 pp.

15. Nawy, E. G., "Crack Control in Reinforced Concrete Structures," ACI JOURNAL, *Proceedings* V. 65, No. 10, Oct. 1968, pp. 825-836.

TABLE 1–FRACTURE COEFFICIENT K IN EQ. $W_{max} = KRf_s\sqrt[3]{I}$

Loading[b] type	Boundary condition[c]	Span ratio[d] S/L	Fracture coeff. K
A	Square slab, 4 edges r.	1.0	2.1×10^{-5}
A	Square slab, 4 edges s.	1.0	3.1
B	Rect. slab, 4 edges r.	0.5	[e]1.6
B	Rect. slab, 4 edges r.	0.7	2.2
B	Rect. slab, 3 edges r. 1 edge h.	0.7	2.3
B	Rect. slab, 2 edges r. 2 edges h.	0.7	2.7
B	Square slab 4 edges r.	1.0	2.8
B	Square slab, 3 edges r. 1 edge h.	1.0	2.9
B	Square slab, 2 edges r. 2 edges h.	1.0	4.2

[a] I = Grid Index = $(\phi_1 s_2/p_{t_1})$ in.^{2}; f_s = reinforced steel stress (ksi). In cases where transverse steel is not used or when its spacing s_2 exceeds 12 in. (30.5 cm), use s_2 = 12 in. in the equation.

[b] Loading type: A = concentrated; B = uniformly distributed.

[c] Boundary condition: r. = restrained; s. = simply supported; h. = hinged.

[d] Span ratio: S = clear short span; L = clear long span.

[e] K interpolated = 1.6×10^{-5}, as minimum for one-way slabs $\left(\frac{S}{L} < 0.5\right)$.

TABLE 1-2–CORRELATION OF OBSERVED AND COMPUTED MAXIMUM CRACK WIDTHS[a]

Test no.	Slab des.	20 ksi			30 ksi			35 ksi			50 ksi			60 ksi		
		w_o	w_c	w_o/w_c	w_o	w_c	w_o/w_c	w_o	w_c	w_o/w_c	w_o	w_c	w_o/w_c	w_o	w_c	w_o/w_c
	4 edges restrained, concentrated loading							Clear spans 5′8″ x 5′8″ $^bK = 2.1 \times 10^{-5}$								
1	CSF1	.005	.0061	0.82	.008	.0092	0.88	.010	.0109	0.92	.022	.0153	1.44	.036	.0183	1.97
2	CSF2	.004	.0056	0.71	.007	.0085	0.82	.009	.0099	0.91	.014	.0141	1.00	.019	.0168	1.13
3	CSG1	.007	.0095	0.74	.012	.0143	0.84	.015	.0167	0.90	.028	.0238	1.18	.037	.0285	1.30
4	CSG2	.006	.0073	0.82	.010	.0109	0.92	.013	.0127	1.02	.021	.0182	1.15	.027	.0219	1.23
5	CSH1	.005	.0053	0.94	.009	.0079	1.14	.010	.0093	1.07	.016	.0132	1.21	.023	.0159	1.45
6	CSH2	.003	.0053	0.57	.004	.0079	0.51	.005	.0093	0.54	.007	.0132	0.53	.009	.0159	0.57
7	CSI1	.009	.0086	1.05	.014	.0129	1.09	.020	.0151	1.33	.044	.0215	2.05	.052	.0258	2.02
8	CSJ1	.006	.0065	0.92	.010	.0097	1.03	.013	.0113	1.15	.022	.0162	1.36	.035	.0195	1.80
9	CSJ2	.007	.0088	0.80	.011	.0131	0.84	.014	.0153	0.91	.022	.0219	1.01	.028	.0264	1.06
10	CSK1	.009	.0086	1.05	.013	.0129	1.01	.015	.0151	0.99	.023	.0216	1.11	.029	.0258	1.12
		$\frac{w_o}{w_c}$	Mean	0.842			0.908			0.974			1.204			1.356
			S.D.	0.152			0.179			0.204			0.322			0.454
	4 edges simply supported, concentrated loading							Clear spans 5′8″ x 5′8″ $K = 3.1 \times 10^{-5}$								
11	SA1	.012	.0085	1.41	.019	.0127	1.50	.024	.0148	1.62	.033	.0211	1.56	.039	.0225	1.73
12	SA2	.006	.0085	0.71	.010	.0127	0.79	.012	.0148	0.81	.019	.0211	0.90	.032	.0225	1.42
13	SA3	.009	.0085	1.06	.013	.0127	1.02	.016	.0148	1.08	.023	.0211	1.09	.034	.0225	1.51
14	SB1	.013	.0228	0.57	.023	.0342	0.67	.028	.0398	0.70	.044	.0569	0.77	.058	.0684	0.85
15	SB2	.007	.0155	0.45	.013	.0232	0.56	.015	.0271	0.55	.024	.0387	0.62	.036	.0465	0.77
16	SC1	.021	.0248	0.85	.032	.0365	0.88	.038	.0425	0.89	.053	.0608	0.87	.064	.0744	0.86
17	SC2	.029	.0238	1.24	.044	.0357	1.23	.056	.0416	1.35	.077	.0595	1.29	.093	.0714	1.30
18	SD1	.020	.0164	1.22	.026	.0246	1.06	.029	.0287	1.01	.041	.0410	1.00	.051	.0492	1.04
19	SD2	.017	.0170	1.00	.025	.0258	0.98	.029	.0301	0.96	.040	.0431	0.93	.050	.0510	0.98
20	SE1	.013	.0185	0.70	.020	.0277	0.72	.024	.0323	0.74	.035	.0462	0.76	.051	.0555	0.92
21	SE2	.006	.0054	1.11	.009	.0081	1.11	.012	.0095	1.26	.019	.0136	1.40	.026	.0162	1.61
22	SE3	.006	.0077	0.78	.009	.0116	0.78	.012	.0135	0.89	.018	.0193	0.93	.025	.0231	1.08
		$\frac{w_o}{w_c}$	Mean	0.925			0.942			0.988			1.010			1.173
			S.D.	0.295			0.264			0.302			0.279			0.328
	4 edges restrained, uniform loading							Clear spans 5′0″ x 5′0″ $K = 2.8 \times 10^{-5}$								
23	WS1	.009	.0070	1.28	.013	.0105	1.24	.016	.0122	1.31	.024	.0175	1.37	.036	.0210	1.72
24	WS2	.007	.0070	1.00	.010	.0105	0.95	.012	.0122	0.98	.017	.0175	0.97	.028	.0210	1.33
25	WS3	.006	.0071	0.85	.009	.0106	0.85	.011	.0124	0.89	.016	.0177	0.91	.033	.0213	1.55
26	WS4	.005	.0071	0.70	.009	.0106	0.85	.013	.0124	1.05	.021	.0177	1.20	.032	.0213	1.50
27	WS5	.009	.0133	0.68	.013	.0201	0.65	.015	.0234	0.64	.021	.0334	0.63	.028	.0400	0.70
28	WS6	.007	.0133	0.53	.009	.0201	0.45	.010	.0234	0.43	.019	.0334	0.57	.022	.0400	0.55
29	WS7	.008	.0067	1.20	.011	.0099	1.11	.013	.0116	1.12	.019	.0166	1.15	.027	.0201	1.35
30	WS8	.006	.0054	1.11	.009	.0814	1.11	.010	.0095	1.05	.014	.0136	1.03	.020	.0162	1.24
31	WS9	.008	.0099	0.81	.011	.0148	0.74	.013	.0173	0.75	.018	.0246	0.73	.027	.0297	0.91
32	WS10	.013	.0114	1.14	.019	.0172	1.10	.024	.0200	1.20	.034	.0286	1.19	.042	.0342	1.23
33	WS11	.014	.0117	1.20	.016	.0176	0.91	.020	.0211	0.95	.031	.0292	1.06	.035	.0352	0.99
34	WS12	.011	.0098	1.12	.017	.0146	1.17	.019	.0171	1.11	.034	.0244	1.40	.045	.0294	1.53
35	WS13	.030	.0288	1.04	.045	.0433	1.04	.052	.0506	1.03	.072	.0723	0.99	.092	.0865	1.06
36	WS14	.022	.0262	0.80	.031	.0393	0.79	.035	.0461	0.76	.051	.0663	0.78	.059	.0886	0.67
37	WS15	.019	.0137	1.39	.023	.0206	1.12	.026	.0240	1.08	.035	.0272	1.29	.042	.0326	1.29
38	[c]WS16	.012	.0094	1.28	.014	.0141	0.99	.016	.0164	0.98	.023	.0234	0.98	.028	.0282	0.99

TABLE 1-2—CORRELATION OF OBSERVED AND COMPUTED MAXIMUM CRACK WIDTHS[a] (CONT.)

Test no.	Slab des.	20 ksi			30 ksi			35 ksi			50 ksi			60 ksi		
		w_o	w_c	w_o/w_c	w_o	w_c	w_o/w_c	w_o	w_c	w_o/w_c	w_o	w_c	w_o/w_c	w_o	w_c	w_o/w_c
39	WS17	.011	.0094	1.17	.013	.0141	0.92	.014	.0164	0.85	.025	.0234	1.06	.033	.0282	1.17
40	WS18	.019	.0163	1.17	.028	.0246	1.04	.037	.0286	1.29	.047	.0410	1.15	.065	.0489	1.33
41	WS19	.014	.0135	1.04	.022	.0202	1.09	.024	.0236	1.02	.034	.0336	1.01	.044	.0405	1.09
42	WS20	.003	.0069	0.43	.006	.0104	0.58	.007	.0121	0.58	.013	.0173	0.75	.015	.0207	0.72
43	WS21	.005	.0069	0.72	.010	.0104	0.96	.013	.0121	1.07	.017	.0173	0.98	.020	.0207	0.97
44	WS22	.010	.0110	0.91	.017	.0165	1.03	.020	.0192	1.04	.026	.0274	0.95	.031	.0333	0.93
45	WS23	.016	.0117	1.37	.022	.0176	1.25	.023	.0206	1.12	.031	.0294	1.06	.037	.0351	1.06
46	WS24	.018	.0183	0.98	.026	.0267	0.92	.031	.0312	0.99	.045	.0455	0.99	.055	.0548	1.00
47	[c]WS25	.015	.0131	1.15	.021	.0197	1.07	.026	.0229	1.14	.038	.0327	1.16	.045	.0393	1.15
48	WS26	.016	.0168	0.95	.025	.0250	1.00	.029	.0294	0.99	.039	.0412	0.85	.047	.0495	0.95
49	WS27	.011	.0126	0.87	.017	.0188	0.90	.021	.0220	0.96	.029	.0314	0.93	.036	.0378	0.96
50	WS28	.013	.0134	0.97	.021	.0201	1.00	.024	.0234	1.03	.034	.0335	1.01	.046	.0402	1.14
51	WS29	.017	.0218	0.78	.026	.0327	0.80	.031	.0381	0.81	.053	.0546	0.97	.076	.0654	1.18
52	WS30	.019	.0241	0.79	.029	.0361	0.80	.034	.0420	0.81	.049	.0604	0.81	.062	.0723	0.86
53	WS31	.012	.0116	1.03	.016	.0176	0.91	.018	.0204	0.88	.027	.0294	0.93	.036	.0348	1.03
54	WS32	.015	.0116	1.29	.019	.0176	1.08	.021	.0204	1.03	.032	.0294	1.09	.039	.0348	1.12
55	WV1	.008	.0077	1.31	.014	.0116	1.21	.017	.0135	1.26	.022	.0193	1.14	.027	.0232	1.16
56	WV2	.008	.0082	0.98	.011	.0123	0.89	.014	.0144	0.97	.021	.0206	1.02	.031	.0247	1.26
57	WV3	.013	.0149	0.87	.019	.0223	0.85	.021	.0261	0.81	.029	.0372	0.78	.035	.0447	0.78
58	WV4	.008	.0089	0.90	.010	.0134	0.75	.013	.0156	0.81	.018	.0223	0.81	.029	.0267	1.09
59	WV5	.013	.0082	1.59	.016	.0123	1.30	.018	.0144	1.25	.021	.0206	1.10	.022	.0247	0.89
60	WV6	.008	.0111	0.72	.015	.0167	0.90	.020	.0195	1.03	.036	.0278	1.30	.044	.0334	1.32
61	WV7	.011	.0175	0.63	.020	.0262	0.76	.025	.0307	0.81	--	--	--	--	--	--
		w_o	Mean	0.981			0.946			0.967			0.996			1.097
		w_c	S.D.	0.215			0.180			0.181			0.185			0.207

3 edges restrained, 1 edge hinged, uniform loading								Clear spans 5′0″ x 5′0″ $K = 2.9 \times 10^{-5}$								
62	WV8	.007	.0080	0.88	.010	.0120	0.83	.013	.0140	0.93	.016	.0200	0.80	.021	.0240	0.87
63	WV9	.014	.0179	0.79	.018	.0253	0.71	.020	.0295	0.68	.029	.0422	0.69	.045	.0506	0.89
64	WV10	.010	.0092	1.08	.013	.0137	0.95	.014	.0160	0.88	.021	.0229	0.92	.028	.0275	1.02
65	WV11	.011	.0126	0.87	.015	.0190	0.79	.018	.0221	0.82	.025	.0316	0.79	.033	.0379	0.87
66	WV12	.018	.0182	0.99	.029	.0272	1.07	.035	.0318	1.10	--	--	--	--	--	--
		w_o	Mean	0.922			0.870			0.882			0.800			0.912
		w_c	S.D.	0.113			0.141			0.154			0.094			0.072
2 edges restrained, 2 edges hinged, uniform loading								Clear spans 5′0″ x 5′0″ $K = 4.2 \times 10^{-5}$								
67	WV13	.024	.0233	1.03	.037	.0350	1.06	.044	.0408	1.08	--	--	--	--	--	--
68	WV14	.017	.0128	1.33	.023	.0190	1.21	.027	.0222	1.22	.040	.0317	1.26	.053	.0380	1.45
69	WV15	.021	.0224	0.93	.040	.0355	1.19	.054	.0391	1.38	--	--	--	--	--	--
70	WV16	.020	.0183	1.09	.027	.0275	0.98	.031	.0321	0.96	.046	.0457	1.00	.060	.0549	1.09
71	WV17	.017	.0132	1.29	.020	.0200	1.00	.022	.0232	0.95	.029	.0322	0.90	.036	.0398	0.91
		w_o	Mean	1.134			1.088			1.118			1.053			1.150
		w_c	S.D.	0.171			0.107			0.183			0.186			0.275
4 edges restrained, uniform loading								Clear spans 5′0″ x 3′6″ $K = 2.2 \times 10^{-5}$								
72	WV18	.013	.0131	0.99	.018	.0197	0.91	.020	.0229	0.87	.027	.0328	0.82	.035	.0394	0.89
73	WV19	.007	.0069	1.01	.012	.0104	1.15	.014	.0122	1.15	.024	.0174	1.40	.034	.0208	1.64
74	WV20	.007	.0054	1.30	.009	.0081	1.11	.010	.0094	1.06	.015	.0134	1.12	.019	.0160	1.19
75	WV21	.007	.0076	0.92	.011	.0114	0.97	.013	.0133	0.98	.019	.0191	1.00	.023	.0229	1.00
76	WV22	.012	.0095	1.26	.017	.0142	1.20	.020	.0166	1.21	.026	.0237	1.10	.035	.0284	1.23

TABLE 1-2–CORRELATION OF OBSERVED AND COMPUTED MAXIMUM CRACK WIDTHS[a] (CONT.)

Test no.	Slab des.	20 ksi			30 ksi			35 ksi			50 ksi			60 ksi		
		w_i	w_c	w_o/w_c	w_o	w_c	w_o/w_c	w_o	w_c	w_o/w_c	w_o	w_c	w_o/w_c	w_o	w_c	w_o/w_c
77	WV23	.013	.0192	0.78	.021	.0288	0.73	.025	.0335	0.75	.041	.0479	0.86	.050	.0575	0.87
78	WV24	.022	.0291	0.68	.023	.0436	0.53	.024	.0508	0.48	.032	.0727	0.44	.045	.0872	0.52
79	WV25	.011	.0122	0.92	.017	.0183	0.93	.020	.0214	0.93	--	--	--	--	--	--
80	WV26	.009	.0117	0.77	.014	.0175	0.80	.016	.0204	0.78	.025	.0292	0.86	.035	.0350	1.00
81	WV27	.007	.0061	1.15	.011	.0091	1.21	.013	.0106	1.22	.019	.0152	1.25	.024	.0182	1.31
82	[c]WV28	--	--	--	--	--	--	--	--	--	--	--	--	--	--	--
83	WV29	.008	.0096	0.94	.012	.0144	0.84	.015	.0168	0.89	.020	.0240	0.83	.025	.0288	0.87
		$\bar{w}_c$	Mean	0.983			0.943			0.938			0.968			1.052
		$\bar{w}_c$	S.D.	0.151			0.176			0.188			0.235			0.227
	3 edges restrained, 1 edge hinged, uniform loading							Clear spans 5′ 0″ x 3′ 6″ $K = 2.3 \times 10^{-5}$								
84	WV30	.008	.0072	1.11	.009	.0109	0.83	.011	.0127	0.87	.016	.0182	0.88	.023	.0218	1.06
85	WV31	.013	.0122	1.07	.018	.0182	0.98	.021	.0214	0.98	.034	.0306	1.11	.044	.0367	1.20
86	WV32	.004	.0069	0.58	.006	.0104	0.58	.008	.0122	0.66	.015	.0174	0.86	.021	.0208	1.01
87	WV33	.012	.0128	0.94	.019	.0192	0.99	.024	.0224	1.07	--	--	--	--	--	--
		$\bar{w}_c$	Mean	0.924			0.844			0.894			0.951			1.088
		$\bar{w}_c$	S.D.	0.241			0.191			0.177			0.139			0.099

	2 edges restrained, 2 edges hinged, uniform loading							Clear spans 5′ 0″ x 3′ 6″ $K = 2.7 \times 10^{-5}$								
88	WV34	.016	.0157	1.02	.025	.0235	1.06	.027	.0275	0.98	.038	.0392	0.97	.045	.0471	0.96
89	WV35	.007	.0079	0.89	.010	.0119	0.84	.012	.0138	0.87	.018	.0198	0.91	.024	.0237	1.01
90	WV36	.014	.0150	0.80	.019	.0225	0.84	.022	.0262	0.84	--	--	--	--	--	--
		$\bar{w}_i$	Mean	0.902			0.916			0.897			0.939			0.984
		$\bar{w}_i$	S.D.	0.111			0.127			0.074			0.042			0.035

[a]Load and boundary conditions defined in Table 1-1. w_o = observed; w_c = computed (in.). 0.01 in. = 0.25 mm.

[b]K = Fracture coefficient.

[c]Not included in analysis.

TABLE 1-3–TESTS BY OTHER INVESTIGATORS

Investigator[a]	No. tests	Scale	No. panels	Panel slab ft	Total slab thick., in.	Clear conc. cover, in.	Flexural reinforcement	Meas. crack width, in.	Steel stress level f_s, ksi	Value of K	Predicted crack width, in
1	2	3	4	5	6	7	8	9	10	11	12
Guralnick-LaFraugh[11]	1	3/4	9	15 x 15	5¼	7/16	½" ϕ bars Top col. strip @ 6 3/8" x 6 3/8" Bot. mid. strip @ 12½" x 12½"	.005 negl.	8.3 2.7	2.45 2.45	.004 .002
Gamble-Sozen-Siess[12]	2	1/4	9	5 x 5	2½	3/4	Top: 1/8" sq. bars @ 2¾" x 2¾"	.005	19.3	2.2	.0045
Cardenas-Kaar[13] f_s evaluated from M-€ diagram	1	prototype	2	13 x 13	5½	3/4	*Panel I:* Top: 3/8" ϕ @ 6" x 6" Bot.: 6" x 6" D5.4/D5.4 WWF[b]	.008	15	2.4	.008
							Adjacent Panel I': Top & bot.: 6" x 6" D5.4/D5.4 WWF + ½" ϕ bars @ 6" x 6" on top col. strip	.014	44		.011
	1	1/2	1	6 x 6	5	3/4	Top & bot.: 6" x 6" D5.4/D5.4 WWF + ½ ϕ bars @ 12" x 12" top	.028	44	2.45	.025
Hopkins Park[14]	1	1/4	9	5½ x 5½ central panel	2.02	13/64	Bot. mid. strip: 1/8" ϕ dia. @ 4¼" x 4¼"	.015	48.5	2.8	.0165

[a]Superscripts are reference numbers.

[b]D5.4 WWF = Deformed welded wire fabric. Area of single wire = .054 in.^{2}; dia. = .2625 in.

TABLE 1-4–PERMISSIBLE CRACK WIDTHS VERSUS EXPOSURE CONDITIONS

Exposure condition	Maximum allowable crack width, in.*
Air or protective membrane	0.016
Humidity, air-water, soil	0.012
De-icing chemicals	0.007
Seawater and seawater spray; wetting and drying	0.006
Water-retaining structure	0.004

*0.001 in. = 0.025 mm.

APPENDIX

CRACK CONTROL DESIGN EXAMPLES

Example #1

The interior panel of a uniformly loaded two-way slab on beams has a span ratio S/L = 1.0 (where S = short span and L = long span). It is 5 in. thick. Find the size and spacing of negative reinforcement to satisfy normal exposure conditions. R = 1.25, f_y = 60 ksi.

Solution

(a) From Table 1-1, required $K = 2.8 \times 10^{-5}$
From Table 1-4, permissible $w_{max} = 0.016$ in.

$$w_{max}/R = \frac{0.016}{1.25} = .0128$$

From Fig. 1-6, Grid Index $I_1 = 370$ in.^{2}

$$I_1 = 370 = \frac{\phi_1 s_2}{p_{t_1}} = \frac{s_1 s_2 t_b}{\phi_1} \cdot \frac{8}{\pi}$$

where t_b = cover to center of first steel layer. Try #4 rebars (ϕ = 0.5 in.), assume $s_1 = s_2$, hence t_b = 1.0 in. hence,

$$370 = \frac{s_1^2 \times 1 \text{ in.}}{0.5 \text{ in.}} \cdot \frac{8}{\pi}, \text{ i.e., } s_1 = 8.5 \text{ in.}$$

(b) From Crack Control Equation:

$$w = KRf_s\sqrt{I}$$

hence,

$$.016 = 2.8 \times 10^{-5} \times 1.25 \times .4 \times 60 \text{ ksi} \sqrt{I}$$

I = 370 giving s_1 = 8.5

Therefore, for crack control, #4 @ 8½ in. is needed.
(ACI 318-71 Section 13.5.1 permits maximum spacing 2t = 2 x 5 = 10 in.)

Example #2

Solve Example #1 using deformed welded wire fabric as reinforcement.

Solution

I = 370 from before
Assume D3.6 gage and $\phi_1 = \phi_2 = 0.214$ in.
hence,

$$t_b = 0.107 + 0.75 = 0.857 \text{ in.}$$

$$I = 370 = \frac{s_1^2 t_b}{\phi_1} \cdot \frac{8}{\pi}$$

$$s_1^2 = \frac{370 \times .214 \times \pi}{8 \times 0.857} = 36.1 \text{ in.}^2, \text{ i.e., } s_1 = 6.02 \text{ in}$$

Therefore, use 6 x 6 - D3.6/D3.6 WWFabric.

Example #3

Solve Example #2 if the span ratio S/L = 0.6.

Solution

From Table 1-1, $K = 1.9 \times 10^{-5}$ by interpolation
From Fig. 1-6, Grid Index I_1 = 810

(a) Trying #4 rebars:

$$810 = \frac{s_1^2 \times 1.0}{0.5} \cdot \frac{8}{\pi}$$

$$s_1^2 = 157, \text{ i.e., } s_1 = 12.5 \text{ in.}$$

Use #4 at 12 in. center to center each way.

(b) Trying deformed WWF size D3.6:

$$\phi_1 = \phi_2 = 0.231 \text{ in.}$$

$$s_1^2 = 36.1 \times \frac{810}{370} = 79.0 \text{ in.}^2 \text{ (from Ex. 2)}; \; s_1 = 8.9 \text{ in.}$$

Use 9 x 9 - D3.6/D3.6 WWF.

Example #4

Find the size and spcing necessary for crack control at the negative region of the column reaction in a flat plate 7 in. thick and loaded uniformly. Span ratio S/L = 1.0, R = 1.20, f_y = 60 ksi. Concrete is subjected to normal exposure.

Solution

From Table 1-1, $K = 2.1 \times 10^{-5}$
From Table 1-4, permissible w = 0.016 in.

Hence,

$$w/R = 0.016/1.20 = 0.0133$$

From Fig. 1-6, Grid Index $I_1 = 700$
Assume $s_1 = s_2$

(a) Trying #4 rebars.

$$t_b = 0.25 + 0.75 \text{ in. cover} = 1.0;\ \phi_1 = 0.5 \text{ in.}$$

$$700 = \frac{s_1^2 \times 1.0}{0.5} \cdot \frac{8}{\pi}$$

$$s_1^2 = 137, \text{ i.e., } s_1 = 11.75 \text{ in.}$$

Use #4 at 12 in. center to center each way

(b) Trying deformed WWF size D3.0:

$$\phi_1 = \phi_2 = 0.195 \text{ in.}$$

$$t_b = 0.097 + 0.75 = 0.847 \text{ in.}$$

$$700 = \frac{s_1^2 \times 0.847}{0.195} \cdot \frac{8}{\pi}$$

$s_1^2 = 63.5 \text{ in.}^2$, i.e., $s_1 = 7.96$ in.
Use 8 x 8 - D3.0/D3.0 WWF.

Example #5

Solve Example #4 for severe exposure conditions.

Solution

From Table 1-4, permissible $w_{max} = 0.012$ in.

$$w/R = 0.012/1.2 = 0.010 \text{ in.}$$

From Fig. 1-6, Grid Index $I = 390 \text{ in.}^2$

(a) Trying #4 rebars:

$$s_1^2 = 137 \times \frac{390}{700} = 76.5 \text{ in.}^2, \text{ i.e., } s_1 = 8.6 \text{ in.}$$

Use #4 @ 8½ in. center to center each way.

(b) Trying deformed WWF size D3.0:

$$s_1^2 = 63.5 \times \frac{390}{700} = 35.5 \text{ in.}^2, \text{ i.e., } s_1 = 5.9 \text{ in.}$$

Use 6 x 6 - D3.0/3.0 WWF.

Note: For yield strength f_y value different from 60 ksi, either the crack control equation is to be directly used, or charts be prepared similar to Fig. 1-6.

NOTATION

- A_s = Area of tensile reinforcement in one direction per foot width of slab
- A_t = Concrete stretched area = $12(2t + \phi)$ for a 12 in. strip, defining the area of concrete stretched in tension
- d = Effective depth to center of one layer of reinforcement
- f'_c = Cylinder compressive strength of concrete, psi
- f_s = Tensile stress in steel reinforcement, ksi
- f'_t = Tensile splitting strength of concrete, psi
- f_y = Yield strength of reinforcement by 0.2 percent offset
- I_1 = Grid Index in direction "1" ($= \phi_1 s_2/p_{t_1}$) closest to outer concrete fibers
- I_2 = Grid Index in direction "2" ($\phi_2 s_1/p_{t_2}$) in direction perpendicular to "1"
- K = Fracture coefficient dependent on load or reaction type and on the support condition (See Table 1-1)
- p = Steel percentage = $A_s/12d$
- p_t = Active steel ratio = A_s/A_t
- R = Cover ratio = ratio of distance from neutral axis to tensile face of concrete to distance from neutral axis to the center of gravity of reinforcement
- s = Spacing of reinforcement, in.
- s.d. = Standard deviation (σ)
- t = Thickness of clear concrete cover, in.
- t_b = Thickness of concrete cover to center of reinforcement layer, in.
- w_c = Computed crack width in inches at concrete face, in.
- w_o = Observed crack width in inches at concrete face, in.
- w_{max} = Maximum crack width in inches at concrete face, in.
- ϕ = Diameter of reinforcing bar or wire, in.
- "1" = Direction of reinforcing elements closest to outer concrete fibers, for which crack control check is to be made

TABLE 1-A–GENERAL PROPERTIES OF SLAB TEST SPECIMENS[a]

Test no.	Slab designation	Average slump, in.	Age at test, days	Cylinder compres. strength f'_c, psi	Cylinder split. strength f'_t, psi	Total center thickness, in.	Center d_1, in.	Reinf.[b] wire gage or bar size	Reinf dia. ϕ_1/ϕ_2, in./in.	Reinf. spacing $s_1 \times s_2$, in.	Reinf. yield strength, 0.2% offset, in.	Center deflec. at ult. load, in.
4 edges restrained, concentrated loading							Clear spans 5′8″ x 5′8″					
1	CSF1	5 1/4	195	5770	540	3.45	2.85	W8.6	0.331	4 x 4	86700	0.29
2	CSF2	3 3/4	12	5000	535	3.64	2.67	W8.6	0.331	4 x 4	86850	0.33
3	CSG1	3	12	4520	425	3.45	2.88	W8.6	0.333	8 x 8	85100	0.76
4	CSG2	3 1/4	9	4060	390	3.30	2.96	W8.6	0.333	8 x 8	78440	0.86
5	CSH1	2 1/2	9	3980	470	3.45	2.93	W4.7	0.244	4 x 4	83120	0.65
6	CSH2	1 3/4	10	5360	570	3.45	2.96	W4.7	0.244	4 x 4	82050	0.68
7	CSI1	2 1/2	17	5010	550	3.50	3.20	W4.7	0.242	8 x 8	80950	1.11
8	CSJ1	1 7/8	17	5710	560	3.40	2.95	W4.7	0.243	4 x 8	81900	0.70
9	CSJ2	1 1/2	17	5100	560	3.40	2.70	W4.7	0.243	4 x 8	83550	0.80
10	CSK1	2	16	4990	530	3.20	2.80	W5.4/ W2.9	0.262/ 0.192	6 x 12	88900	1.18
4 edges simply supported, concentrated loading							Clear spans 5′8″ x 5′8″					
11	SA1	1 3/4	7	4420	365	3.85	3.20	W4.7	0.244	4 x 4	96600	1.62
12	SA2	9 1/2	14	4060	360	3.75	3.10	W4.7	0.244	4 x 4	88100	1.95
13	SA3	1 3/4	13½	5275	515	3.65	3.00	W4.7	0.244	4 x 4	80500	1.34
14	SB1	2 1/4	11	5660	450	3.60	2.55	W8.6	0.331	8 x 8	78900	1.42
15	SB2	3 1/2	12	4470	370	3.95	3.25	W8.6	0.331	8 x 8	78400	1.63
16	SC1	3 3/4	9½	4270	470	3.95	2.90	W4.7	0.244	8 x 8	80600	2.16
17	SC2	5 1/3	12	4500	470	3.60	2.60	W4.7	0.244	8 x 8	82700	2.34
18	SD1	2 1/2	11	5340	515	4.10	3.50	W5.4/ W2.9	0.263/ 0.192	6 x 12	94200	1.46
19	SD2	3	13	5300	540	4.00	3.40	W5.4/ W2.9	0.263/ 0.192	6 x 12	95700	1.50
20	SE1	3	12	5530	510	4.10	1.80	W8.6	0.331	4 x 4	84200	1.95
21	SE2	7 1/2	11	3810	410	4.10	3.75	W8.6	0.331	4 x 4	77600	1.38
22	SE3	6 1/2	11	4340	505	4.10	3.45	W8.6	0.331	4 x 4	82100	1.22
4 edges restrained, uniform loading							Clear spans 5′0″ x 5′0″					
23	WS1	8	86	3300	280	3.00	2.45	D4.6	0.242	4 x 4	83500	1.40
24	WS2	8	80	3300	280	3.00	2.45	D4.6	0.242	4 x 4	83500	1.48
25	WS3	3 1/2	42	4870	535	3.00	2.56	D2.0	0.159	4 x 4	86300	1.18
26	WS4	3 1/2	50	4870	535	3.00	2.69	D2.0	0.159	4 x 4	86300	1.52
27	WS5	2	32	5880	570	3.00	2.05	D2.0	0.159	4 x 4	86300	1.94
28	WS6	2	41	5880	570	3.00	1.90	D2.0	0.159	4 x 4	86300	1.50
29	WS7	8	64	2830	335	3.00	2.56	D2.9	0.191	4 x 4	93000	1.46
30	WS8	8	64	2830	335	3.00	2.56	D2.9	0.191	4 x 4	93000	1.38
31	WS9	7	53	4170	450	3.00	2.25	D2.9	0.191	4 x 4	93000	1.63
32	WS10	7	53	4170	450	3.00	2.25	D2.9	0.191	4 x 4	93000	1.68
33	WS11	7	55	4400	470	3.00	2.62	D4.6	0.242	8 x 8	67500	1.34
34	WS12	7	55	4400	470	3.00	2.62	D4.6	0.242	8 x 8	67500	1.42
35	WS13	7	55	4070	410	3.00	1.75	W8.6	0.331	8 x 8	83500	2.52
36	WS14	7	55	4070	410	3.00	2.00	W8.6	0.331	8 x 8	83500	2.60
37	WS15	7 1/2	40	3930	420	3.00	1.94	W2.1	0.162	4 x 4	72000	2.54
38	WS16	7	48	4530	420	3.00	2.32	W2.1	0.162	4 x 4	72000	1.72
39	WS17	7	48	4530	420	3.00	2.32	W2.1	0.162	4 x 4	72000	1.48
40	WS18	7 1/2	40	3930	420	3.00	1.87	W2.1	0.162	4 x 4	72000	1.96
41	WS19	6	49	4850	500	3.00	1.81	D2.0	0.159	3 x 3	81900	1.54
42	WS20	7	44	4420	440	3.00	2.25	D2.0	0.159	3 x 3	81900	1.58

TABLE 1-A1—GENERAL PROPERTIES OF SLAB TEST SPECIMENS[a] (CONT.)

Test no.	Slab designation	Average slump, in.	Age at test, days	Cylinder compres. strength f'_c, psi	Cylinder split. strength f_t, psi	Total center thickness, in.	Center d_1, in.	Reinf.[b] wire gage or bar size	Reinf. dia. ϕ_1/ϕ_2, in./in.	Reinf. spacing $s_1 \times s_2$, in.	Reinf. yield strength, 0.2% offset, in.	Center deflec. at ult. load, in.
43	WS21	7	45	4420	440	3.00	2.25	D2.0	0.159	3 x 3	81900	1.37
44	WS22	6	49	4850	500	3.00	1.94	D2.0	0.159	3 x 3	81900	1.42
45	WS23	7	45	4190	430	3.00	2.25	D2.0	0.159	4 x 4	81900	1.55
46	WS24	7	45	4190	430	3.00	1.75	D2.0	0.159	4 x 4	81900	1.92
47	WS25	9 1/2	33	3800	360	3.00	1.87	D4.6	0.242	4 x 8	67500	2.46
48	WS26	9 1/2	32	2800	360	3.00	1.87	D4.6	0.242	4 x 8	67500	1.94
49	WS27	10	34	3550	390	3.00	2.12	D4.6	0.242	4 x 8	67500	1.92
50	WS28	10	34	3550	390	3.00	2.00	D4.6	0.242	4 x 8	67500	1.80
51	WS29	8	26	3800	425	3.00	1.75	D4.6	0.242	6 x 6	67500	2.24
52	WS30	8	27	3800	420	3.00	1.62	D4.6	0.242	6 x 6	67500	1.76
53	WS31	9	28	3780	390	3.00	1.25	D4.6	0.242	6 x 6	67500	1.84
54	WS32	9	65	3780	390	3.00	1.25	D4.6	0.242	6 x 6	67500	1.76
55	WV1	5	21	5590	580	2.50	2.00	D4.6	0.242	4 x 4	68300	2.22
56	WV2	5	28	5590	580	2.50	2.00	D2.9	0.191	4 x 4	68900	2.03
57	WV3	5 1/2	28	4810	500	2.50	2.00	D4.6	0.242	8 x 8	68300	2.20
58	WV4	6	32	5590	580	2.50	2.00	D2.0	0.159	4 x 4	68700	2.05
59	WV5	6	27	4990	530	2.50	2.00	D2.9	0.191	4 x 4	68900	2.04
60	WV6	6	34	4990	530	2.50	2.00	D4.6	0.242	6 x 6	68300	2.14
61	WV7	6 1/4	28	5660	570	2.50	2.00	#3	0.375	9½ x 9½	41600	2.04
	3 edges restrained, one edge hinged, uniform loading						Clear spans 5'0" x 5'0"					
62	WV8	6 1/4	22	5590	570	2.50	2.00	D4.6	0.242	4 x 4	68300	2.02
63	WV9	5 1/2	28	5590	570	2.50	2.00	D4.6	0.242	8 x 8	68300	2.20
64	WV10	5 1/2	30	6080	660	2.50	2.00	D2.9	0.191	4 x 4	68900	1.94
65	WV11	6	36	6080	660	2.50	2.00	D4.6	0.242	6 x 6	68300	2.04
66	WV12	7	26	5660	550	2.50	2.00	#3	0.375	9½ x 9½	68300	2.20
	2 edges restrained, 2 edges hinged, uniform loading						Clear spans 5'0" x 5'0"					
67	WV13	7 1/2	32	4100	410	2.50	2.00	#3	0.375	9½ x 9½	41600	2.56
68	WV14	6	34	4100	410	2.50	2.00	D4.6	0.242	4 x 4	68300	2.82
69	WV15	6	31	5200	590	2.50	2.00	D4.6	0.242	8 x 8	68300	2.30
70	WV16	6 1/4	33	5200	590	2.50	2.00	D4.6	0.242	6 x 6	68300	2.58
71	WV17	6 1/4	17	4780	530	2.50	2.00	D2.9	0.191	4 x 4	68900	2.28
	4 edges restrained, uniform loading						Clear spans 5'0" x 3'6"					
72	WV18	4	7	3370	390	2.50	1.83	D9.2	0.342	8 x 8	62000	2.10
73	WV19	4	83	4200	400	2.50	1.92	D2.9	0.191	4 x 4	68000	1.77
74	WV20	7	24	3750	400	2.50	1.91	D2.5	0.177	3 x 3	91000	1.41
75	WV21	7	58	4280	380	2.50	1.66	D2.5	0.177	3 x 3	91000	1.64
76	WV22	6 1/2	53	5700	470	2.50	1.88	D4.6	0.242	6 x 6	91000	1.70
77	WV23	6 1/2	59	5700	520	2.50	1.83	D9.2	0.342	12 x 12	76000	2.28
78	WV24	5 1/2	18	5490	500	2.50	1.21	D9.2	0.342	8 x 8	62000	1.90
79	WV25	7 1/4	37	4780	530	2.50	2.00	#3	0.375	9½ x 9½	41600	1.86
80	WV26	6	35	5770	590	2.50	2.00	D4.6	0.242	8 x 8	68300	1.62
81	WV27	6	38	5770	590	2.50	2.00	D4.6	0.242	4 x 4	68300	1.56
82	WV28	6	22	5020	540	2.50	2.00	D2.9	0.191	4 x 4	68900	1.70
83	WV29	7	23	5020	540	2.50	2.00	D4.6	0.242	6 x 6	68300	1.70

TABLE 1-A1–GENERAL PROPERTIES OF SLAB TEST SPECIMENS[a] (CONT.)

Test no.	Slab designation	Average slump, in.	Age at test, days	Cylinder compres. strength f'_c, psi	Cylinder split. strength f'_t, psi	Total center thickness, in.	Center d_1, in.	Reinf.[b] wire gage or bar size	Reinf. dia. ϕ_1/ϕ_2, in./in.	Reinf. spacing $s_1 \times s_2$, in.	Reinf. yield strength, 0.2% offset, in.	Center deflec. at ult. load, in.
3 edges restrained, 1 edge hinged, uniform loading							Clear spans 5′0″ x 3′6″					
84	WV30	7	25	3930	440	2.50	2.00	D2.0	0.191	4 x 4	68900	2.05
85	WV31	6	26	3960	440	2.50	2.00	D4.6	0.242	8 x 8	68300	1.80
86	WV32	6	21	4950	520	2.50	2.00	D4.6	0.242	4 x 4	68300	1.80
87	WV33	6	22	4950	520	2.50	2.00	#3	0.375	9½ x 9½	41600	1.88
2 edges restrained, 2 edges hinged, uniform loading							Clear spans 5′0″ x 3′6″					
88	WV34	6 1/2	21	4320	490	2.50	2.00	D4.6	0.242	8 x 8	68300	1.78
89	WV35	6 1/2	22	4320	490	2.50	2.00	D2.9	0.191	4 x 4	68900	2.00
90	WV36	6 1/2	14	4350	470	2.50	2.00	#3	0.375	9½ x 9½	41600	2.00

[a]Edge support described in footnote to Table 1-1.

[b]W = Smooth wire gage. D = Deformed wire gage. Number after letter W or D indicates area of cross-section in 0.01 in.^{2} # = Rebar size.

Note: In slabs restrained at boundaries, the same pattern and amount of reinforcement used for the positive moment was also used for the negative moment.

TABLE 1-A2–PROPERTIES OF CONCRETE STRETCHED CRACKED ZONES

Test no.	Slab des.	Failure load P_u, lb	Concr. stret. area A_{t_1}, in.	Concr. stret. area A_{t_2}, in.	Cover factor R	Active steel ratio p_{t_1}, %	Active steel ratio p_{t_2}, %	Grid index $I_1 = \frac{\phi_1 s_2}{p_{t_1}}$	Grid index $I_2 = \frac{\phi_2 s_1}{p_{t_2}}$	Control. initial crack pattern O; YL*
1	CSF1	49700	18.38	22.36	1.50	1.407	1.155	94.1	114.7	O
2	CSF2	57600	18.49	22.34	1.40	1.433	1.189	92.4	112.6	O
3	CSG1	43400	17.67	21.84	1.20	.730	.598	358.2	445.2	YL
4	CSG2	40600	12.15	16.20	1.10	1.073	.808	248.1	329.6	YL
5	CSH1	41500	15.65	18.29	1.20	.881	.755	110.3	128.9	O
6	CSH2	41000	14.68	17.61	1.20	.940	.770	110.1	126.6	O
7	CSI1	37000	12.50	15.41	1.10	.556	.452	347.9	427.6	YL
8	CSJ1	41300	13.72	16.63	1.10	.993	.413	196.1	235.7	O-YL
9	CSJ2	41000	19.72	22.64	1.30	.706	.303	257.1	321.1	YL-O
10	CSK1	30900	11.90	15.05	1.10	.902	.191	349.7	603.1	YL
11	SA1	25000	18.52	21.45	1.20	.755	.652	129.1	150.0	O
12	SA2	23900	18.52	21.45	1.20	.755	.652	129.1	149.4	O
13	SA3	27000	18.52	21.45	1.20	.755	.652	129.1	149.4	O
14	SB1	18000	29.17	33.14	1.50	.442	.389	598.6	740.7	YL
15	SB2	22000	20.77	24.74	1.20	.621	.521	432.4	508.3	YL
16	SC1	13000	28.12	31.05	1.40	.249	.225	783.6	865.0	YL
17	SC2	12200	26.92	29.85	1.40	.260	.234	750.1	831.7	YL
18	SD1	12000	16.70	18.16	1.20	.648	.159	486.1	722.7	YL
19	SD2	14300	18.41	19.85	1.20	.588	.146	535.9	790.1	YL
20	SE1	27600	25.61	29.59	2.60	1.008	.873	131.4	151.8	O

TABLE 1-A2–PROPERTIES OF CONCRETE STRETCHED CRACKED ZONES (CONT.)

Test no.	Slab des.	Failure load P_u, lb	Concr. stret. area A_{t_1}, in.	Concr. stret. area A_{t_2}, in.	Cover factor R	Active steel ratio p_{t_1}, %	Active steel ratio p_{t_2}, %	Grid index $I_1 = \frac{\phi_1 s_2}{p_{t_1}}$	Grid index $I_2 = \frac{\phi_2 s_1}{p_{t_2}}$	Control. initial crack pattern O; YL*
21	SE2	53500	12.37	16.34	1.10	2.087	1.579	63.5	83.8	O
22	SE3	41000	19.57	23.54	1.20	1.319	1.096	108.9	131.0	O
23	WS1	119600	13.20	18.96	1.30	1.05	.73	92.4	132.8	O
24	WS2	104100	13.20	18.96	1.30	1.05	.73	92.4	132.8	O
25	WS3	98600	10.56	7.44	1.20	.57	.81	111.6	78.4	O
26	WS4	79600	7.44	10.56	1.20	.81	.57	78.4	111.6	O
27	WS5	104800	22.80	26.40	1.50	.26	.23	244.8	276.8	O-YL
28	WS6	105000	26.40	22.80	1.50	.23	.26	276.8	244.8	O-YL
29	WS7	81200	10.56	15.12	1.20	1.17	.58	65.2	131.6	O
30	WS8	84000	10.56	10.56	1.20	1.17	.58	65.2	131.6	O
31	WS9	73700	18.00	24.00	1.40	.48	.36	159.2	212.4	O-YL
32	WS10	82900	18.00	24.00	1.85	.48	.36	159.2	212.4	O-YL
33	WS11	85400	9.00	13.51	1.20	.77	.51	251.2	379.2	YL
34	WS12	81000	9.00	13.51	1.10	.77	.51	251.2	379.2	YL
35	WS13	105900	30.00	36.00	2.00	.43	.36	616.0	736.0	YL
36	WS14	109500	24.00	30.00	1.90	.54	.43	489.6	616.0	YL
37	WS15	74100	25.51	30.00	1.80	.25	.21	259.2	308.8	YL-O
38	WS16	631.00	16.30	18.00	1.30	.39	.35	166.4	185.2	O-YL
39	WS17	65300	16.30	18.00	1.30	.39	.35	166.4	185.2	O-YL
40	WS18	65300	27.00	31.49	1.70	.23	.20	281.6	324.0	YL
41	WS19	68300	28.49	33.00	1.80	.30	.24	159.0	198.9	YL

42	WS20	73000	18.00	15.00	1.30	.44	.53	108.6	90.0	O
43	WS21	73000	18.00	15.00	1.30	.44	.53	108.6	90.0	O
44	WS22	71900	25.51	22.46	1.60	.31	.36	153.9	132.6	O
45	WS23	68300	18.00	24.00	1.40	.33	.25	192.8	254.4	YL
46	WS24	62700	30.00	33.00	1.80	.20	.22	318.0	298.2	YL
47	WS25	84700	27.00	21.00	1.20	.26	.66	372.4	290.4	YL
48	WS26	74500	27.00	24.00	1.60	.26	.58	372.4	333.6	YL
49	WS27	79200	21.00	18.00	1.40	.32	.78	266.0	231.0	YL
50	WS28	84000	24.00	18.00	1.40	.29	.74	339.0	261.6	YL
51	WS29	73000	30.00	27.00	1.80	.31	.34	468.6	427.2	YL
52	WS30	70800	33.00	30.00	1.90	.28	.31	518.4	468.6	YL
53	WS31	68300	18.00	15.00	1.30	.51	.61	285.0	238.2	YL
54	WS32	77000	18.00	15.00	1.30	.51	.61	285.0	238.2	YL
55	WV1	81700	14.90	20.71	1.35	.926	.666	104.5	145.3	O
56	WV2	67700	14.29	18.88	1.30	.601	.455	127.1	167.9	O
57	WV3	63200	14.90	20.71	1.30	.463	.333	418.1	581.4	YL
58	WV4	63200	13.91	17.72	1.30	.427	.336	149.1	189.2	O-YL
59	WV5	69500	14.29	18.88	1.30	.601	.455	127.1	167.9	O
60	WV6	73000	14.90	20.71	1.30	.617	.444	235.1	327.2	O-YL
61	WV7	84000	16.50	25.50	1.35	.842	.545	423.1	653.7	YL
62	WV8	70500	14.90	20.71	1.35	.926	.666	104.5	145.3	O
63	WV9	57000	14.90	20.71	1.30	.463	.333	418.1	581.4	YL
64	WV10	66700	14.29	18.88	1.30	.801	.455	127.1	167.9	YL
65	WV11	76500	14.90	20.71	1.30	.617	.444	235.3	327.0	O-YL
66	WV12	70000	16.50	25.50	1.35	.842	.545	423.1	653.7	YL
67	WV13	65000	16.50	25.50	1.35	.842	.545	423.1	653.7	YL
68	WV14	74200	14.90	20.71	1.35	.926	.666	104.5	145.3	O
69	WV15	59000	14.90	20.71	1.30	.463	.333	418.1	581.4	YL
70	WV16	64000	14.90	20.71	1.30	.617	.444	235.3	327.0	O-YL

TABLE 1-A2—PROPERTIES OF CONCRETE STRETCHED CRACKED ZONES (CONT.)

Test no.	Slab des.	Failure load P_u, lb	Concr. stret. area A_{t_1}, in.	Concr. stret. area A_{t_2}, in.	Cover factor R	Active steel ratio P_{t_1}, %	Active steel ratio P_{t_2}, %	Grid index $I_1 = \frac{\phi_1/s_2}{P_{t_1}}$	Grid index $I_2 = \frac{\phi_2 s_1}{P_{t_2}}$	Control. initial crack pattern O; YL*
72	WV18	93200	16.10	24.31	1.45	.857	.567	319.3	482.5	YL
73	WV19	74300	14.29	18.88	1.40	.601	.455	127.1	167.9	O-YL
74	WV20	73600	14.12	18.37	1.30	.694	.533	76.5	99.6	O
75	WV21	70800	20.12	24.37	1.65	.487	.402	109.0	132.1	O
76	WV22	75600	14.90	20.71	1.40	.617	.444	235.3	327.0	YL
77	WV23	70600	16.10	24.31	1.45	.571	.378	718.7	1085.7	YL
78	WV24	83400	31.10	39.31	2.50	.443	.351	617.6	779.5	YL
79	WV25	77300	16.50	25.50	1.35	.842	.545	423.1	653.7	YL
80	WV26	67900	14.90	20.71	1.30	.463	.333	418.1	581.4	YL
81	WV27	80900	14.90	20.71	1.35	.926	.666	104.5	145.3	O
82	WV28	75800	14.29	18.88	1.30	.601	.455	127.1	167.9	O
83	WV29	73300	14.90	20.71	1.30	.617	.444	235.3	327.0	O-YL
84	WV30	51200	14.29	18.88	1.30	.601	.455	127.1	167.9	O-YL
85	WV31	47400	14.90	20.71	1.30	.463	.333	418.1	581.4	O-YL
86	WV32	72100	14.90	20.71	1.35	.926	.666	104.5	145.3	O
87	WV33	65500	16.50	25.50	1.35	.842	.545	423.1	653.7	YL
88	WV34	44300	14.90	20.71	1.30	.463	.333	418.1	581.4	YL
89	WV35	45600	14.29	18.88	1.30	.601	.455	127.1	167.9	O-YL
90	WV36	59600	16.50	25.50	1.35	.842	.545	423.1	653.7	YL

Fig. 1-1—Typical stress-strain diagram of reinforcement

Fig. 1-2—Reinforcement grid unit

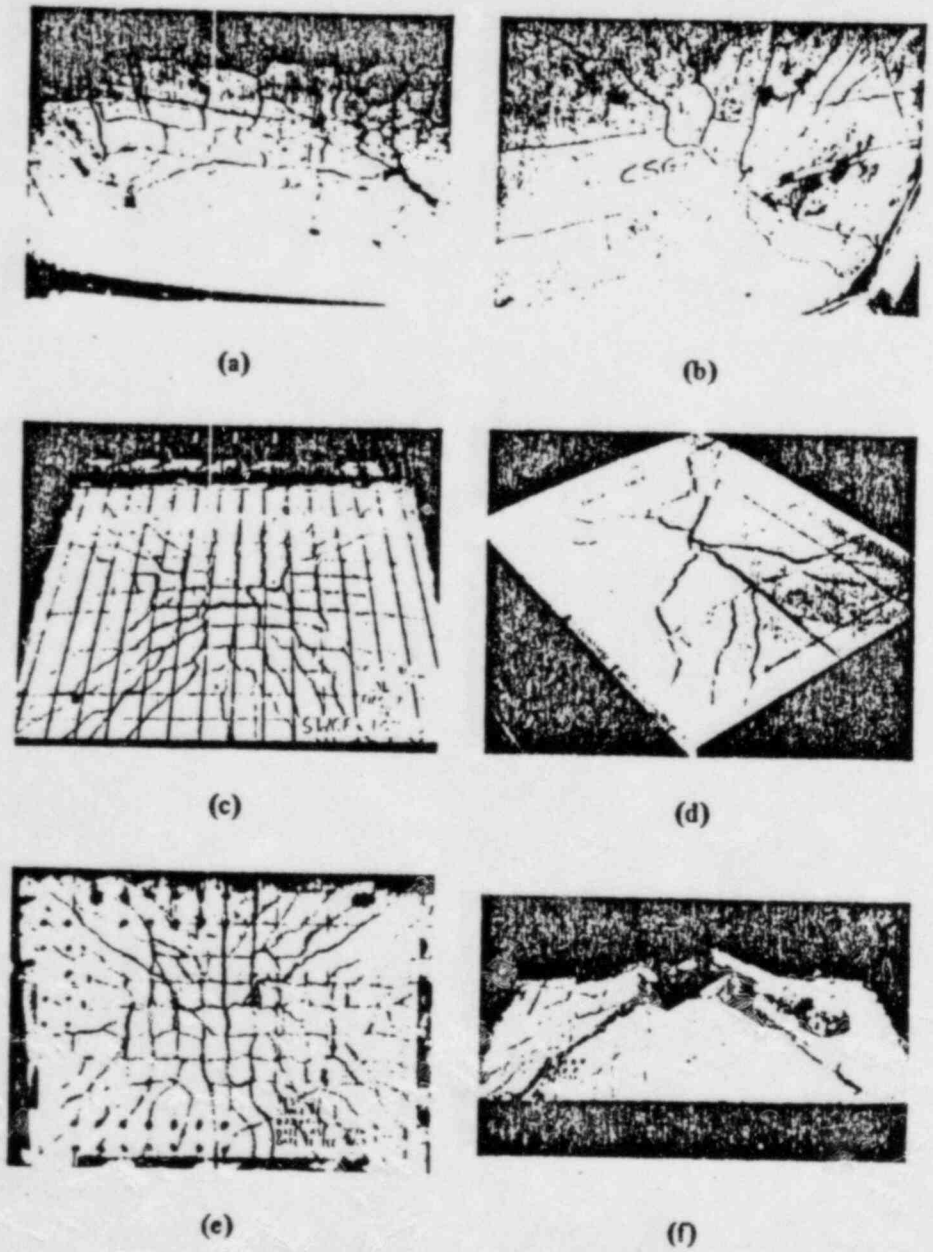

(a) (b) (c) (d) (e) (f)

Fig. 1-3—Typical controlling cracking patterns. (a) Orthogonal: centrally loaded square slab. (b) Yield-line: centrally loaded square slab. (c) Orthogonal: uniformly loaded square slab. (d) Yield-line: uniformly loaded rectangular slab. (e) Orthogonal: uniformly loaded rectangular slab. (f) Slab at rupture.

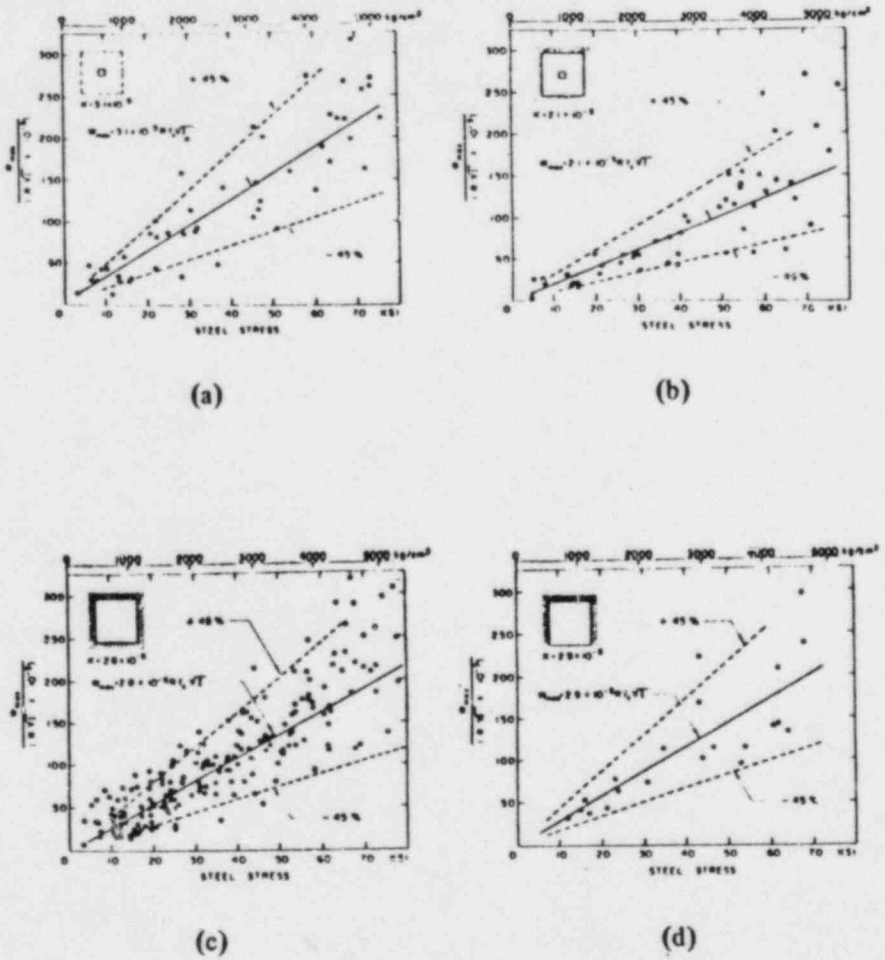

(a) (b) (c) (d)

Fig. 1-4—Crack width vs. reinforcement steel stress. (a) Centrally loaded square slabs simply supported on all edges. (b) Centrally loaded square slabs restrained on all edges. (c) Uniformly loaded square slabs restrained on all edges. (d) Uniformly loaded square slabs restrained on three edges, hinged on one.

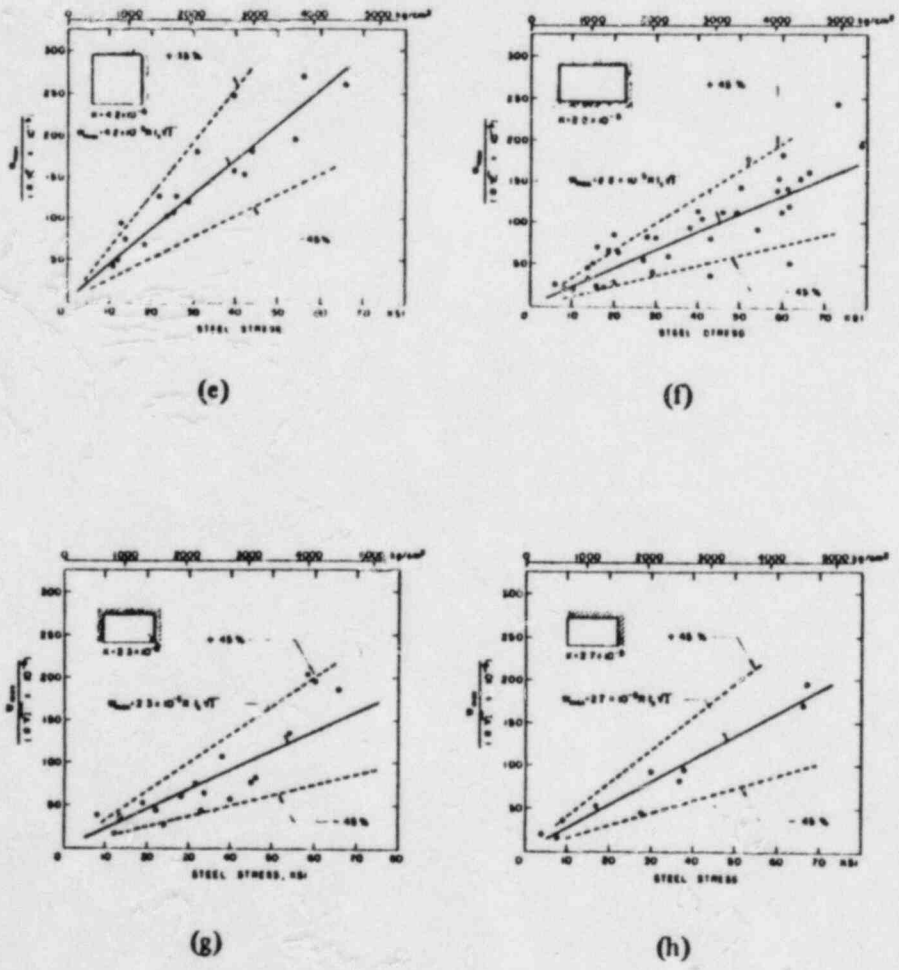

(e) (f) (g) (h)

Fig. 1-4—Crack width vs. reinforcement steel stress. (e) Uniformly loaded square slabs restrained on two adjacent edges, hinged on the other two. (f) Uniformly loaded rectangular slabs restrained on all edges. (g) Uniformly loaded rectangular slabs restrained on three edges, hinged on one long edge. (h) Uniformly loaded rectangular slabs restrained on two adjacent edges, hinged on the other two

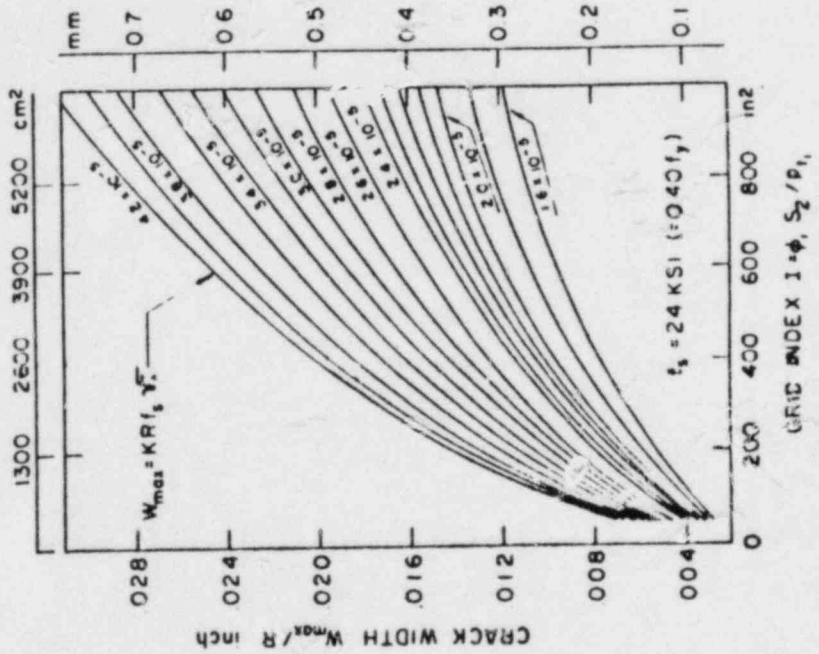

Fig. 1-6—Plots of grid index versus crack width at 24 ksi stress level for various load and support conditions

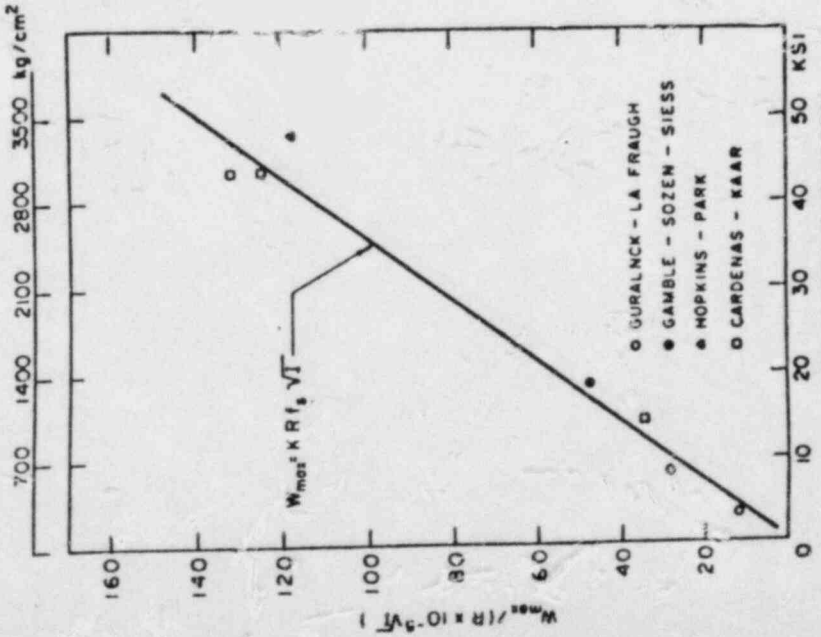

Fig. 1-5—Comparison with tests by others